

UNIVERSIDADE ESTADUAL DE CAMPINAS
FACULDADE DE ENGENHARIA MECÂNICA
COMISSÃO DE PÓS-GRADUAÇÃO EM ENGENHARIA MECÂNICA

**Análise Dinâmica de Problemas não
Determinísticos usando Métodos
Baseados em Conjuntos Nebulosos**

Autor: **Ronaldo Fernandes Nunes**

Orientador: **Prof. Dr. José Roberto de França Arruda**

01/2005

UNIVERSIDADE ESTADUAL DE CAMPINAS
FACULDADE DE ENGENHARIA MECÂNICA
COMISSÃO DE PÓS-GRADUAÇÃO EM ENGENHARIA MECÂNICA
DEPARTAMENTO DE MECÂNICA COMPUTACIONAL

Análise Dinâmica de Problemas não Determinísticos usando Métodos Baseados em Conjuntos Nebulosos

Autor: **Ronaldo Fernandes Nunes**

Orientador: **Prof. Dr. José Roberto de França Arruda**

Curso: Engenharia Mecânica

Área de Concentração: Mecânica dos Sólidos e Projeto Mecânico

Tese de doutorado apresentada à comissão de Pós Graduação da Faculdade de Engenharia Mecânica, como requisito para a obtenção do título de Doutor em Engenharia Mecânica.

Campinas, 2005

S.P. - Brasil

UNIVERSIDADE ESTADUAL DE CAMPINAS
FACULDADE DE ENGENHARIA MECÂNICA
COMISSÃO DE PÓS-GRADUAÇÃO EM ENGENHARIA MECÂNICA
DEPARTAMENTO DE MECÂNICA COMPUTACIONAL

TESE DE DOUTORADO

Análise Dinâmica de Problemas não
Determinísticos usando Métodos
Baseados em Conjuntos Nebulosos

Autor: Ronaldo Fernandes Nunes

Orientador: Prof. Dr. José Roberto de França Arruda

Prof. Dr. José Roberto de França Arruda, Presidente
FEM/UNICAMP

Prof. Dr. Arcanjo Lenzi
EMC/UFSC

Prof. Dr. Ney Roitman
COPPE/UFRJ

Prof. Dr. Renato Pavanello
FEM/UNICAMP

Prof. Dr. José Maria Campos dos Santos
FEM/UNICAMP

Campinas, 27 de Junho de 2005

Dedication

To my father Sebastião Nunes (1944 - 2003).

The less we know, the more certain and precise we are in our explanations; the more we know, the more we realize the limitations of being certain and precise.

Socrates

Acknowledgments

I would like to express my appreciation to all these who contributed to the success of this work:

- With special thanks to my wife Andrea Miti Dobashi, for the patience, help and comprehension that I needed during this busy time.

- I would like to thank my parents Sebastião Nunes and Alaide Fernandes Nunes, who gave me the opportunity that themselves did not have. To my sister, Valquiria Fernandes Nunes and her husband, André Barros, which during my academic life, gave me support and strength.

- I would like to express my gratitude with special thanks to my supervisor, Professor Dr. José Roberto de França Arruda, Unicamp, who pointed me in the right direction in this work, to the fruitful and innumerable discussions and also for the friendship during the development of this thesis.

- To Andreas Klimke from Stuttgart University for the very important discussions in the fuzzy set based methods area and for giving me the opportunity to learn and to develop the basis of my topic of research. Also, to Professor Dr. Hanss of Stuttgart University for the initial discussions on fuzzy arithmetic, I express my gratitude.

- To Stefan Oexl for the meaningful discussions in fuzzy arithmetic and giving me the first insights in this area, many thanks.

- I also would like to thank Professor Hermann Matthies from Technical University of Braunschweig for sending me very interesting papers in the field of finite

elements for stochastic problems.

- To the Computational Mechanics Department for the support to my work and for giving me the opportunity to develop my thesis.

- For all of my colleagues of the Computational Mechanics Department - Vibro-acoustics Laboratory, with very special attention to Khaled, Lázaro, Belisário, Éder, Elson, Edmilson and Allan Pereira, who gave me support to make this work possible.

- To my colleagues of the TPC Department, DaimlerChrysler, Stuttgart, Germany, who read and reviewed my work and gave me some important comments. With special thanks to Fantini, McKellip, Linnick, Thorsten and Manfred Bach. Also, to my colleagues from Freightliner, Craig and Greg.

- I would like also to thank my former company, T-Systems (debris Humaitá), in the name of Marcos Argentino, Celso Nogueira and Arnaldo Camarão, who gave me the opportunity, during my daily work, to conclude the subjects that I used as a basis to write this thesis. Without this great opportunity, I wouldn't be able to write these acknowledgments.

Resumo

Nunes, Ronaldo Fernandes, *Análise Dinâmica de Problemas não Determinísticos usando Métodos Baseados em Conjuntos Nebulosos*, Campinas: Faculdade de Engenharia Mecânica, Universidade Estadual de Campinas, 2005, 142 p., Tese (Doutorado).

Neste trabalho, o problema da análise dinâmica de estruturas em médias frequências é abordado. Em geral, métodos numéricos tais como elementos finitos e elementos de contorno não são apropriados para tratar estes casos. As principais razões são a necessidade do refinamento das malhas com o aumento da frequência e o cálculo da influência dos parâmetros incertos, cujo efeito em particular, para médias e altas frequências, tende a ser significativo. O problema do refinamento do modelo pode ser superado através de métodos semi-analíticos, como por exemplo o método do elemento espectral. Em relação à simulação dos sistemas com parâmetros de entrada incertos, métodos baseados em conjuntos nebulosos e métodos probabilísticos são adotados. Nesta tese, uma proposta combinando o método do elemento espectral com conjuntos nebulosos é conduzida. O principal foco deste trabalho é apresentar uma nova abordagem para o problema em médias frequências. Neste contexto, funções de resposta em frequência são adotadas para representar o efeito dos parâmetros de entrada não determinísticos na resposta dinâmica de estruturas. Para ilustrar o procedimento proposto, exemplos numéricos são tratados, como o caso simples de uma placa retangular reforçada com vigas e também o caso de uma estrutura do tipo pórtico.

Palavras Chave

Método dos elementos espectrais, médias frequências, conjunto nebulosos, parâmetros de entrada incertos, método de transformação.

Abstract

Nunes, Ronaldo Fernandes, *Dynamic Analysis of Non-Deterministic Problems using Fuzzy Set Based Methods*, Campinas: Faculdade de Engenharia Mecânica, Universidade Estadual de Campinas, 2005, 142 p., Thesis (Doctorate).

It is well-known that, in the mid-frequency range, numerical methods such as finite and boundary elements are not suitable for structural dynamic analysis. One of the reasons is the fine mesh resolution required to accurately model the physical problem, leading to large computational models. The other reason is associated with the difficulty in estimating the response statistics for system parameter variations. The mesh refinement problem can be addressed using semi-analytical methods, such as the spectral element method. However, in general, these methods are very limited with respect to the geometry and boundary conditions that can be treated. With respect to parameter variation, the simulation of systems with uncertain parameters has in the past been addressed with different techniques, such as finite elements applied to stochastic problems and fuzzy set based methods. In this thesis, the spectral element method is combined with a special implementation of a fuzzy set based method that avoids the well-known effect of overestimation in interval computations. In this regard, some efficient alternatives, such as the transformation method and the sparse grids approach are proposed. In this work, the main goal is to provide alternatives to address dynamic problems under uncertainty in the mid-frequency range. In this context, envelopes for frequency response functions are used to represent the effect of non-deterministic input parameters in the dynamic response of structures. To illustrate the proposed procedure, numerical examples are treated, such as a simple rectangular plate reinforced with beams and a frame-type model.

Key words

Spectral element method, mid frequencies, fuzzy set based methods, uncertainty parameters, transformation method.

Introdução

Mesmo quando se pode obter um modelo determinístico do comportamento dinâmico de uma estrutura através de métodos numéricos como o método de elementos finitos, por mais exato que seja este modelo para descrever a resposta dinâmica, o seu resultado é apenas uma representação de uma estrutura nominal. Porém, sabe-se que, em uma situação real, a análise determinística é insuficiente. Por exemplo, se tomarmos o caso de várias amostras de um veículo comercial na saída da linha de produção, sabe-se que a resposta dinâmica irá apresentar grandes variações apesar de serem veículos nominalmente idênticos. Estruturas similares podem apresentar, durante o seu processo de fabricação, variações em suas propriedades individuais que, de certa forma, refletirão na sua resposta dinâmica. Algumas pequenas mudanças nas propriedades físicas da estrutura podem afetar diretamente os resultados finais (Kompella e Bernhard, 1993).

Neste contexto, muitas pesquisas têm sido conduzidas na área de simulação numérica para que os modelos numéricos de elementos finitos sejam capazes de estimar as respostas levando em conta a influência dos parâmetros de entrada não determinísticos e para que limites em frequência sejam estendidos em aplicações de frequências mais altas.

Considerando a discussão acima, o objetivo deste trabalho é apresentar alternativas para o estudo da resposta de sistemas dinâmicos em médias frequências considerando os efeitos dos parâmetros de entrada não determinísticos. Métodos numéricos, tais como elementos finitos e elementos de contorno, em geral não são apropriados para tratar tais problemas. Uma das razões é a necessidade do refinamento dos modelos e a outra é a influência dos parâmetros de entrada incertos, cujo efeito, em particular para médias e altas frequências, torna-se mais evidente. Considerando o comprimento de onda das vibrações, para se obter uma boa correlação entre soluções analíticas e numéricas, recomendam-se de 6 a 10 elementos lineares por comprimento de onda para manter as respostas dentro de limites aceitáveis de erro de predição (Desmet, 2002).

Indo mais adiante, outro ponto importante no contexto acima é que, à medida que a frequência aumenta, a resposta dinâmica da estrutura fica mais sensível à influência dos parâmetros incertos, como, por exemplo, detalhes geométricos e variações das propriedades dos materiais. Outro problema que também deve ser considerado diz respeito aos modos de vibração de ordem elevada que, em particular para altas frequências, tendem a apresentar uma flutuação espacial mais complexa (Shorter, 1998).

Ao longo do tempo, muitas pesquisas foram conduzidas de forma a criar alternativas aos problemas descritos acima. Para o problema do refinamento do modelo, este pode ser resolvido em alguns casos através de métodos semi-analíticos, tais como o método dos elementos espectrais (SEM), que são menos afetados pelo pequeno comprimento de onda. Em relação à simulação dos sistemas com parâmetros de entrada não determinísticos, por exemplo, métodos baseados em conjuntos nebulosos (Hanss, 2002b; Klimke et al., 2004a; Nunes et al., 2005) e métodos estocásticos (Elishakoff e Ren, 2003; Ghanem e Spanos, 2003; Manohar e Ibrahim, 1999) são sugeridos na literatura. Neste trabalho, para o termo em inglês *Fuzzy Sets*, será adotado o termo em português conjuntos nebulosos ou, quando combinado com o SEM, simplesmente SEM/Fuzzy.

Vários outros métodos para descrever o problema em médias e altas frequências têm sido considerados na literatura, tais como técnicas probabilísticas de modelagem e o uso da Análise Estatística de Energia (SEA), a qual pode ser considerada de grande aplicabilidade para altas frequências.

Lyon e DeJong (1995) postulam que, em altas frequências, a representação da resposta de uma estrutura em termos de energia torna-se mais apropriada. Na SEA o problema é tratado através do balanço de energia e do fluxo de potência entre os diferentes grupos de modos em um sistema dinâmico. Neste caso, grupos modais são tratados como subsistemas, onde, para cada subsistema, modos naturais com características semelhantes devem ser considerados. Para cada subsistema dentro de uma determinada banda, a resposta é calculada através dos níveis médios de energia.

Por exemplo, a Figura 1 apresenta o modelo de duas barras acopladas, onde a barra 1, em função das características geométricas e propriedades físicas adotadas, apresenta uma densidade modal muito inferior à barra 2. Neste caso, o objetivo é obter a resposta dinâmica da estrutura no ponto de conexão da barra 1 com a barra 2, assumindo uma excitação unitária em uma das extremidades, i.e., para uma força longitudinal P de 1 N. Para a barra 2, um

comprimento de $L_2 = 2.46$ m é adotado, enquanto a barra 1 possui um comprimento de apenas $L_1 = 0.20$ m. Para as propriedades físicas das barras tem-se valores médios de Módulo de Young igual a $E_{1/2} = 2.71 \times 10^9$ N/m², densidade $\rho_{1/2} = 1140$ kg/m³, amortecimento igual a $\eta_{1/2} = 1.0 \times 10^{-2}$ e áreas da seção transversal $A_1 = 1.735 \times 10^{-3}$ m² e $A_2 = 1.862 \times 10^{-4}$ m², respectivamente.

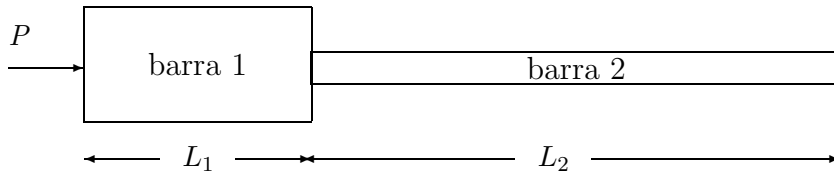


Figura 1: Esquema de duas barras acopladas.

A Figura 2 compara os resultados obtidos com o método da SEA e com o método dos SEM para o caso simples de duas barras acopladas. Com base no resultado apresentado, o que se nota é que para altas frequências, o resultado obtido via SEA fica muito próximo do valor médio da curva obtida via SEM, enquanto que, para as baixas frequências, o resultado não é tão representativo.

Em geral, para que o uso da SEA produza resultados precisos, algumas pré-condições devem ser atendidas. Por exemplo, uma das principais condições a ser atendida diz respeito à alta densidade modal dentro da banda de frequência de interesse, o que não é atendido para as baixas frequências. Neste caso, é importante ressaltar que caso não haja um número mínimo de modos por banda de frequência ou mesmo um valor de sobreposição modal superior (*modal overlap factor*) a 1, grandes erros podem ser introduzidos com o uso da SEA (Langley e Brown, 2002). Assim, para casos de estruturas com baixa densidade modal, o uso da SEA não é recomendado, pois suas hipóteses não são válidas (Lyon e DeJong, 1995).

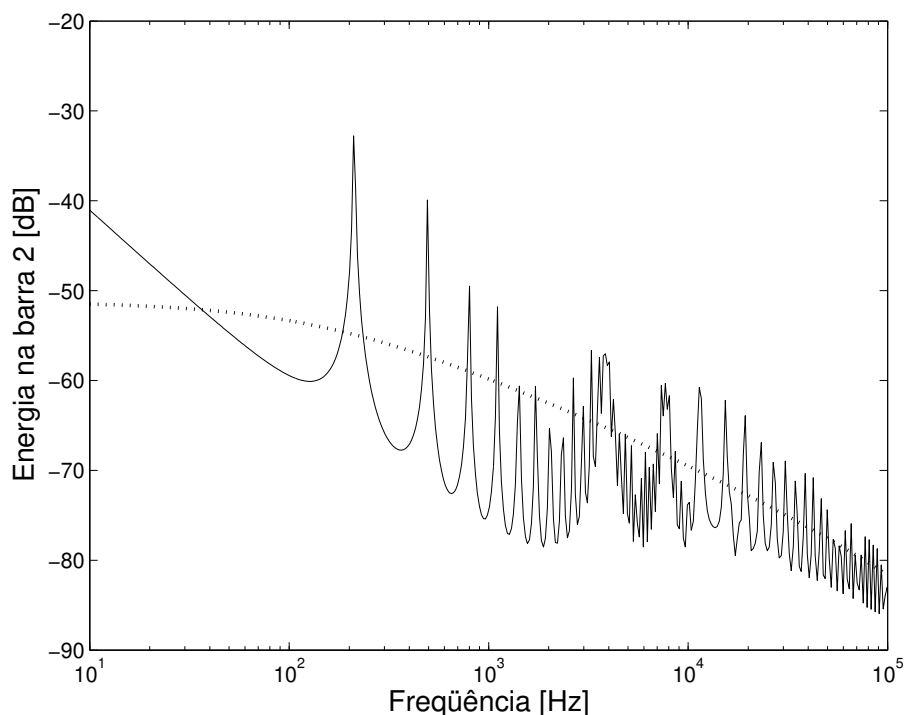


Figura 2: Energia obtida via SEA (linha pontilhada) e SEM (linha sólida).

De acordo com a discussão anterior, a faixa que se convencionou denominar de médias frequências está situada entre o limite de aplicação dos métodos determinísticos e o limite onde a SEA é aplicável ou, simplesmente, onde as hipóteses da SEA são válidas (Lyon e DeJong, 1995).

Em relação ao termo médias frequências, este ainda não foi consolidado, porém algumas definições são tratadas na literatura, como, por exemplo, Langley (1998) descreve que o problema deve ser considerado para cada tipo de estrutura independentemente do número de modos presentes. Lyon e DeJong (1995) definem o termo como sendo a faixa de frequência onde os métodos determinísticos como elementos finitos e elementos de contorno não são mais válidos e onde as hipóteses para aplicações da SEA ainda não são válidas.

Para abordar tal problema, vários métodos combinando elementos finitos e SEA têm sido sugeridos. Indo mais adiante, quatro diferentes métodos têm obtido destaque especial: o método de fluxo de energia ou também chamado método de coeficientes de influência de energia (Zhang et al., 2003), o método da SEA virtual/experimental (Gagliardini et al., 2003), métodos híbridos combinando SEA e elementos finitos (Langley e Bremner, 1999) e o método baseado em propagação de ondas (WBM) (Desmet, 2002).

Neste trabalho, uma proposta combinando o método do elemento espectral com métodos

baseados em conjuntos nebulosos será formulada. Um dos focos deste trabalho é apresentar uma abordagem para tratar o problema em médias frequências considerando a influência dos parâmetros de entrada não determinísticos. Neste contexto, funções de resposta em frequência são adotadas para representar a resposta dinâmica de alguns exemplos numéricos considerando os limites máximos e mínimos (Nunes et al., 2005). A Figura 3 apresenta um exemplo onde o cálculo de energia para a barra 2 obtida via SEA apresentado anteriormente na Figura 2 é comparado com o método proposto nesta tese, ou seja, o SEM combinado com métodos baseados em conjuntos nebulosos (SEM/Fuzzy). Para este exemplo, os parâmetros Módulo de Young igual a $E = 2.71 \times 10^9$ N/m² e fator de perda $\eta = 0.01$ são considerados não determinísticos, assumindo-se um desvio padrão de 10% em relação aos respectivos valores médios. Neste caso, os resultados apresentados deixam de ser apenas determinísticos para também inserir os efeitos dos parâmetros de entrada incertos. Portanto, o principal objetivo nesta tese é lançar bases para a aplicação de métodos baseados em conjuntos nebulosos, apresentando os principais pontos positivos e as respectivas limitações. Ao longo do trabalho, diversos exemplos serão tratados, tendo como foco principal o problema das médias frequências.

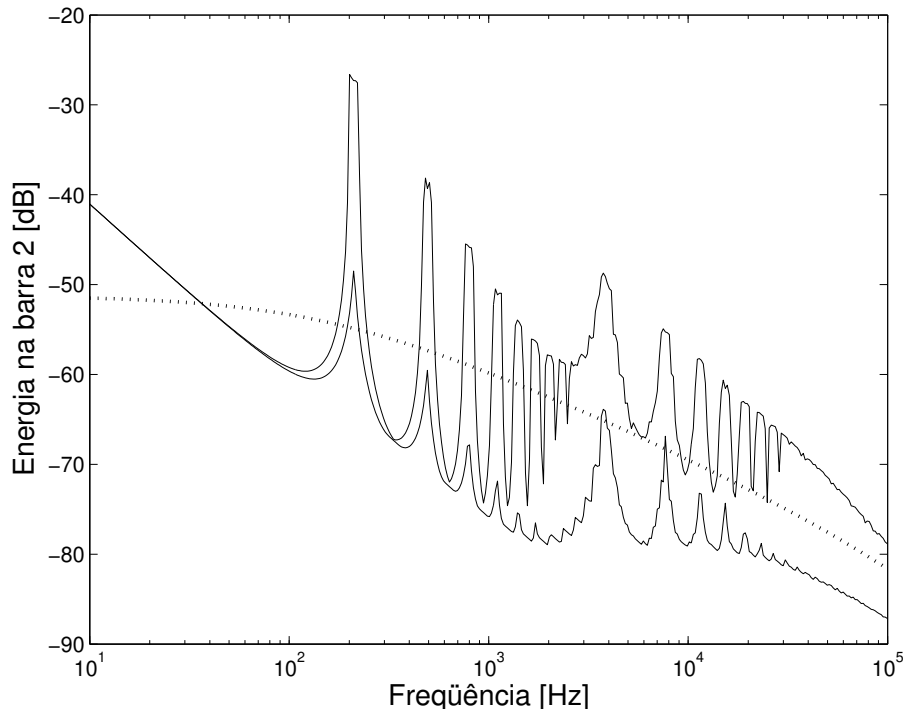


Figura 3: Energia obtida via SEA (linha pontilhada) e SEM/Fuzzy (linha sólida).

Conclusões e Comentários

Nesta tese, importantes questões relacionando o problema da análise dinâmica de médias frequências foram discutidas. Neste caso, o uso do método do elemento espectral combinado com conjuntos nebulosos foi proposto. Considerando os parâmetros de entradas não determinísticos, funções de resposta em frequência usando envelopes foram adotadas para representar os limites máximos e mínimos encontrados.

Na primeira parte do trabalho, uma introdução com uma breve revisão das principais alternativas para o problema de médias frequências foi apresentada. Neste caso, os seguintes métodos foram destacados: o método conhecido como Híbrido, que combina FEA/SEA, o método chamado Virtual/Experimental SEA, o método usando coeficiente de influência de energia (EIC) e também o método baseado em ondas (WBM).

No Capítulo 2, os efeitos da análise dinâmica de estruturas levando em consideração a influência dos parâmetros de entradas incertos foram considerados. Neste capítulo, uma implementação especial do princípio de extensão conhecida como método de transformação foi introduzida. A principal idéia foi mostrar um método eficiente baseado em conjuntos nebulosos para ser combinado com o método do elemento espectral. Neste caso, foi recomendado que, no caso de poucos dados estatísticos disponíveis, os métodos baseados em conjuntos nebulosos são mais adequados do que as técnicas probabilísticas.

No Capítulo 3, antes de apresentar a implementação do método do elemento espectral combinado com conjuntos nebulosos, algumas eficientes alternativas para os métodos de conjuntos nebulosos foram apresentadas. Assim, um método alternativo que considera a remoção dos pontos recorrentes no método de transformação original e mais o uso dos *sparse grids* foram introduzidos como alternativas atrativas para serem combinadas com o método do elemento espectral.

No Capítulo 4, alguns exemplos numéricos foram apresentados para mostrar a aplicação do método proposto nesta tese. Três problemas básicos usados como teste foram apresentados: o

caso simples de um sistema de barras acopladas, um modelo de placa com reforços e também uma estrutura constituída de duas vigas acopladas. Neste mesmo capítulo, aplicações usando a Análise Estatística de Energia (SEA) foram apresentadas para o cálculo dos fatores de perda por acoplamento (CLF).

No Capítulo 5, para apresentação da metodologia de forma mais detalhada, um exemplo numérico aplicado dentro do contexto da engenharia foi apresentado. Neste caso, importantes aspectos, tais como o processo a ser adotado durante um projeto de engenharia, o uso de dados estatísticos disponíveis, os *limites* de aceitabilidade durante o projeto e tipo de incertezas foram discutidos.

Adicionalmente, nos Apêndices A, B, C e D, uma revisão do método dos elementos espectrais foi apresentada para os elementos de barra, viga e placa.

Principais contribuições

As principais contribuições desta tese podem ser resumidas como:

- i. Definição de uma alternativa para o problema das médias frequências considerando os efeitos da resposta dinâmica de estruturas com dados de entradas não determinísticos. Para tanto, o método dos elementos espectrais combinado com conjuntos nebulosos foi proposto. Através deste método, alternativas para dois aspectos negativos encontrados no método tradicional dos elementos finitos foram sugeridas: a extensão do limite de frequência para as médias e altas frequências e o uso de dados de entrada não determinísticos no cálculo da resposta dinâmica de estruturas.
- ii. Apresentação de uma descrição eficiente baseada no princípio de extensão para ser combinada com o método dos elementos espectrais.
- iii. Um novo esquema para a estimativa dos fatores de perda por acoplamento (CLFs) usados em SEA, cobrindo os *limites* de confiança através do uso do método do elemento spectral combinado com conjuntos nebulosos.
- iv. Discussão com apresentação das vantagens e desvantagens de cada método utilizado nesta tese, baseados em conjuntos nebulosos para combinação com métodos determinísticos, como o método dos elementos espectrais.

Sugestões para pesquisas futuras

Para o desenvolvimento de futuras pesquisas, duas áreas devem ser consideradas como principais: Considerando aplicações mais realísticas, ainda há a necessidade do desenvolvimento de elementos espectrais que tenham maior flexibilidade nas condições de contorno e também aplicado para estruturas mais gerais. Em geral, o uso do método dos elementos espectrais pode ser considerado uma ferramenta poderosa para aplicações de problemas dinâmicos em médias frequências. No entanto, para aplicações do tipo industrial, uma biblioteca mais geral dos elementos deve ser desenvolvida. Por exemplo, elementos do tipo casca com condições de contorno mais gerais podem ser consideradas uma grande área a ser explorada. Igualmente, o estudo de um método híbrido, no caso combinando elementos espectrais com elementos finitos ou mesmo com a Análise Estatística de Energia, também pode ser considerada uma interessante área a ser desenvolvida.

Em relação aos métodos baseados em conjuntos nebulosos, a primeira área de interesse de desenvolvimento pode ser considerada a área de implementação de novos algoritmos. Neste campo de pesquisa, o principal foco está no desenvolvimento de algoritmos para tornar a área mais atrativa do ponto de vista industrial. Por exemplo, considerando o método de transformação geral removendo os pontos recorrentes da sua formulação original, para casos com dimensões maiores que dez parâmetros de entradas incertos, sua complexidade aumenta consideravelmente. Para o caso dos *sparse grids*, este depende da superfície de interpolação em função dos parâmetros de entrada incertos.

Uma outra área também de grande importância está relacionada com o desenvolvimento de algoritmos capazes de selecionar os parâmetros de entrada mais importantes, evitando com isto alto custo computacional nas análises envolvendo parâmetros não determinísticos. Esta área tem sido objeto de pesquisa e alguns trabalhos já podem ser encontrados na literatura, por exemplo os trabalhos de Hanss e Klimke (2004) e Hanss (2003). No mesmo contexto, implementações de softwares comerciais que combinem métodos determinísticos com conjuntos nebulosos também pode ser considerada uma área a ser explorada. Para casos mais simples, como os apresentados nesta tese, o uso do método de elemento espectral pode ser uma excelente alternativa.

Trabalhos publicados

Durante o desenvolvimento desta tese, foram publicados os seguintes trabalhos em anais de congressos internacionais, relatórios e submetidos para periódicos internacionais:

Submetido para periódicos internacionais

Nunes, R. F., Ahmida, K. M. and Arruda, J. R. F. Applying a Fuzzy Set Based Method for Robust Estimation of the Coupling Loss Factors. *Submetido para o Journal of Sound and Vibration, 2005.*

Nunes, R. F., Klimke, A. and Arruda, J. R. F. On estimating frequency response function envelopes using the spectral element method and fuzzy sets. *Aceito para publicação no Journal of Sound and Vibration, 2005.*

Anais de congressos internacionais

Nunes, R. F., Ahmida, K. M. and Arruda, J. R. F. A SEM/Fuzzy Method for the Estimation of the SEA Coupling Loss Factors. *Proceedings of the NOVEM 2005*, Saint Raphael, France, paper 52, 2005.

Arruda, J. R. F., Donadon, L. **Nunes**, R. F. and Albuquerque, E. On the modeling of reinforced plates in the mid-frequency range, *Proceedings of the ISMA2004*, Leuven, Belgium, paper number 308, 2004.

Nunes, R. F., Oexl, S. and Arruda, J. R. F. Taking uncertainties into account in spectral element modeling of structures, *Proceedings of the Inter-Noise 2004*, Prague, Czech Republic, paper number 436, 2004.

Relatórios

Nunes, R. F., Klimke, A. and Arruda, J. R. F. *On estimating frequency response function envelopes using the spectral element method and fuzzy sets.* IANS report 2004/020, Tech. rep., University of Stuttgart, 2004, URL <http://preprints.ians.uni-stuttgart.de>. 09/11/2004.

Contents

1	Introduction and Motivation	1
1.1	Alternatives based on the FE method	2
1.1.1	Dynamic reduction	3
1.1.2	Hierarchical FE	3
1.1.3	Component Mode Synthesis (CMS)	4
1.1.4	Monte-Carlo Simulation	5
1.2	SEA Method	7
1.2.1	Statistical Energy Analysis (SEA)	7
1.3	Developments in the Mid-Frequency Range	10
1.3.1	Virtual/Experimental SEA	10
1.3.2	Energy Influence Coefficient (EIC)	12
1.3.3	FEA/SEA Hybrid Method	13
1.3.4	Wave Based Method (WBM)	16
1.4	Thesis Outline	18
2	Dynamic Analysis of Structures for Design Under Uncertainty	19
2.1	Introduction	19
2.2	Probabilistic Methods	21
2.2.1	General aspects	21
2.2.2	Probability density function (PDF) and central moments	23
2.2.3	Variability, uncertainty and error	23
2.3	Fuzzy Set Based Methods	25
2.3.1	Standard fuzzy arithmetic	25
2.4	Fuzzy Numbers Implementation	26
2.4.1	LR-fuzzy numbers	26

2.4.2	Discretization of the fuzzy numbers	29
2.5	Constrained Fuzzy Arithmetic	31
2.6	Implementation of the Transformation Method	32
2.6.1	General transformation method	33
2.6.2	Reduced transformation method	34
2.6.3	Applying the general transformation method for a simple one DOF system	35
2.6.4	Advantages and disadvantages of the transformation method	36
2.7	Summary	38
3	Efficient Fuzzy Set Based Methods to be Combined with SEM	39
3.1	Introduction	39
3.2	Transformation Method Removing Recurring Points	40
3.3	Fuzzy Set Method using Sparse Grids Interpolation	43
3.4	Estimating of Envelopes for FRF using SEM and Fuzzy Set Based Methods . .	49
3.5	Summary	52
4	Numerical Applications using the SEM Combined with Fuzzy Set Based Methods	53
4.1	Coupled Rods System	53
4.2	Plate with Reinforcements	54
4.2.1	Envelopes for FRF: coupled rods system	55
4.2.2	Envelopes for FRF: plate model	58
4.2.3	Error plots	58
4.2.4	Interpretation of the results	62
4.3	SEA Coupling Loss Factors Estimation	64
4.3.1	Case 1: Estimation of SEA CLFs for two coupled rods	64
4.3.2	Case 2: Estimation of SEA CLFs for frame-type structures	66
4.3.3	Estimation of CLFs using the SEM combined with the fuzzy method- <i>gtrmrecur</i>	71
4.3.4	Estimation of energies using the SEM with the fuzzy method- <i>gtrmrecur</i>	74
4.4	Summary	78

5	Initial Design Phase Considering a Non-Deterministic Dynamic Analysis	79
5.1	Describing our Example Problem	79
5.2	Dynamic Modelling of the Example Structure	80
5.2.1	Finite element model	80
5.2.2	Spectral element model	81
5.3	Non-Deterministic Input Data	82
5.3.1	<i>Uncertainty, variability and error</i>	82
5.4	Sensitivity Analysis: Degree of Influence of the Non-Deterministic Input Pa- rameters	86
5.4.1	Results using a sensitivity analysis	87
5.5	<i>Targets</i> during the initial design phase	89
5.6	Dynamic Behavior of the Reinforced Plate Model	89
5.6.1	Initial design requirements	89
5.6.2	Deterministic receptance response and <i>target</i>	90
5.6.3	Envelopes for the Receptance	91
5.6.4	Interpretation of the results	95
5.7	Summary	96
6	Concluding Remarks	97
6.1	Main contributions	98
6.2	Discussion for further research	98
6.3	List of Publications	100
	Bibliography	101
	Appendices	112
A	The Spectral Element Method	112
B	The Spectral Element applied to Rods	113
B.0.1	Dynamic stiffness matrix of a <i>throw-off</i> element	116
B.0.2	Application to two coupled rods	116
B.0.3	Numerical results: case 1	117
B.0.4	Numerical and experimental results	119

B.0.5	Numerical results: case 2	122
C	The Spectral Element applied to Beams	125
C.0.6	Dynamic Stiffness Matrix - Bernoulli-Euler beam <i>two nodes</i> element . .	126
C.0.7	Dynamic Stiffness Matrix - Bernoulli-Euler beam <i>throw-off</i> element . .	128
C.0.8	Numerical Example	129
D	The Spectral Element applied to Plates	132
D.0.9	Introducing the beam reinforcements on the plate element	136
D.0.10	Numerical results for a plate with reinforcements	137

List of Figures

2.1	Triangular membership function with standard deviation σ and mean value \bar{m} .	27
2.2	Triangular (a) and quasi-Gaussian (b) membership functions for a linear Young's modulus.	28
2.3	Symmetric fuzzy number of quasi-Gaussian shape expressed by their membership functions with mean value \bar{m} and standard deviation σ , <i>crisp</i> number c and closed interval $[a, b]$	29
2.4	Implementation of a fuzzy number \tilde{p} decomposed into intervals.	30
2.5	Decomposition scheme for the general transformation method for $m = 5$	34
2.6	Envelope FRFs for the one DOF system using the general transformation method. (a) envelope and nominal value, (b) zoom between 4.0 Hz and 6.0 Hz.	36
2.7	Degree of possibility for different α -cuts at $f = 5.25$ Hz. 2 α -cuts (solid), 5 α -cuts (dashed line) and 15 α -cuts (plus sign).	36
3.1	General transformation method and its recurring points (Klimke, 2003).	41
3.2	Sparse grid $H_{3,2}$ construction using Clenshaw-Curtis for 2D case.	46
3.3	Comparison for sparse grids: (a) $H_{7,2}^M$, (b) $H_{7,2}^{NB}$ and (c) $H_{7,2}^{CC}$	47
3.4	Sparse grids method: (a) original surface and (b) result using the interpolation.	49
4.1	Schematic of the coupled rods system.	54
4.2	Schematic diagram of the stiffened plate (units in meters).	54
4.3	Envelopes for FRF for the uncoupled rod system. (a) MC, (b) <i>rtrm</i> , (c) <i>gtrm-recur</i> , (d) <i>sparse grid</i> ; (i) full spectrum, (a,ii-iv) zoom for $N = 10, 100, 1000$, (b-c,ii-iv) zoom for $m = 2, 5, 17$ α -cuts, (d,ii-iv) zoom for level $n = 1, 3, 5$; (a,v) range of MC results depending on N at $f_{892} = 7796.4$ Hz, (b-d,v) fuzzy-valued result at f_{892} depending on m, n	56

4.4	Envelopes for FRF for the coupled rod system. (a) MC, (b) <i>rtrm</i> , (c) <i>gtrmrecur</i> , (d) sparse grid; (i) full spectrum, (a,ii-iv) zoom for $N = 10, 100, 1000$, (b-c,ii-iv) zoom for $m = 2, 5, 17$ α -cuts, (d,ii-iv) zoom for level $n = 1, 3, 5$; (a,v) range of MC results depending on N at $f_{867} = 3986.6$ Hz, (b-d,v) fuzzy-valued result at f_{867} depending on m, n	57
4.5	Envelopes for FRF for the plate system. (a) MC, (b) <i>rtrm</i> , (c) <i>gtrmrecur</i> , (d) <i>sparse grid</i> ; (i) full spectrum, (a,ii-iv) zoom for $N = 10, 100, 1000$, (b-c,ii-iv) zoom for $m = 2, 5, 17$ α -cuts, (d,ii-iv) zoom for level $n = 1, 3, 5$; (a,v) range of MC results depending on N at $f_{849} = 897.90$ Hz, (b-d,v) fuzzy-valued result at f_{849} depending on m, n	59
4.6	Error plots for the SEM combined with fuzzy set based methods and with MC: (a-b) uncoupled rod (c-d) coupled rod (e-f) plate case.	61
4.7	Energies for rods 1 and 2 performed by standard SEA and SEM.	67
4.8	CLFs performed by standard SEA and analytical expressions with Fuzzy - <i>gtrmrecur</i>	68
4.9	Nominal energy performed via standard SEA and energies by SEM combined with the fuzzy set based method- <i>gtrmrecur</i>	69
4.10	SE model for connected beams with arbitrary angle.	70
4.11	Estimation of CLFs using S&L approximation and their envelopes: (a) η_{B1B2} and (b) η_{B1L2} . SEM-nominal (solid), SEM with the fuzzy method- <i>gtrmrecur</i> (dotted-line) and SEM with MC (dashed +)	73
4.12	Estimation of CLFs using S&L approximation and their envelopes: (a) η_{L1B2} and (b) η_{L1L2} . SEM-nominal (solid), SEM with the fuzzy method- <i>gtrmrecur</i> (dotted-line) and SEM with MC (dashed +)	73
4.13	Energy levels for the beams 1 and 2 using CLFs estimated with SEM combined with fuzzy method- <i>gtrmrecur</i> : (a) Transversal energy in beam 1 and (b) Transversal energy in beam 2. <i>Max</i> and <i>Min</i> energies (dotted-line) and nominal energy (solid)	75
4.14	Energy levels for the beams 1 and 2 using CLFs estimated with SEM combined with the fuzzy method- <i>gtrmrecur</i> : (a) Longitudinal energy in beam 1 and (b) Longitudinal energy in beam 2. <i>Max</i> and <i>Min</i> energies (dotted-line) and nominal energy (solid)	75

4.15	Energy levels for the beams 1 and 2 using CLFs and power input estimated with the SEM combined with the fuzzy method- <i>gtrmrecur</i> : (a) Transversal energy in beam 1 and (b) Transversal energy in beam 2. <i>Max</i> and <i>Min</i> energies (dotted-line) and nominal energy (solid)	77
4.16	Energy levels for the beams 1 and 2 using CLFs and power input estimated with the SEM combined with the fuzzy method- <i>gtrmrecur</i> : (a) Longitudinal energy in beam 1 and (b) Longitudinal energy in beam 2. <i>Max</i> and <i>Min</i> energies (dotted-line) and nominal energy (solid)	77
5.1	Floor area with reinforcement applied in the automotive industry.	80
5.2	Scheme for the spectral element and finite element mesh for the reinforced plate: (a) SEM and (b) FEM.	82
5.3	Experimental data for the thickness h with respective histogram and quasi-Gaussian approximation adopted for membership function.	83
5.4	Uncertain parameter for the (a) internal loss factor $\tilde{\eta}$ and (b) force \tilde{P} for the reinforced plate model.	85
5.5	Degree of influence for the non-deterministic input parameters of the reinforced plate model.	88
5.6	Deterministic receptance response (solid line) at the drive point with the <i>target</i> (dashed line) proposed.	91
5.7	SEM- <i>deterministic</i> (solid), SEM combined with <i>gtrmrecur</i> using 3 α -cuts: envelopes (dotted line) and <i>target</i> value (dashed line).	92
5.8	SEM- <i>deterministic</i> (solid), SEM combined with <i>gtrmrecur</i> using 5 α -cuts: envelopes (dotted line) and <i>target</i> value (dashed line).	92
5.9	SEM- <i>deterministic</i> (solid), SEM combined with <i>gtrmrecur</i> using 9 α -cuts: envelopes (dotted line) and <i>target</i> value (dashed line).	93
5.10	Fuzzy-valued results for different number of α -cuts: at 84 Hz (a) and at 304 Hz (b) with 3 α -cuts (solid line), 5 α -cuts (dotted line) and 9 α -cuts (dash dot line).	93
5.11	SEM- <i>deterministic</i> (solid), <i>target</i> value (dashed line) and the improved version with $h = 5.5$ mm (dotted line).	94

5.12 SEM- <i>deterministic</i> improved version with $h = 5.5$ mm (dotted line), <i>target</i> value (dashed line) and the envelopes with 3 α -cuts (dash dot line).	94
B.1 Coupled rods system with axial force P applied to free end of uncoupled rod 1.	117
B.2 SE model for the coupled rods applied to case 1.	117
B.3 FRFs for the uncoupled rod 1: comparison of FEM (dashed) and SEM (continuous).	118
B.4 FRFs for the coupled rods 1 and 2: comparison of FEM (dashed) and SEM (continuous).	118
B.5 Comparison for the uncoupled rod 1 (continuous) and coupled rods 1 and 2 (dashed) using SEM.	119
B.6 Coupled rods experimental set-up.	120
B.7 Accelerometers in details.	120
B.8 Numerical (continuous) and experimental (dashed) results for the uncoupled rod case.	121
B.9 Numerical (continuous) and experimental (dashed) results for the coupled rods case.	121
B.10 Coupled rods system with axial force P applied at the middle of rod 1.	122
B.11 SEM model for the coupled rods applied to case 2.	122
B.12 FRFs for the uncoupled rod 1: comparison of FEM (dashed) and SEM (continuous)	123
B.13 FRFs for the coupled rods 1 and 2: comparison of FEM (dashed) and SEM (continuous).	123
B.14 Comparison for the uncoupled rod 1 (continuous) and coupled rods 1 and 2 (dashed) using the SEM.	124
C.1 Cantilever beam model.	130
C.2 SEM model applied to a Cantilever beam model.	130
C.3 Comparison of FEM (dashed) and SEM (continuous) results at the point mobility for the Cantilever beam model.	130
C.4 Comparison of FEM (dashed) and SEM (continuous) results at the end of the Cantilever beam model.	131
D.1 Scheme of image sources for two simply supported edges.	135

D.2	Equilibrium for a plate with an edge rigidly connected to a beam (Donadon et al., 2004).	136
D.3	Schematic diagram of the stiffened plate (units in meters).	137
D.4	Scheme of the spectral elements used in the model (Arruda et al., 2004).	138
D.5	Comparison of FEM (dashed) and SEM (continuous) results for the plate without reinforcements.	140
D.6	Comparison of FEM (dashed) and SEM (continuous) results for the plate in Fig.D.3 (Arruda et al., 2004).	141
D.7	Comparison of FEM (dashed) and SEM (continuous) results for the plate in Fig.D.3 with $\eta = 0.01$ (Arruda et al., 2004).	142

List of Tables

2.1	Coefficient of variation (ν) for same typical aerospace materials (Marczyk, 2004).	21
2.2	Coefficient of variation (ν) for same typical aerospace loads (Marczyk, 2004).	21
3.1	Comparison of the number of function evaluations in <i>gtrm</i> and in the <i>gtrmrecur</i> (Klimke, 2003).	42
3.2	Comparison of number of grid points for refinement level $n = q - d$ (Klimke, 2005).	47
4.1	Physical and geometrical properties of the coupled rods system.	54
4.2	Physical properties of the plate with non-deterministic input parameters.	55
4.3	Discretization parameters and approximation error for the simulation runs.	60
4.4	Physical properties: beams with non-deterministic input parameters.	70
5.1	Plate properties with non-deterministic input parameters.	86
B.1	Physical properties for rods 1 and 2.	117
C.1	Physical properties to the Cantilever beam model.	129
D.1	Physical properties defined to the plate.	138

List of Symbols

Greek letters

α	intervals of confidence, α -cut, levels
β	SEA parameter for modal factors
Δ	space, step, average half-power bandwidth of the modes
$\Delta_{p,i}$	average half-power bandwidth of the modes of subsystem i
ϵ	absolute error
η	internal loss factor
η_{ij}	coupling loss factor between subsystem i and j
θ	angular coordinate
λ	length of wave, eigenfunctions and eigenvalues
$\mu(x)$	membership functions
ν	Poisson's ratio
$\rho, \rho_i, \rho I$	mass density, measure of influence, rotational inertia
σ	standard deviation
τ	transmission coefficient used in SEA
ϕ, ϕ_1, ϕ_2	rotation, slopes
ξ	critical damping ratio
$\Psi(x)$	shape functions
Ω	universal set
ω	central frequency band

Latin symbols

A, B, C, D	frequency dependent coefficient
A	matrix of the energy influence coefficients (EICs), area
A_{n+d}	sparse grid interpolants
a, b, c	bounds of the interval
C	damping matrix
c	certain modes, damping, crisp numbers

Latin Symbols

c_{crit}	critical damping
c_g	group speed
c_o	longitudinal wave speed
D	dynamic stiffness, transverse displacement, dimension
d	problem dimension for sparse grid interpolation
E	elasticity Young's modulus, vector of subsystems energies
E_i	energy to subsystem i
EI_b	beam flexural stiffness
\hat{E}	complex elasticity Young module
F	vector of the generalized forces, function
F_0	concentrated driving force
\hat{F}	complex amplitude of applied force (frequency domain)
f	function, frequency
G	shear modulus
$GA\kappa$	shear stiffness for the beam element
GJ_b	torsional stiffness for the beam element
\hat{g}	frequency dependent rod shape functions
\hat{g}_i	element shape functions
H	inverse of the matrix of energy influence coefficients
h	plate thickness
I_b	moment of inertia of the beam
J_b	polar moment of inertia of the beam
K	stiffness matrix
$k, k_{1n}, k_{2n}, k_p, k_{yn}$	element defined into the array, wave numbers
\hat{k}_e	complex dynamic stiffness matrix for rod element
L	length of element
M	mass matrix, subsystem mass
M_x, M_{xy}	moment
m	segments of interval, levels of membership, modal overlap
\bar{m}	mean value
N	number of propagation modes and function evaluations
n	modal density, uncertain parameters, random variable
P_{coupl}	coupling power
P_{diss}	dissipated power
P_{in}^i	input power from external loading
\tilde{p}	fuzzy numbers
Q	Fourier transform of $q(t)$ and $f(t)$
$q(t)$	vector of co-ordinates (time domain)
$q_v(x, t)$	transverse load (time domain)
\tilde{q}	fuzzy-valued response

Latin Symbols

q_ϕ	distribute torque (time domain)
$q(x, t)$	extern force (time domain)
R_{min}, R_{max}	reference solutions to compute error analysis
s	discrete steps, different entries
$T, T_{kinetic}$	vibration energy, rod average kinetic energy
t	time domain, size of the array
u	uncertain modes
$\hat{u}(x)$	vector of the complex amplitude node displacement
V_x	shear force for the plate element
v	velocity
\hat{v}_i	displacement for the beam spectral element
$w(x, y)$	transverse displacement of the plate
X, \hat{X}	interval definition, arrays defined in fuzzy arithmetic
x	co-ordinate system
y	co-ordinate system
y_0	position of the concentrated driving force
Z, \hat{Z}	impedance, interval definition, arrays (transformed form)

Operations

$ $	absolute value
$()^*$	complex conjugate
$\langle \rangle$	ensemble average
$E[]$	mathematical expectation
$\Im()$	imaginary part
$\Re()$	real part
$()^T$	transpose of the matrix
\mathcal{O}	order of operations
∇^2	differential operator, $\frac{\partial^2}{\partial x^2} + \frac{\partial^2}{\partial y^2}$
\cdot	dot, time derivative
$'$	derivative
$\hat{}$	frequency domain (transformed) quantity
\sim	wavenumber domain, fuzzy numbers, fuzzy-valued response
i	$\sqrt{-1}$, imaginary number
\setminus	set minus
\emptyset	empty set
\subset	subset

Subscripts

c, d, i, j, k, p, u indices adopted for fuzzy set methods and SEA equations

Superscripts

i, j, k, m, n indices adopted for fuzzy set methods and SEA equations

Abbreviations

BEM	Boundary Element Method
CAD	Computer Aided Design
CAE	Computer Aided Engineering
CLF	Coupling Loss Factor
CMS	Component Mode Synthesis
COV_P	Desired Coefficient of Variation of Probability of Failure
CV	Coefficient of Variation
DLF	Damping Loss Factor
DOF	Degree of Freedom
EIC	Energy Influence Coefficient
FE	Finite Element
FEA	Finite Element Analysis
FEM	Finite Element Method
FRF	Frequency Response Function
FWA	Fuzzy Weighted Averages Algorithm
GFN	Gaussian Fuzzy Numbers
$gtrm$	General Transformation Method
$gtrmrecur$	General Transformation avoiding recurring permutations
$rtrm$	Reduced Transformation Method
HFE-WBM	Hybrid Finite Element - Wave Based Method
LR	Left and Right Fuzzy Numbers
LM/P	Local Modal Perturbation Method
MC	Monte Carlo
MCA	Monte Carlo Analysis
MDOF	Multiple Degree of Freedom
PIM	Power Injection Method
QGFN	Quasi-Gaussian Fuzzy Numbers
RAND	Pseudo-Random Number Generator in MATLAB
SEA	Statistical Energy Analysis
SEM	Spectral Element Method
TFN	Triangular Fuzzy Numbers
WBM	Wave Based Method

Chapter 1

Introduction and Motivation

Even the most accurate Finite Element (FE) model of a structural dynamic system is just a representation of a nominal structure. In this context, several similar structures taken out of the production line will exhibit variations on all of these individual properties and this dispersion will reflect in the global response of the structure. Small changes in the physical properties of the structure can directly affect the results, and the prediction error can increase with frequency (Kompella and Bernhard, 1993).

The above statement summarizes one of the main challenges in adopting numerical models to cover the full range of structural dynamic analysis response. To date, much research has been done towards improving the numerical models, hence towards achieving full spectrum response. However, deterministic models, such as the finite element (FE) and the boundary element (BE) methods, have limitations at higher frequencies due to the necessity of refining the mesh, whereas analytical methods, such as the spectral element (SEM) are less sensitive to the higher wave-numbers.

In terms of wavelength, it is well known that to achieve sufficient agreement between numerical and analytical solutions, 6 to 10 linear elements per wavelength are necessary to keep the prediction error within acceptable limits (Desmet, 2002). Experience shows that, as the frequency range increases, the structure becomes very sensitive to small uncertainties in material properties and geometrical details. Additionally, the high order modes of vibration also tend to have more complex spatial fluctuations. As a result, the size of the finite element model increases with frequency (Shorter, 1998). Therefore, in terms of a frequency response function (FRF), the response of the structure is not adequately predicted, and it is more convenient to predict the frequency averaged response in terms of the energy (Lyon and

DeJong, 1995).

In order to address the limitation described above, probabilistic techniques have been proposed. In this case, the Statistical Energy Analysis (SEA) has been considered the most applicable modelling strategy (Lyon and DeJong, 1995). SEA is a procedure for calculating the flow and storage of dynamical energy in complex systems. It is a sub-structuring technique where the response in each subsystem is the space averaged, mean-squared vibration (or sound pressure) level within a given frequency band. In this methodology, the main focus is to describe the dynamic response in terms of the space averaged energy response levels for each subsystem. As it is normally the case when such assumptions are made, the accuracy of the model response depends on the validity of these assumptions. For instance, a simple look at one of the main assumptions in SEA, i.e., high modal density in the frequency range of interest, leads to the result that, at lower frequencies ranges, the accuracy of the SEA becomes questionable (Desmet, 2002).

Considering the above, it appears that there is a gap in the mid-frequency range, above the range of applicability of deterministic methods and below the frequency range where SEA is applicable. Research is under way to try to address this problem. Many papers have been published combining deterministic and statistical methodology. In this context, four different methods have emerged: the Energy Influence Coefficient (EIC), also called the Energy Flow Method, the Virtual/Experimental SEA, the Hybrid FEA/SEA and the Wave Based Method (WBM). There are, however, disadvantages that restrict the applicability of the methodologies proposed above. See, for instance, (Zhang et al. (2003), Gagliardini et al. (2003), Langley and Bremner (1999), Desmet (2002)).

To overcome some of the above drawbacks, the present work proposes a Spectral Element Method (SEM) combined with fuzzy set based methods, in order to address the frequency response function envelopes in the mid-frequency range applied to dynamic structural problems. See for instance Nunes et al. (2004ab).

1.1 Alternatives based on the FE method

This section intends to present some relevant aspects and possible improvements achieved with FE modelling methods. According to Zienkiewicz (2000), the short wavelength dynamic problems are among the currently unsolved problems of the FE method, which means the FE dynamic analysis is restricted in practice to low frequency applications (Desmet, 2002).

Considering the limitations of the FE method, other alternatives to the conventional FE method have been proposed. In what follows, some important aspects of the dynamic model reduction technique, the hierarchical FE, and the sub-structuring method, with special attention to the Component Mode Synthesis (CMS), are discussed. In addition, the Monte Carlo simulation is also presented.

1.1.1 Dynamic reduction

In several practical engineering problems, dynamic reduction can be considered an option to reduce the number of degrees of freedom (DOF) in a dynamic model. Broadly speaking, the main idea is to work with small matrices, where the original dynamic characteristic of the model is maintained.

Basically, two methodologies dominate: the static condensation and the generalized dynamic reduction. The first one is also called the Guyan Reduction approach, which considers a partition of the global DOF into master and slave DOF (Bathe, 1996). The procedure is done defining two sets which contain master and slave DOF, respectively. In this case, a set defined as master DOF is retained and the remaining set which contains the slave DOF is removed by using condensation process. In such a case, during the condensation, only stiffness properties are taken into account; inertia coupling of master and slave nodes are simply ignored. Following that, the eigenvalue problem can be solved considering the master DOF by adopting a coordinate transformation (Bathe, 1996).

In comparison to the Guyan reduction, the generalized dynamic reduction can be shown to be more accurate, which can be explained by the fact that dynamic effects are taken into account during the transformation process, i.e., by using the coordinate transformation (Bathe, 1996).

1.1.2 Hierarchical FE

To improve the accuracy of the FE method, adaptive strategies, such as the h -, p - and hp -method have been proposed.

In the h -version, the method is applied to refine the mesh of the FE model. This case, which has been implemented in many commercial FE codes, the convergence is achieved by adopting small elements, which increase the mesh refinement. This version is based on elements with low-order polynomials that can be used to describe the displacement field

(Zienkiewicz and Taylor, 1989). According to Babuska et al. (1981) and Zienkiewicz et al. (1983), the *h-version* is appropriate for treating problems in the low frequency range, however less so for medium and high frequencies.

In order to address the limitation of the *h-version*, the *p-version* of the FE has been proposed. See for instance: Meirovitch and Baruh (1983), Babuska et al. (1981), Zienkiewicz et al. (1983). The idea is to increase the order of the polynomial shape functions considering a fixed mesh. According to Zienkiewicz and Taylor (1989), the *p-version* converges more rapidly per DOF introduced.

Nowadays, the *h* and *p-versions* have also been applied simultaneously to increase the frequency range of FE analysis. The method, called *hp-version* of the FE is constructed based on higher order finite elements and refined meshes to address the dynamic response for higher frequency application (Langley and Bardell, 1998).

Behind the idea of the hierarchical methods or adaptive strategies is the ability to achieve the optimal polynomial function order for each element within the mesh. Nevertheless, in most cases, polynomial functions are ill-conditioned. West et al. (1997) concluded that in *h-p* applications, one has to restrict the degree of polynomial enrichment to: (1) 24 or less in 1-D applications, (2) 14 or less in 2-D applications, and (3) 8 or less in 3-D applications. In this case, the *p-version* application is drastically limited. In order to address this problem, Leung and Chan (1998) have suggested the use of products of polynomials and Fourier series, instead of polynomials alone in the *p-version*. In that work, the Fourier *p-element* shape functions are applied to the analysis of beams and plates and the limitation observed in the *p-version* with the polynomial functions is overcome.

In addition, there are several works with application of the *h-* and *hp* methods to address the acoustic Helmholtz problems. The adaptive techniques might be also applied with high computational efficiency to more challenging problems, such as those involving fluid/structure coupling. However, according to a recent review by Desmet (2002), there has not yet been an application to industrial problems.

1.1.3 Component Mode Synthesis (CMS)

Consider now a large system to be analyzed with an FE dynamic analysis. One alternative to solve the FE dynamic problem is to split up the global system into small additional subsystems, and to perform local analyses on those components or subsystems, which represent

the global system as whole. Such a procedure is called Component Mode Synthesis, and can be adopted in FE analysis to reduce the size of a model (Craig, 1995).

The Component Mode Synthesis (CMS) was introduced by Hurty in 1965. The idea behind this method is to adopt individual substructures to describe the global behavior of a structure. In such an approach, the size of the global model can be drastically reduced in performing the structural dynamic FE analysis. The synthesis of the model as a whole is carried out by imposing continuity of co-ordinates at interfaces nodes.

In order to perform the synthesis of a model, two basic methods have been proposed: the fixed-interface methods and the free-interface component mode methods (Craig, 1995).

In the fixed-interface methods, which adopt normal modes of the components with fixed boundary conditions at interfaces nodes, a general improvement of the characteristics of convergence can be achieved. This can be done by using constraint modes, which are defined as the shapes of the deformed substructure when a unit displacement is applied to each interface DOF with the other interface DOF fixed (Craig and Bampton, 1968).

In the free-interface mode method the modal basis must be enriched with the so-called attachment modes. This approach is used only when experimentally obtained modes are used in the synthesis. Otherwise, in most FE modelling applications, including commercial codes, the fixed-interface methods are preferred (Craig, 2000).

1.1.4 Monte-Carlo Simulation

Even considering the possibility of extending the frequency range of application of the FE methods, the computational time becomes in most cases prohibitive. Moreover, the wavelength of interest becomes smaller, which leads to the model becoming very sensitive to small perturbations in the properties. This is one of the main problems in the deterministic methods. Such a problem is concerned with the uncertainties in the properties of the system, which are not taken into account in FE deterministic modelling.

In practical engineering problems, most real models possess some kind of uncertainty, such as in domain geometry, material properties or even loads which are not known for certain. In fact, another possibility is that uncertainty can also be considered due to a lack of knowledge.

The amount of research in this area and also the interest in new methodologies has been increased. One possibility is to adopt updating techniques, where a conventional FE model is used with measurement data. In such an approach, the FE models are compared with

experimental data and the simulation results must be matched to the measurements. This technique allows to increase the accuracy of the FE prediction with respect to one particular realization of the structure, but does not improve the representation of the statistics of the predicted response (Shorter, 1998).

Another possible way to describe the uncertainty parameters may through the use of approximate methods. For instance, in a Monte-Carlo simulation, the global structure is described in terms of sample individual structures, which can be used to achieve the statistical information responses. Monte Carlo simulation is considered a stochastic technique, when used to solve mathematical problems in general. The word *stochastic* means that it uses random numbers and *probability statistics* to obtain results. Monte Carlo methods were originally developed for the Manhattan Project during World War II. However, this technique has found application in many fields, such as stock market, forecasting, biology, etc. Regarding the name *Monte Carlo*, it originated from the city Monte Carlo in Monaco, whose main attractions are casinos and gambling. In a fashion similar to gambling, Monte Carlo simulations use a random selection process which is repeated many times to create multiple scenarios for the proposed problem. Each time a value is randomly selected, it forms one possible scenario and solution to the problem. Taking all scenarios together gives a range of possible solutions, some of which are more probable, and others less so. It is clear that for many scenarios, say 10,000 or more, the average solution will give an approximate answer to the problem. Naturally, to improve the accuracy of this answer, more scenarios should be used.

In terms of practical application, unfortunately, due to the number of members to be sampled and the number of samples to perform the statistical responses, the use of the Monte Carlo approach can be prohibitive. For more details on Monte Carlo simulation, please refer to Huber (1999) and Klieber and Hien (1992).

Thus, the Monte Carlo approach is usually associated with methods to reduce the computational burden of the FE dynamic model, such as model reduction methods and the response surface methods.

1.2 SEA Method

Before developing deeper into the medium frequency review, an introduction to the Statistical Energy Analysis (SEA) will be given. Following that, some important developments achieved for mid-frequency range application is presented.

1.2.1 Statistical Energy Analysis (SEA)

Statistical Energy Analysis (SEA) is a technique that is suited for the study of sound and vibration transmission through complex structures at high frequency range. SEA has been proposed to address the limitations of deterministic approaches, such as FE, which in the high frequency range becomes very sensitivity to small changes in the structural model. On the other hand, the number of DOFs required to describe the high frequency behavior becomes excessive in terms of computational resources and computing power.

In the SEA application, in contrast to deterministic approaches, the average value of an energy response over the frequency band is the main issue. In this case, the description is statistical, which means that the systems being studied are presumed to be drawn from populations of similar design construction having known distributions of their dynamical parameters (Lyon and DeJong, 1995).

SEA is a procedure for calculating the flow and storage of dynamical energy in complex systems. It is a sub-structuring technique where the response in each subsystem is the space averaged energy, mean-squared vibration (or sound pressure) level within a given frequency band.

In the SEA methodology, a system is subdivided into subsystems where the main attempt is made to predict the time and space average energy within a subsystem. The idea is to estimate the power in each subsystem by taking into account the input power acting on each subsystem and the coupling power which flow from one subsystem to another (Mace, 1993). This fact leads to a power balance equation, which is the basic fundamental equation of SEA, defined as

$$P_{in}^i = P_{diss}^i + P_{coup}^i \quad (1.1)$$

where P_{in}^i is the input power from external loading to the system i , P_{diss}^i is the dissipated power, due, for instance, to internal damping, radiation, etc and the P_{coup}^i is the coupling

power flowing from subsystem i to all the other connected subsystems.

The dissipated power can be related to the subsystem energies E_i by considering the following expression

$$P_{diss}^i = \Delta_p^i E_i \quad (1.2)$$

where Δ_p^i is the average half-power bandwidth of the modes of subsystem i .

As described above, the primary interest in the SEA method is to assess the ensemble energy response, which can be done by averaging across the ensemble as follows

$$\langle P_{in}^i \rangle = \langle P_{diss}^i \rangle + \langle P_{coup}^i \rangle \quad (1.3)$$

The symbol $\langle \rangle$ indicates the ensemble average, which means the variable is an appropriate representation of the ensemble member. Now, considering that Δ_p^i is constant across the ensemble leads to

$$\langle E_i \rangle = (\langle P_{in}^i \rangle - \langle P_{coup}^i \rangle) / \Delta_p^i \quad (1.4)$$

According to Eq.(1.4) the main problem is to assess the coupling powers. However, there are several assumptions which are generally made in the development of SEA models. One of them is that the ensemble average coupling energy flow from subsystem i to subsystem j is related to the ensemble average subsystem energies by (Mace, 1993)

$$\langle P^{ij} \rangle = \omega \eta_{ij} \left\{ \langle E_i \rangle - \frac{n_i}{n_j} \langle E_j \rangle \right\} \quad (1.5)$$

where η_{ij} is the Coupling Loss Factor (CLF), and is defined as a constant independent of the levels of the excitation applied to the individual subsystems. Also, the following terms, defined as n_i and n_j , are respectively the asymptotic modal densities of the subsystems and ω is the central frequency band of the problem considered. According to SEA assumptions, the coupling power between subsystems i and j is proportional to the difference in the average modal energies of subsystems i and j , which leads equation (1.5) to be rewritten as follows

$$P^{ij} = \omega n_i \eta_{ij} \left(\frac{E_i}{n_i} - \frac{E_j}{n_j} \right) \quad (1.6)$$

The assumption of proportional coupling power has been discussed in several papers, which is known to be exact for two coupled oscillators, as described by Lyon and Maidanik

(1962) and also considering broadband excitation described by Lyon and Eicher (1964). In addition, Scharton et al. (1968) presented the power flow sharing in random vibration. In that work, they show that the coupling power proportionality between two oscillators holds for any strength of coupling, considering the energy of the oscillator system. Other works have shown that coupling power proportionality holds for general dynamic systems provided weak coupling is considered (Langley (1989), Langley (1990)). In this context, other alternatives have been proposed in the literature for estimating coupling loss factors, such as the wave approach in which the effects of reflections are not considered (Mace (1992), Mace (1994)). Several authors have proposed the use of FE to assess the coupling loss factor, which in this sense leads to a new approach called FEA/SEA methodology. This approach will be discussed in the next section.

In addition to SEA assumptions, it is assumed that the input power spectra are broadband, which means that there are no strong pure tones in the input spectra. In this sense, white noise excitation uniformly distributed spatially over the structure surface is adopted, the so called *rain-on-the-roof* excitation. Another hypothesis is that the Damping Loss Factor (DLF) is equally distributed for all modes within a subsystem and in the frequency band proposed. The SEA method assumes that energy is not created in the coupling between subsystems. Energy can be dissipated in junctions between subsystems, such as in isolation mounts. The SEA method considers that the effect of isolation is generally added to subsystem DLF. Modes within a subsystem do not interact except to share an equipartition of energy.

Following the original idea proposed by Lyon and Madanik (1962), much research has been done in this area to improve the conventional SEA, as well as to address the main limitations of this methodology. Additional information can be found, for example, in (Fahy, 1994) and (Fahy, 1993), where a critical overview of the limits of SEA following the assumptions used to derive the power balance is presented.

In this context, there are several areas where SEA should be improved, such as application to the strong coupling instead of just weak coupling system application, non-conservative coupling, the applicability of SEA to the low frequency range and also to address correctly the mid frequency range, where SEA assumptions are not well fulfilled.

In addition, however, in the same context, Langley and Cotoni (2003), Langley et al. (2003), Langley and Brown (2002) presented a method to predict the variance of the energy levels in built-up systems. The idea is to predict not only the mean energy of each subsystem,

but also the higher order statistics, such as the variance. In both works, expressions for predicting the variance of energy levels in a built-up system are presented. Additionally, Lyon and DeJong (1995) in a previous work, have also discussed this possibility for built-up systems.

1.3 Developments in the Mid-Frequency Range

In this section, some recent developments achieved in the mid-frequency range are discussed. Considering the discussion from the former sections, one can note that the Statistical Energy Analysis has been established as a powerful technique for addressing dynamic problems in the high frequency range. The Finite Element Analysis (FEA) has been considered as a standard methodology to assess problems in the low-frequency range. Both techniques work well in their respective frequency ranges. It has also been pointed out the former sections that to extend the applicability of SEA and FEA methods, i.e., SEA for low and mid-frequency ranges and FEA for mid-high frequencies, some theoretical and numerical restrictions are found.

To address some of these limitations, in this section four separate methods have been chosen for review: the Virtual/Experimental SEA, the Energy Influence Coefficient (EIC), the FE/SEA Hybrid and the Wave Based Method (WBM).

1.3.1 Virtual/Experimental SEA

In the proposed Virtual/Experimental SEA, the FE model is adopted to predict the CLFs instead of using experimental measurements. In this approach, the Frequency Response Functions (FRF) are computed for a very fine FE structural model to allow the FE to be applied to the medium frequency range.

In this methodology, the first question that arises is why one should not apply directly the FE analysis to assess the full spectrum dynamic response. First of all, in a realistic structure, the responses in the medium and high frequency range are very sensitive to the physical material uncertainties. (See for example the Monte-Carlo simulation described in a previous section). Secondly, to assess the response of such structure in the medium and high frequency ranges, the energy response is a more convenient way to understand the structure-borne

problem. In this regard, as described in Lyon and DeJong (1995), the computer programs used to evaluate mode shapes and frequencies directly are known to be inaccurate for higher order modes.

The concepts of the Virtual/Experimental SEA was applied recently to the floor of a minivan, where an automatic sub-structuring process was proposed to optimize the model identification (Gagliardini et al., 2003). In their work, computed energetic transfer functions based on an FE model are compared with measurement data. Very similar results are found for the structure proposed, which is represented by four sub-systems (Gagliardini et al., 2003). To find the energetic transfer functions, uniform structural damping is taken into account in the FE model, which for a SEA model the definition is applied as a Damping Loss Factor (DLF). Additionally, they also propose that the squared transfer function due to the variance among input power is considered small, which in practical terms, means more information about the dynamic behavior of the structure response (Gagliardini et al., 2003).

Going further, they also proposed an automatic sub-structuring process, where after all energetic transfer mobility functions have been performed, the size of the database is compressed to add in the SEA model. The next step involves an inverse SEA process, which makes use of the sub-systems defined in a substructure process and SEA parameters identified. The CLFs are found considering a balance of energy for a unit power.

In contrast to traditional Experimental SEA, in the Virtual/SEA, an equivalent mass is adopted before the computation of the CLFs is carried out. During this process, some values of the CLFs can be identified negative. In practical terms, it is indicate that the coupling sub-systems estimated is not physical. Alternatives to address this problem have also been proposed, considering a least square problem with multiple excitation points defined in a structure (Gagliardini et al., 2003).

One of the main disadvantages of this technique is related to the strong coupling, which is not considered in this approach. In terms of computational time, many commercially available codes provide efficient schemes for improving the solution of the FE analysis. See for instance, the Automatic Component Mode Synthesis (ACMS) available in the MSC.NASTRAN (2004ab).

1.3.2 Energy Influence Coefficient (EIC)

The Energy Influence Coefficient (EIC) method has been proposed for dynamic structural analysis in the mid and high frequency range. The theory is based on the power injection method, in which the structure is discretised into a number of subsystems. The energy response is performed considering spatially incoherent *rain-on-the-roof* excitation, e.g., spatially uniform distributed white noise is applied. The methodology described is also called the Energy Flow Method, perhaps a more common name adopted in the literature. See for instance, Mace and Shorter (2000). Basically, the main difference between the EIC and the Virtual/Experimental SEA is that the EIC is based on exact expressions for the energies and input powers, instead of estimating them using Frequency Response Functions (FRFs).

In terms of mathematical description, the linear system can be described as

$$E = AP_{in} \quad (1.7)$$

where E is described as a vector of subsystem energies, i.e., the potential and kinetic energies of various responding subsystems, P_{in} is a vector of input powers, and the matrix A represent the energy influence coefficients (Mace and Shorter (2000)).

Eq.(1.7) can be written in inverse form, which leads to

$$P_{in} = HE \quad (1.8)$$

where in this case $H = A^{-1}$. In the EIC method, the matrix A is assumed to be defined; if A is a singular matrix, then H is undefined. In this case the response becomes independent of the particular subsystem to which the power is applied and the energy is equipartitioned (Shorter, 1998).

Considering that the matrix A is defined, as well as conservation of energy, the input power can be written as sum of the dissipated and coupling powers, which leads to

$$P_{in} = P_{diss} + P_{coup} \quad (1.9)$$

where P_{diss} and P_{coup} are, respectively, vectors which represent the dissipated and coupling power for each subsystem.

Assuming next that the system to be analyzed is lightly damped and the potential and kinetic energies are equal, and the coupling is also conservative, the following expressions can

be defined according to Lyon and DeJong (1995)

$$P_{diss} = \omega\eta E \quad (1.10)$$

$$P_{coup} = [H - \omega\eta]E \quad (1.11)$$

The net coupling power can be treated as a linear combination of the subsystems energies, which can be defined as

$$P_{coup} = \sum_{j \neq i} P^{ij} \quad (1.12)$$

where P^{ij} defines the coupling power between subsystem i and j . Eq.(1.12) enables the CLFs (Coupling Loss Factors) to be determined in terms of subsystem energies.

Recently, this method was proposed and implemented in a commercial code MSC Nastran (Zhang et al., 2003). The description of this implementation and some details concerning the bulk data cards and additional case control cards are also discussed in Zhang et al. (2003). One important point to add is that the EIC is currently restricted to groups of plate and shell elements, and is also computationally expensive for large models. Another inherent problem is that the method requires that the entire matrix of CLFs be performed as a new design is proposed, which is unfeasible for some applications.

With regard to advantages and disadvantages of the EIC, two main concerns can be addressed. The first is that the EIC does not provide any kind of sub-structuring process, which is considered one of the most critical points to identify a SEA model. Second, the EIC technique provides an exact value of energy into the subsystems, i.e., it does not take into account uncertainties in the properties, which can be also considered as a deterministic one.

1.3.3 FEA/SEA Hybrid Method

The equations of motion for the discrete multi-degree-of-freedom (MDOF) model of a continuous system formulated using Lagrange-Rayleigh-Ritz theory are now considered (Meirovitch, 1986). In this approach, the response can be expressed in terms of a complete set of admissible functions. The continuous systems can be generated in terms of shape functions $\Psi(x) = (\Psi_1, \Psi_2, \dots, \Psi_N)$, $x = (x_1, x_2, x_3)$ and generated coordinate expressed by

$q(t) = (q_1, q_2 \dots, q_N)^T$, which in terms of the displacement field $u(x, t) = (u_1, u_2, u_3)$ is then written in the following form

$$u(x, t) = \sum_{n=1}^N q_n(t) \Psi_n(x) \quad (1.13)$$

It is well know that, the equations of motion applied to Lagrange's equation which govern the amplitude q is expressed in the form

$$M\ddot{q}(t) + C\dot{q}(t) + Kq(t) = F(t) \quad (1.14)$$

where M , C , and K are the mass, damping and stiffness matrices, and the vector F contains the generalized forces. In this approach, the mass, damping and stiffness matrices are determined as a function of the shape functions, which are based on a variational formulation of the governing partial differential equation. Additionally, the mass and the stiffness matrices are assumed to be positive definite, the damping matrix is symmetric, i.e., $M = M^T$, $K = K^T$ and also $C = C^T$.

In terms of the frequency domain solution, applying a Fourier transform, the following expression can be expressed

$$DQ = F \quad (1.15)$$

$$D = -\omega^2 M + i\omega C + K \quad (1.16)$$

where D is the dynamic stiffness matrix of the system and Q and F the respectively Fourier transform of $q(t)$ and $f(t)$. In general, the basic formulation described above is adopted in FE to predict the modal parameters, described in terms of eigenfrequencies and eigenmodes or mode shapes.

As described in former sections, it is well know that FE is able to predict structural response of a model in the low frequency range. However, in the high frequencies, some errors can be expected compared to measurement of a real structure data. One of the expected errors is caused by uncertainties present in the physical material properties, which in terms of FE response functions becomes very sensitive as the frequency range increases. On the other hand, another distinction can be made between modal responses, which can be performed with sufficient accuracy and others that cannot be accurately predicted (Langley and Bremner,

1999). In this context, the equation of motion described can be partitioned into sets which contain *certain* and *uncertain* modes, or, respectively, *global* and *local* as shown below

$$u(x, t) = \sum_{j=1}^{N_c} q_j^c(t) \Psi_j^c(x) + \sum_{j=1}^{N_u} q_j^u(t) \Psi_j^u(x) \quad (1.17)$$

Eq.(1.17) can be also partitioned as follows

$$\begin{bmatrix} D_{cc} & D_{cu} \\ D_{uc} & D_{uu} \end{bmatrix} \begin{bmatrix} Q^c \\ Q^u \end{bmatrix} = \begin{bmatrix} F^c \\ F^u \end{bmatrix} \quad (1.18)$$

In a more convenient form, Eq.(1.18) can be rewritten in the following form

$$(D_{cc} - D_{uu} D_{uu}^{-1} D_{cu}^T) Q^c = F^c - D_{cu} D_{uu}^{-1} F^u \quad (1.19)$$

$$D_{uu} Q^u = F^u - D_{cu}^T Q^c \quad (1.20)$$

Following that, the global equation of motion which contain the response of the *certain* modes is described by Eq.(1.19) and the response of the *uncertain* modes is described by equation Eq.(1.20). The solution of this approach is that equation Eq.(1.19) may be solved by FEA, while Eq.(1.20) is based on the SEA approach. This approach has been called the Hybrid FEA/SEA method, which adopts a combination of FE and SEA methodologies in a rigorous way to describe the full structural dynamic response of a system.

In additional, as described in Eq.(1.19), the dynamic stiffness matrix and global forcing vector must be modified. FE is adopted to solve the long wavelength global behavior, while the short wavelength local behavior is modelled statistically using SEA in Eq.(1.20).

Since Langley and Bremner in (1999) proposed this approach, much progress in this area has been seen, see for instance Shorter and Langley (2004) in a recent work that they demonstrated some numerical and experimental validation of this method.

In terms of advantages of such a technique, the concept of the hybrid method is based on the development of junctions which can be used to couple the FE and SEA subsystems. In terms of a solution of a given structure-borne problem, FE is adopted to model the local junction details, i.e., only the stiff parts described into the model are taken by account in a deterministic manner. In terms of computation resource, this can be consider an advantage, since the short wavelength subsystems are not treated using a FE method.

Some disadvantages of this methodology are that the approach must be modelled by FE or SEA subsystems, which for some complex structure models can not be easily established, or it may be difficult to identify the in-plane response for the subsystem. In such cases, one way out is to model the entire system with FE in order to check the response of the system modelling. In addition, the proposed method is currently restricted to point and line junctions between the FE and the SEA subsystems, which in terms of practical application, can be also considered a limitation as a whole.

1.3.4 Wave Based Method (WBM)

The Wave Based Method (WBM) has been developed in the KULeuven-Noise and Vibration Research group. In this methodology, an indirect Trefftz approach has been adopted. The idea is to express the entire domain in terms of a wave function, which represents the homogeneous solution of the governing dynamic equation (Desmet, 2002). The Trefftz approach was introduced in 1926 as an alternative to the Rayleigh-Ritz method. In contrast to the FE method that adopts polynomial shape functions for field variable expansion, the Trefftz method adopts exact solution functions of the governing partial differential equations. For instance, the Spectral Element Method (SEM) has also been proposed, which combines the Trefftz and the element method approaches of the FE method (Doyle, 1997).

In this context, Desmet (2002) has developed an alternative method for dynamic analysis called the Wave Based Method (WBM). The technique proposed, which adopts an indirect Trefftz approach, has been applied for many vibro-acoustic problems; see for instance Hepberger et al. (2002) and Van Hal et al. (2002).

The use of the WBM has been suggested as an alternative for the FE method, which for comparison has been shown to converge better than the FE method. The WBM was also applied to the mid-frequency range, where better convergence and improvements compared to the FE method were found (Hepberger et al., 2002).

The main disadvantages of the WBM is that the system matrix cannot be decomposed in frequency independent matrices due to the implicit frequency dependence of the wave functions. Also, the fully populated and complex matrix are defined in the entire continuum domain (Desmet, 2002).

In general, the WBM has been shown to be a promising technique for addressing the problem in the mid-frequency range. Also, some hybrid alternatives using WBM coupled with

element based models have been proposed (Hal et al., 2004). In this paper, they developed the so-called hybrid finite element - wave based method (HFE-WBM), which the main idea is to take the advantages and efficiency of each method. In addition, to show the potential applicability of the HFE-WBM, they applied such a technique for a test problem comparing the FEM with the WBM applied separately. Basically, they concluded that, for higher frequency range, the HFE-WBM is more accurate than FEM. However, due to the irregularity shape of the cavity proposed, the FEM provides better and more accurate results in the low frequency range. Therefore, future research in this area should be done to improve the accuracy of the proposed method as a whole.

1.4 Thesis Outline

In Chapter 2, methods to address the influence in the uncertain parameters to the dynamic analysis are discussed. A review of this area is presented for the probabilistic and fuzzy set based methods. As the main subject of this thesis, special attention is drawn to the fuzzy set based methods. The so-called transformation method is introduced in its original version. Additionally, some important aspects to be improved with the general transformation method are discussed.

In Chapter 3, efficient alternatives to be implemented with fuzzy set based methods are presented, such as the transformation method implemented via multi-dimensional arrays and avoiding recurring permutations. Likewise, the sparse grids interpolation method is also suggested as an efficient alternative to be combined with the SEM.

In Chapter 4, the Spectral Element Method (SEM) combined with fuzzy set based methods is applied for selected test problems. Numerical examples adopting the reduced, general transformation method avoiding recurring permutations and the sparse grids interpolation method are treated for the case of two connected rods, as well as for a reinforced plate, which are compared with Monte Carlo simulation. For SEA applications, numerical tests covering the SEA coupling loss factors (CLFs) estimation are also proposed.

In Chapter 5, the SEM combined with a fuzzy set based method called general transformation method avoiding recurring permutations or simply called SEM combined with *gtrmrecur* is applied to a typical engineering problem. In this regard, a reinforced plate modelled by SEM is proposed. One important thing to add is that, due to present development stage of the SEM, the numerical example suggested here consists only of a simply supported plate with reinforced beams. The main focus in this chapter is to show that such a method can be successfully applied for some specific engineering problems, especially during the initial design phase, where, in general, little information is available.

In Chapter 6, the main conclusions and contribution achieved in this thesis are discussed. Following that, some additional areas that can be used as future research are proposed.

At the end of this work, to give a review of the SEM, including rod, beam and plate elements, Appendices A, B, C and D are presented. In this sense, the main advantage of the SEM and the applicability to the medium frequency range analysis is discussed. Additionally, examples adopting rod, beam and plate elements are presented and compared with FEM.

Chapter 2

Dynamic Analysis of Structures for Design Under Uncertainty

Many alternative methods that address the influence of uncertain parameters in dynamic analysis have been discussed in literature. In general, probabilistic and fuzzy set based methods have been suggested. As discussed in the former chapter, one of the main challenges in using deterministic approaches, such as FE, BE or SE methods, is to consider the influence of non-deterministic input parameters in the mid- and high-frequency range responses. In this chapter, a brief review of this area is presented, including the probabilistic and fuzzy set based methods. Special attention is given to the fuzzy set based method, which is the main focus in this thesis.

2.1 Introduction

In recent years, an important research effort has been deployed in the mid-frequency range problem in structural dynamics. In this regard, one of the most important issues is the numerical simulation of dynamic systems taking into account the influence of non-deterministic input parameters.

In order to describe how uncertainty can influence the engineering design process, both the variability of physical artifacts and their interaction with environments have to be taken into account. Many possible factors can lead to uncertainty, such as variations in the measurement process, variation in the outer environment, geometrical and material variation of the same product and so on (Battil et al., 2000).

According to a review paper by Manohar and Gupta (2002), the sources of uncertainties in dynamic structural engineering problems can be split up into four categories: physical or

inherent uncertainties, model uncertainties, estimations errors and human errors. Some of the sources, such as inherent uncertainties, are beyond the control of engineers. With regard to model uncertainty some assumptions, usually done in the mathematical models based on simplifying assumptions, also lead to model uncertainty. The study of estimation errors belongs to the science of statistics, while human errors can arise at any stage of the design process.

Other authors, such as Keese (2003) summarize that uncertainties can be caused either by the intrinsic variability of physical quantities such as irregularities in material properties caused by the manufacturing process or simply by lack of knowledge, which can be called epistemic uncertainty.

In the context of non-deterministic numerical modelling, different methods using different approximate models of uncertainties have been proposed to deal with this problem. Basically, some important methods include worst-case scenario, safety factors, Taguchi methods, probabilistic and fuzzy set based methods. According to Maglaras et al. (1997), the worst-case scenario concept used to improve safety factors in many cases lead to over design. Also, for Taguchi methods in general, the concept is to find values of some parameters for which system performance is close to the *target* values and is insensitive to uncertainties.

In Maglaras et al. (1997), experimental comparison of probabilistic and fuzzy set based methods was conducted. They state that a model with uncertainty and enough statistical information available, is better represented by stochastic description; otherwise fuzzy theory is better suited.

In terms of stochastic approach, the finite element method for stochastic problems applied to dynamic analysis is a fast growing area of research. Many authors have discussed such an application in papers reviews and books, see for instance in (Keese (2003), Elishakoff and Ren (2003), Ghanem and Spanos (2003), Manohar and Gupta (2002) and Manohar and Ibrahim (1999)).

In order to give some examples of non-deterministic input parameters, in Marczyk (2004) some typical values of the coefficient of variation (ν) defined as $\nu = \sigma/\mu$, where σ is the standard deviation and μ the mean value for aerospace-type materials and loads are presented. See some examples in Tables 2.1 and 2.2. For instance, the level of scatter for transient loads can achieve something around 60%, which is not considered in any deterministic approach. Such an example illustrates how important it is to take into account the influence of uncertain

parameters during the development process of a new engineering system.

Table 2.1: Coefficient of variation (ν) for same typical aerospace materials (Marczyk, 2004).

Material	Characteristic	ν (%)
Metallic	Rupture	8 – 15
Metallic	Buckling	14
Carbon fiber	Rupture	10 – 17
Screw, Rivet, Welding	Rupture	8
Bonding	Adhesive strength	12 – 16
Bonding	Metal/Metal	8 – 13
Honeycomb	Tension	16
Honeycomb	Shear, compression	10
Honeycomb	Face wrinkling	8
Inserts	Axial Loading	12
Thermal Protection (QA60)	In-plane Tension	12 – 24
Thermal Protection (QA60)	In-plane compression	15 – 20

Table 2.2: Coefficient of variation (ν) for same typical aerospace loads (Marczyk, 2004).

Load Type	Origin of Results	ν (%)
Launch vehicle thrust	STS, ARIANE	5
Transient	ARIANE 4	60
Thermal	Thermal tests	8 – 20
Deployment shocks (solar array)	Aerospace tests	10
Thrusts burner	Calibration tests	2
Acoustic	ARIANE 4 and STS 4 (flights)	30
Vibration	Satellite tests	20

In what follows, some important aspects covering probabilistic and fuzzy set methods are discussed. Thus, in this section, the main idea is to present important aspects of both methods, showing the advantages and disadvantages of each methodology.

2.2 Probabilistic Methods

2.2.1 General aspects

The idea of probabilistic methods is to include uncertainties of the input parameters in the analysis. Basically, important aspects as a risk of failure, safety factors or simply targets

established in the industry are possible examples of the application of probabilistic approach.

In terms of mathematical foundation, the concept of probability is defined as a number assigned to events of a universal set (Chen, 2000). Probability also satisfies the three axioms of Kolmogorov, which state that (Papoulis, 1965)

- i. *The probability of any single event occurring is greater or equal to zero.*
- ii. *The probability of the universal set is one, i.e., in case the universal set includes all possible outcomes.*
- iii. *The probability of the union of mutually exclusive events is equal to the sum of the probabilities of these events. This is also called the additivity axiom.*

In other words, considering the objective sense, the probability concept is the relative frequency of occurrence of an event (Siddall, 1983). In this context, one important factor to add is that to give a confidence interval, probability must be estimated considering a large number of observations. In this scenario, it is important to stress the quote proposed by Freudenthal cited in Moens and Vandelpitte (2004) that ” ... *ignorance of the cause of variation does not make such variation random*”. Besides that, the concept of probability is also defined in terms of a subjective view, which in general is called *Bayesian* interpretation. The probability concept is then defined as a likelihood that an event will occur (Savage, 1972). On one hand, it is important to add that with the Bayesian method, it is possible to add objective information if it becomes available. On the other hand, when no information is available, the Bayesian approach is just a subjective representation of real-life cases (Moens and Vandelpitte, 2004).

Going further, in terms of assumptions, one assumption which is very often applied in probability theory is that variables are uncorrelated. However, this is not true or at least it cannot be defined when little information is available. This can lead to very inaccurate models or can be unrealistic in terms of real applications. In the same context, it is important to add that modelling errors should also be considered in the problem formulation. However, in general, they are not taken into account. Considering, for instance, an optimization problem, where little statistical information is available, this can also lead to poor results as a whole.

In addition, in Maglaras et al. (1997), the effect of the choice of probability distribution is also discussed. According to results presented by Fox and Safie in 1992, it is concluded that probability of failure is very sensitive to the choice of distribution.

Therefore, in real life applications, to give all statistical information which is necessary to satisfy the probability method assumptions is, in general, time consuming or, in most cases, impracticable.

2.2.2 Probability density function (PDF) and central moments

One important property is used in the context of probabilistic concept, which defines a probability density function (PDF) $f(x)$ for the probabilistic quantity X considering a domain of possible values. In this case, for a interval $[a, b]$, the PDF can be defined as follows

$$P(a \leq X \leq b) = \int_a^b f(x)dx \quad (2.1)$$

In terms of mathematical expectation of a function $g(X)$ with respect to $f(X)$, we have

$$E\{g(X)\} = \int_{-\infty}^{\infty} g(X)f(x)dx \quad (2.2)$$

In this regard, the mean value of the distribution $f(X)$ equals $E\{X\}$. In addition, the concept of central moments might also be defined associated with the PDF. The n^{th} central moment m_n is defined from the mean value using the following relation

$$m_n = \int_{-\infty}^{\infty} (x - E\{X\})^n f(x)dx \quad (2.3)$$

Following that, the second order central moment is defined as the variance of the distribution simply defined as $var(X)$. The measure for the dispersion of the distribution about the mean, which is called standard deviation is also defined as $\sigma = \sqrt{var(X)}$. For more insight into this area, please refer to Miller and Freund (1985).

2.2.3 Variability, uncertainty and error

Recently, Moens and Vandelpitte (2004) presented a survey on the use of non-probabilistic methods for non-deterministic dynamic FE analysis. In this paper review, they discussed the main methods available with basic concepts, types of application for imprecisely defined structures and notably the organization of the terminology to be applied for non-determinist approaches. According to Oberkampf in 1999, cited in Moens and Vandelpitte (2004), the term *variability*, *uncertainty* and *error* should be defined as follows

- i. *Variability covers the variation which is inherent to the physical system or the environment under consideration.*
- ii. *Uncertainty is a potential deficiency in any phase of activity of the modelling process that is due to lack of knowledge.*
- iii. *Error is defined as a recognizable deficiency in any phase of modelling or simulation that is not due to lack of knowledge.*

The reason for presenting the above definitions is to clarify or at least to give some definition that can be useful to distinguish the probabilistic and non-probabilistic quantities.

In addition, Moens and Vandelpitte (2004) also suggest some extension for the definitions proposed above, where some correlation between *uncertainty* and *variability* can be found. For instance, for the term *variability*, when no information on its range or likelihood is missing, a *variability* should be subject to lack of knowledge, which means that such a *variability* is also an *uncertainty*. In this regard, they suggest the term *uncertain variability*. However, assuming that the likelihood is exactly known, the term *certain variability* should be used. Another case is where for some model properties that are implemented as constant deterministic values, a possible lack of knowledge in the deterministic properties should be considered. This is the case of model properties that are difficult to model, e.g. damping, loads and so on. For those model properties, the concept of *invariable uncertainty* is defined.

Going further, the main question that arises is which method is in general recommended to deal with engineering problems for designing under uncertainty. In Maglaras et al. (1997), a review comparing fuzzy set based methods and probabilistic methods were presented. Although this review was focused in the last decade, the answer to the question on how to treat non-deterministic input parameters still remains unclear.

Today, there is a consensus that in the presence of statistical information about the random variables, probability methods are better suited. On the other hand, i.e., if little information is available, which is usually true for most realistic engineering problems, it would be better to adopt possibility theory based on fuzzy set methods. The author agrees with the statements above, especially in the case of engineering applications considering the initial design phase. Additionally, Moens and Vandelpitte (2004) also suggested that fuzzy set theory is well suited for the initial phase of a project. When more information becomes available, which is usually the case of a project in industry, probability methods are recommended.

In this thesis, instead of applying the probabilistic approach, the possibility theory based on the Zadeh's (1965) extension principle will be the focus. For a comparison of probabilistic and fuzzy set approaches with numerical and experimental results, please refer to Chen (2000) and Maglaras et al. (1997). Also, for a comparison of probabilistic and deterministic approaches for optimization process, refer to Ponslet (1995).

In what follows, fuzzy set based method will be introduced covering important aspects of fuzzy arithmetic concepts including some discussion about interval and fuzzy set as a whole. By doing so, in the context of fuzzy set based method, the transformation method proposed by Hanss (2002b) is reviewed and suggested to be combined with SEM.

2.3 Fuzzy Set Based Methods

2.3.1 Standard fuzzy arithmetic

Fuzzy arithmetic has been proposed in the literature as a methodology that can be very helpful to analyze systems with respect to uncertain model parameters. The concept of fuzzy has been developed to deal with *imprecision* and also what is called *verbal information*. In the context of engineering applications, a fuzzy model adopted for a dynamic problem can help in determining the range of results or simply intervals of confidence, considering a variability of materials, geometrical dimensions, manufacturing process and so on.

Going one step further, Zadeh's extension principle provides the fundamental basis of fuzzy arithmetic. He states that real valued functions can be extended to functions of fuzzy numbers (Zadeh, 1965). In this concept, also a fuzzy set can be defined as a class with a continuum of grades of membership. This is the case that an element belongs to a fuzzy set to a certain degree.

The main idea behind the concept of the fuzzy set is to model uncertainty considering subjective information or simply *vagueness*. In terms of practical applications, the fuzzy arithmetic based on Zadeh's extension principle, such as LR-fuzzy numbers according to Dubois and Prade (1980) and the standard fuzzy arithmetic described in Kaufmann and Gupta (1991), lead to a serious drawback. Such effect is well known in interval arithmetic as the effect of overestimation or simply defined as *dependency effect*. In Hanss (2002b) the effect of overestimation is discussed and simple examples are treated to show the major drawback in applying standard fuzzy arithmetic.

In order to address the limitation described above, other alternatives in the literature have been proposed. In this context, algorithms for fuzzy arithmetic based on interval-based branch-and-bounds codes according to Hansen (1992) and point-based methods or just called constrained fuzzy arithmetic, such as proposed by Hanss (2002b), Dong and Wong (1987), Dong and Shah (1987) have been suggested.

In this thesis, the transformation method proposed by Hanss (2002b) will be the main focus. By doing so, in the next section, before presenting the main concepts of the proposed method, implementations for fuzzy numbers are introduced, which include the LR- and discretized approaches.

2.4 Fuzzy Numbers Implementation

According to Hanss and Willner (1999), the following requirements for fuzzy numbers must be filled out to represent the uncertain model parameters: representation of fuzzy numbers with arbitrarily shaped membership functions. In this case, special attention must be given to the set of fuzzy numbers with representation from measured data. The second requirement is to avoid any loss of information in the uncertainty and to allow a practical realization of arithmetical operations between fuzzy numbers.

In this context, the concept of implementing fuzzy numbers is represented using LR-fuzzy numbers and, in a more appropriate way, using discretized fuzzy numbers.

In what follows, the LR- and discretized fuzzy numbers are discussed in more detail.

2.4.1 LR-fuzzy numbers

Here we define a fuzzy number according to Dubois and Prade (1980), for different types of fuzzy numbers and definition, please refer to Hanss (2004b).

Assuming the definition proposed by Dubois and Prade (1980), a fuzzy number \tilde{p} is called LR-fuzzy number if two shape functions L (left) and R (right) with three parameters $\bar{m} \in \mathbb{R}$, $\alpha \in \mathbb{R}^+$, and $\beta \in \mathbb{R}^+$ exist as follows

$$\forall x : \mu_{\tilde{p}}(x) = \begin{cases} L(\frac{\bar{m}-x}{\alpha}) & \text{if } x < \bar{m} \\ 1 & \text{if } x = \bar{m} \\ R(\frac{x-\bar{m}}{\beta}) & \text{if } x > \bar{m} \end{cases} \quad (2.4)$$

respectively the following description, \bar{m} is the modal value or also called the *peak value*, α and β are called the left-hand and the right-hand spread parameters.

In short notation, LR-fuzzy number p can be defined as

$$\tilde{p} = \langle \bar{m}, \alpha, \beta \rangle_{LR} \quad (2.5)$$

In addition, special cases of LR fuzzy numbers are also used, such as *triangular fuzzy numbers (TFN)*, in which the shape function is defined as

$$L(u) = R(u) = \max(0, 1 - u) \quad (2.6)$$

where $u = (\bar{m} - x)/\alpha$. We can also define the triangular fuzzy numbers simply as

$$\tilde{p} = \langle \bar{m}, \alpha, \beta \rangle_{TFN} \quad (2.7)$$

Note that, in the definition above, $\beta = \alpha$, which leads to TFN symmetric, otherwise, semi-symmetric.

Figure 2.1 shows an example of a triangular membership function. According to Moens and Vandelpitte (2004), in most practical engineering problems, triangular and quasi-Gaussian membership functions are used to represent fuzzy sets.

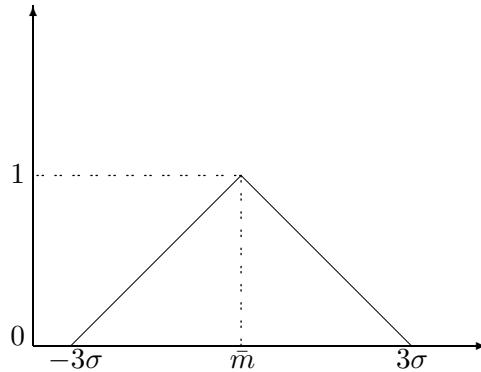


Figure 2.1: Triangular membership function with standard deviation σ and mean value \bar{m} .

A *Gaussian fuzzy numbers (GFN)* is represented as follows

$$L(u) = R(u) = \exp\left(-\frac{1}{2}u^2\right) \quad (2.8)$$

or also

$$\tilde{p} = \langle \bar{m}, \sigma, \sigma \rangle_{GFN} = \langle \bar{m}, \sigma \rangle_{GFN} \quad (2.9)$$

and we can also adopt a *quasi-Gaussian fuzzy numbers (QGFN)* defined as follows

$$L(u) = R(u) = \begin{cases} \exp(-\frac{1}{2}u^2) & \text{if } |\bar{m} - x| \leq r\sigma \\ 0 & \text{if } |\bar{m} - x| > r\sigma \end{cases} \quad (2.10)$$

or simply defined as

$$\tilde{p} = \langle \bar{m}, \sigma, r \rangle_{QGFN} \quad (2.11)$$

For instance, taking a symmetric fuzzy number of a *QGFN* shape function which is defined by the membership with $r = 3$:

$$\begin{aligned} \mu(x) &= e^{-\frac{(x - \bar{m})^2}{2\sigma^2}} & \text{for } |x - \bar{m}| \leq 3\sigma & \text{ and} \\ \mu(x) &= 0 & \text{for } x > \bar{m} + 3\sigma & \text{ or } x < \bar{m} - 3\sigma \end{aligned} \quad (2.12)$$

where \bar{m} is the mean value and σ the standard deviation of the Gaussian distribution.

Now consider that a Young's modulus with a nominal value of $E = 2.0 \times 10^{11}$ N/m² is set up with a standard deviation of 5%. Assuming the proposed standard deviation and adopting triangular and quasi-Gaussian membership functions, its approximation can be represented according to Figures 2.2 (a) and (b).

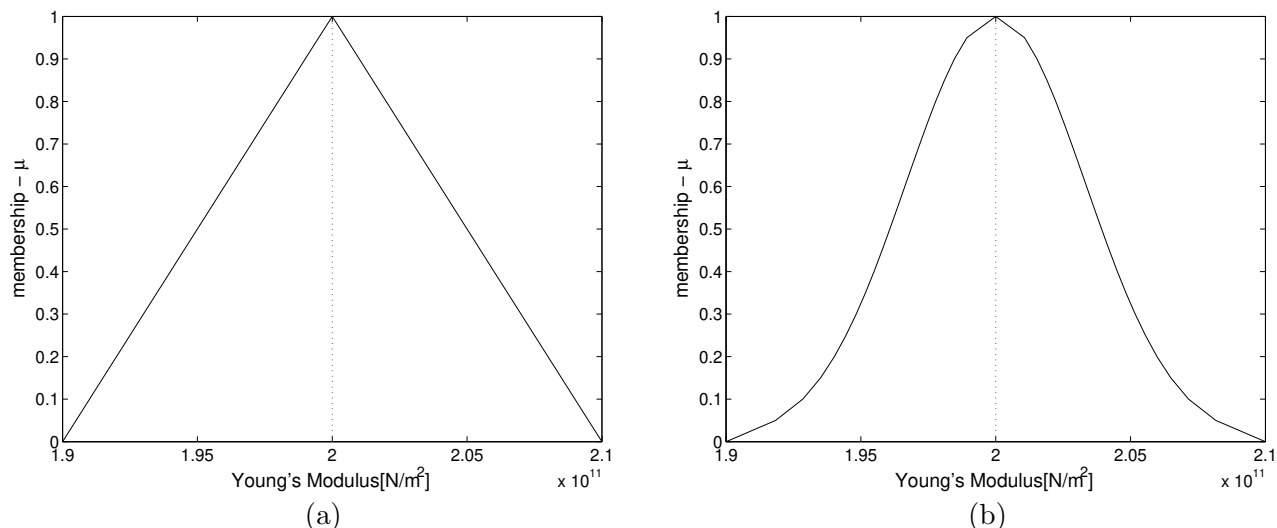


Figure 2.2: Triangular (a) and quasi-Gaussian (b) membership functions for a linear Young's modulus.

In addition, a closed interval $[a, b]$ and the concept of *crisp* value number considering conventional subsets of the *universal* set Ω are described in the following form

$$\mu_{[a,b]}(x) = \begin{cases} 1 & \text{for } a \leq x \leq b \\ 0 & \text{for all other } x \end{cases} \quad \text{and} \quad (2.13)$$

$$\mu_c(x) = \begin{cases} 1 & \text{for } x = c \\ 0 & \text{for all other } x \end{cases} \quad (2.14)$$

with membership functions $\mu(x) \in [0, 1]$, and with $\mu(x) = 1$ true only for the single value $x = \bar{m}$ (Oexl et al., 2002). See Figure 2.3.

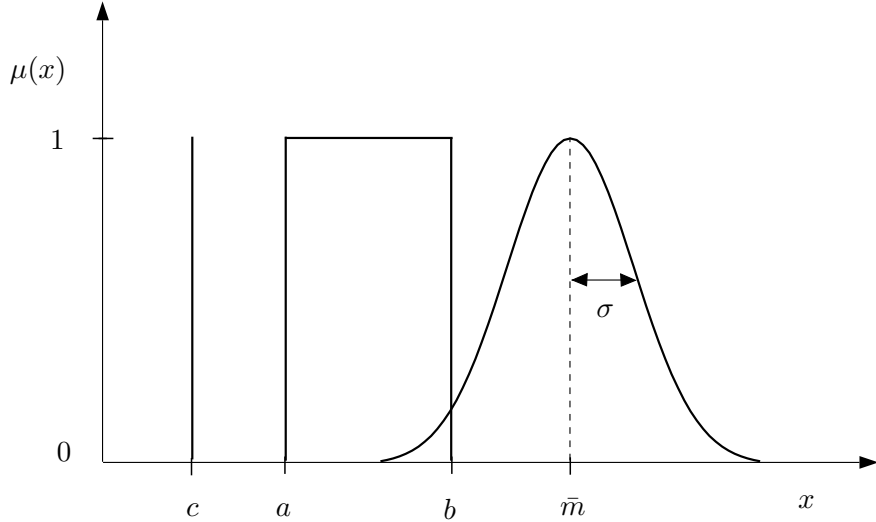


Figure 2.3: Symmetric fuzzy number of quasi-Gaussian shape expressed by their membership functions with mean value \bar{m} and standard deviation σ , *crisp* number c and closed interval $[a, b]$.

2.4.2 Discretization of the fuzzy numbers

As discussed above, the concept of LR-fuzzy numbers is not complicated to implement and does not require complex computation. However, according to Hanss and Willner (1999), it is unsuitable to treat fuzzy numbers with arbitrary shape.

In this sense, in Hanss (2002b) one alternative is described based on subdividing the axis for the degree of membership μ into a number of m segments, equally spaced by $\Delta_\mu = 1/m$. Such an alternative is based on the practice of sampling analog signals, which consists in describing the fuzzy number in a discrete form. Moreover, the $m + 1$ levels of membership μ_j for a given α -cut at the level α -level $\in [0, 1]$ are then given by

$$\mu_j = \frac{j}{m}, \quad j = 0, 1, \dots, m \quad (2.15)$$

Figure 2.4 shows an implementation of a fuzzy number \tilde{p} using decomposition into intervals by the discrete fuzzy numbers representation (Hanss, 2002b).

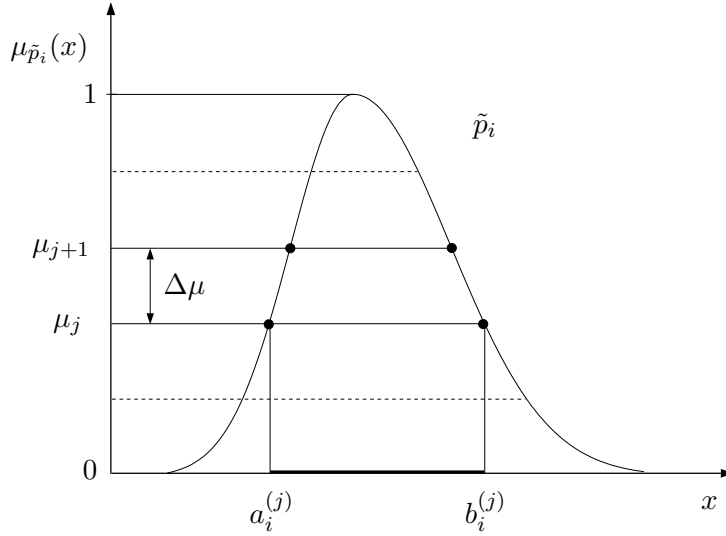


Figure 2.4: Implementation of a fuzzy number \tilde{p} decomposed into intervals.

One important point to add is that, in the fuzzy application, the intervals of confidence are called simply α -cuts with the α -level $\alpha = j/m \in [0, 1]$. According to Hanss and Willner (1999), this discretization is also called in literature as α -cut representation or α -sublevel technique.

In this case, the fuzzy number to be implemented either using approximation by discrete number or decomposed into a number of intervals, for instance $[a^j, b^j]$, $a^j \leq b^j$, $j = 0, 1, \dots, m$ given by α -cuts and the α -levels μ_j .

Additionally, an interesting question in the context of finding an approximation of a fuzzy number in its discrete solution is how to measure the error of the final result. This question is discussed in Klimke (2003) based on work of Giachetti (1997a). In that work, they suggest that the error measure is defined by comparing the approximation and the actual results separately for the left and right parts of the fuzzy numbers for a given α -level with $\alpha \in [0, 1]$.

For instance, taking \tilde{p} defined as the actual result and \tilde{p}_* as the approximation with $[a^{(\alpha)}, b^{(\alpha)}]$ the actual interval and $[a_*^{(\alpha)}, b_*^{(\alpha)}]$, the approximate interval for a given α -level, the following absolute error ϵ can be defined as

$$\epsilon_{left}^{(\alpha)} = |a^{(\alpha)} - a_*^{(\alpha)}| \quad \text{and} \quad \epsilon_{right}^{(\alpha)} = |b^{(\alpha)} - b_*^{(\alpha)}| \quad (2.16)$$

Following that, the measure suggested above can also be defined as distance to the left $\Delta_{left}^{(\alpha)} = \epsilon_{left}^{(\alpha)}$ and distance to the right $\Delta_{right}^{(\alpha)} = \epsilon_{right}^{(\alpha)}$ of two intervals of confidence with the distance given by $\Delta^{(\alpha)} = \Delta_{left}^{(\alpha)} + \Delta_{right}^{(\alpha)}$.

In Klimke (2003), the absolute error is defined integrating over all membership levels $\alpha \in [0, 1]$, which leads to the following integral

$$\epsilon = \int_{\alpha=0}^1 \Delta^{(\alpha)} d\alpha \quad (2.17)$$

or also defined as

$$\epsilon = \int_{\alpha=0}^1 (|a^{(\alpha)} - a_*^{(\alpha)}| + (|b^{(\alpha)} - b_*^{(\alpha)}|)) d\alpha \quad (2.18)$$

The relative error is found by dividing the absolute error by the area of fuzzy number, i.e.,

$$e = \epsilon / \text{area}(\tilde{p}) \quad (2.19)$$

where

$$\text{area}(\tilde{p}) = \int_{\alpha=0}^1 (b^{(\alpha)} - a^{(\alpha)}) d\alpha \quad (2.20)$$

In addition, the following properties can be defined for the error e

- i. $e \geq 0$.
- ii. $(\tilde{p}_* = \tilde{p}) \longrightarrow e = 0$.
- iii. For \tilde{p}_* defined as a *crisp* number with real value p , the peak value of \tilde{p} is equal to p and $e = 1$.

2.5 Constrained Fuzzy Arithmetic

The well known overestimation effect in fuzzy arithmetic is discussed in the literature and different approaches have been proposed. A non-overestimating approach, also called fuzzy weighted averages (FWA) has been proposed by Dong and Wong (1987) as an alternative to address this problem. However, in its initial proposal, only monotonic functions with respect to all of their fuzzy variables were used.

In Wood et al. (1992), an enhancement is achieved for the case of non-monotonic function applications. According to Klimke (2003), the proposed algorithm requires an additional routine that should be used to locate the internal extrema. For such kind of application, numerical and analytical approaches are used combined with special algorithms that take into account the non-linear functions as input.

Additionally, a new theoretical framework proposed by Klir (1997) takes into account dependencies of the fuzzy parameters. Such an approach in literature is called *constrained fuzzy arithmetic*.

In this sense, the transformation method is proposed by Hanss (2002b) as a practical approach to evaluate fuzzy parameterized models in order to avoid any other extra optimization routine such as suggested by Wood et al. (1992). The transformation method is considered an advanced approach of the Vertex Method proposed by Dong and Shah (1987).

Thus, in the next section, the transformation method is introduced and the main advantages and disadvantages are discussed.

2.6 Implementation of the Transformation Method

The implementation of fuzzy arithmetic using the transformation method was introduced by Hanss (2002b). In what follows, some of the main characteristics of this method will be reviewed. For more detailed explanation about the fundamental ideas of the transformation method, please refer to a recent book published by Hanss (2004b).

Consider a problem with n independent uncertain parameters, represented by fuzzy numbers \tilde{p}_i , $i = 1, 2, \dots, n$, each decomposed into a set P_i of $m + 1$ intervals defined by $X_i^{(j)}$ with $j = 0, 1, \dots, m$, of the form

$$P_i = \left\{ X_i^{(0)}, X_i^{(1)}, \dots, X_i^{(m)} \right\} \quad (2.21)$$

where

$$X_i^{(j)} = [a_i^{(j)}, b_i^{(j)}], \quad a_i^{(j)} \leq b_i^{(j)}, \quad (2.22)$$

$$i = 1, 2, \dots, n, \quad j = 0, 1, \dots, m$$

Based on this representation of the fuzzy numbers, the general and reduced transformation method in its standard form will be introduced according to Hanss (2002b). In what follows, the same notation proposed by Hanss (2002b) is used to introduce the general transformation method.

2.6.1 General transformation method

In the proposed transformation method, instead of applying standard interval arithmetic to the intervals $X_i^{(j)}$, $i = 1, 2, \dots, n$ for each level of membership μ_j , $j = 0, 1, \dots, m$, the intervals are transformed into arrays $\widehat{X}_i^{(j)}$ of the following form (Hanss, 2002b)

$$\widehat{X}_i^{(j)} = \overbrace{(\gamma_{1,i}^{(j)}, \gamma_{2,i}^{(j)}, \dots, \gamma_{(m+1-j),i}^{(j)}, \gamma_{1,i}^{(j)}, \gamma_{2,i}^{(j)}, \dots, \gamma_{(m+1-j),i}^{(j)})}^{(m+1-j)^{i-1}(m+1-j)\text{-tuples}} \quad (2.23)$$

with

$$\gamma_{l,i}^{(j)} = \underbrace{(c_{l,i}^{(j)}, \dots, c_{l,i}^{(j)})}_{(m+1-j)^{n-1} \text{ elements}} \quad (2.24)$$

and also

$$c_{l,i}^{(j)} = \begin{cases} a_i^{(j)} & \text{for } l = 1 & \text{and } j = 0, 1, \dots, m, \\ \frac{1}{2}(c_{l-1,i}^{(j+1)} + c_{l,i}^{(j+1)}) & \text{for } l = 2, 3, \dots, m-j & \text{and } j = 0, 1, \dots, m-2, \\ b_i^{(j)} & \text{for } l = m-j+1 & \text{and } j = 0, 1, \dots, m, \end{cases} \quad (2.25)$$

In Figure 2.5, decomposition scheme proposed of the general transformation method is shown for $m = 5$ (Hanss, 2003). In this case, addition points within the intervals $X_i^{(j)}$, $i = 1, 2, \dots, m-2$ are considered.

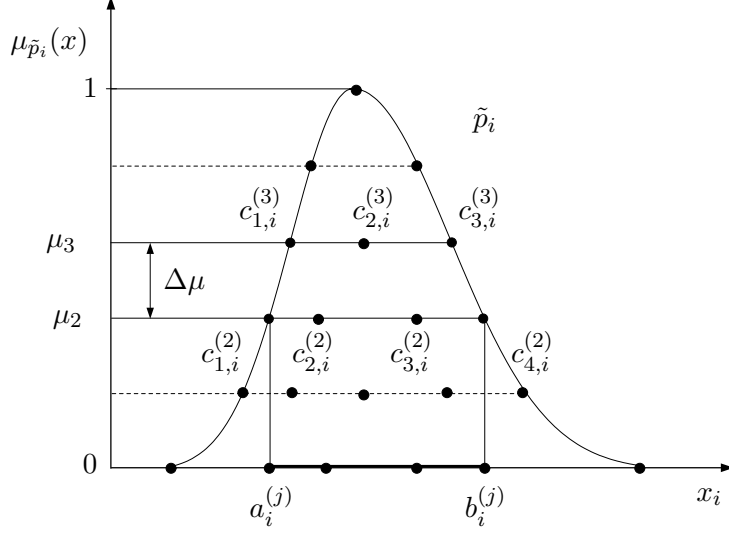


Figure 2.5: Decomposition scheme for the general transformation method for $m = 5$.

2.6.2 Reduced transformation method

To reduced form, the transformation method is defined as follows

$$\widehat{X}_i^{(j)} = \overbrace{(\alpha_i^{(j)}, \beta_i^{(j)}, \alpha_i^{(j)}, \beta_i^{(j)}, \dots, \alpha_i^{(j)}, \beta_i^{(j)})}^{2^{i-1} \text{ pairs}} \quad (2.26)$$

with

$$\alpha_i^{(j)} = \underbrace{(a_i^{(j)}, \dots, a_i^{(j)})}_{2^{n-i} \text{ elements}}, \quad \beta_i^{(j)} = \underbrace{(b_i^{(j)}, \dots, b_i^{(j)})}_{2^{n-i} \text{ elements}} \quad (2.27)$$

where $a_i^{(j)}$ and $b_i^{(j)}$ are the lower and upper bounds of the interval at membership level μ_j for the i -th uncertain model parameter.

Assuming that the uncertain system response is given by a function F defined as follows

$$\tilde{q} = F(\tilde{p}_1, \tilde{p}_2, \dots, \tilde{p}_n) \quad (2.28)$$

its evaluation can be carried out separately at each of the values of the arrays using conventional arithmetic for *crisp* numbers. If the output \tilde{q} of the system can be expressed in its decomposed and transformed form by the arrays $\widehat{Z}^{(j)}$, $j = 0, 1, \dots, m$, the k -th element ${}^k \hat{z}^{(j)}$ of the array $\widehat{Z}^{(j)}$ is then given by

$$\begin{aligned}
{}^k\hat{z}^{(j)} &= F \left({}^k\hat{x}_1^{(j)}, {}^k\hat{x}_2^{(j)}, \dots, {}^k\hat{x}_n^{(j)} \right), \\
k &= 1, 2, \dots, 2^n,
\end{aligned} \tag{2.29}$$

where ${}^k\hat{x}_i^{(j)}$ denotes the k -th element of the array $\widehat{X}_i^{(j)}$. For a conclusion, the fuzzy-valued response \tilde{q} of the system can be obtained in its decomposed form

$$Z^{(j)} = [a^{(j)}, b^{(j)}], \quad j = 0, 1, \dots, m, \tag{2.30}$$

by back-transforming the arrays $\widehat{Z}^{(j)}$ as follows

$$\begin{aligned}
a^{(j)} &= \min_k ({}^k\hat{z}^{(j)}) \\
b^{(j)} &= \max_k ({}^k\hat{z}^{(j)}) \quad , \quad j = 0, 1, \dots, m
\end{aligned} \tag{2.31}$$

In order to give an interpretation of the transformation scheme, an example for $n = 3$ uncertain parameters using the reduced transformation method is presented in Hanss (2002b). In this case, the process can be interpreted as a coordinates of points on the $(n-1)$ dimensional hypersurfaces of a number of $m+1$ n -dimensional cuboids according to the membership level. In addition, one interesting to add is that, for $\mu = 1$, it represents just one single point. Also, its is important to emphasize that in its reduced form just the 2^n vertex points of the n -dimensional cuboids are considered during the evaluation of the problem.

2.6.3 Applying the general transformation method for a simple one DOF system

In order to give a simple example adopting the transformation method, we consider a mass-spring system. In this example, we assume force and structural damping as non-deterministic input parameters with 20% and 10% standard deviation, respectively. The numerical mean values used are: $k = 1000 \text{ N.m}^{-1}$, $m = 1 \text{ kg}$, $F = 1 \text{ N}$ and internal loss factor $\eta = 0.01$. For the non-deterministic input parameters, quasi-Gaussian shape membership function is assumed. Figure 2.6 (a) and (b) shown the FRF and a *zoom* between 4.0 Hz and 6.0 Hz. Additionally, in Figure 2.7, fuzzy-valued result depending on three different numbers of α -cuts at 5.25 Hz are shown. Basically, we see that using only 2 α -cuts, the resolution for the fuzzy-valued is very poor. On the other hand, increasing the number of α -cuts to 5, we found

a similar convergence using 15 α -cuts. Therefore, in this simple case, we can adopt only 5 α -cuts to assess the envelopes for receptance response.

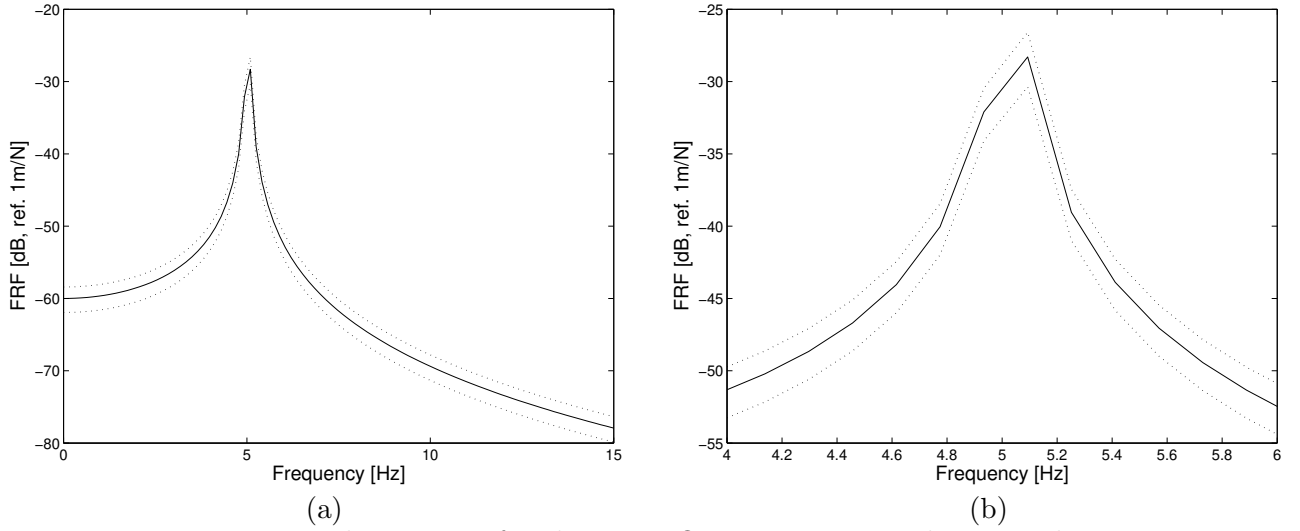


Figure 2.6: Envelope FRFs for the one DOF system using the general transformation method. (a) envelope and nominal value, (b) zoom between 4.0 Hz and 6.0 Hz.

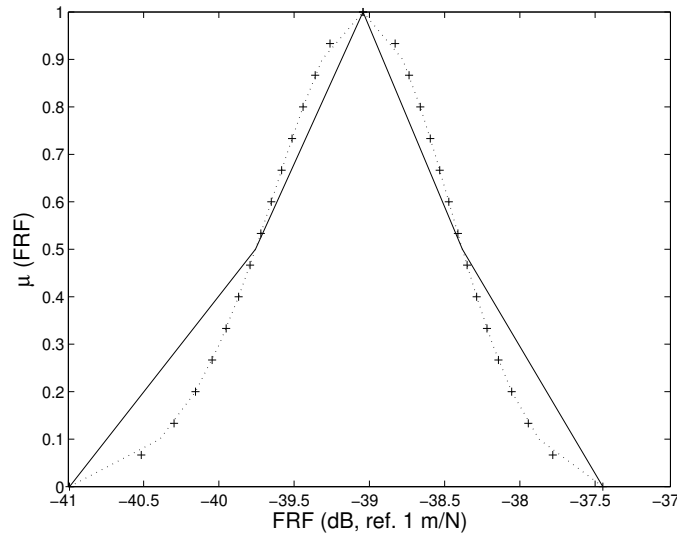


Figure 2.7: Degree of possibility for different α -cuts at $f = 5.25$ Hz. 2 α -cuts (solid), 5 α -cuts (dashed line) and 15 α -cuts (plus sign).

2.6.4 Advantages and disadvantages of the transformation method

In what follows, the main advantages and disadvantages of the transformation method proposed as a practical implementation of the Zadeh's (1965) extension principle will be discussed.

- i. The most important point is that for the transformation method, there is no need to add any external optimization routine to evaluate fuzzy-parameterized models. In contrast to the (extension) of the FWA proposed by Wood et al. (1992) for FWA, an additional routine to locate internal extrema is required.
- ii. The process to combine the lower and upper interval bounds, also values described in the middle, are correctly described, without any ambiguities.
- iii. The relative influence of the uncertainty of each parameter on the overall uncertainty of the model output can be quantified. In addition, it can also be used as an alternative method to provide a sensitivity analysis. Nevertheless, in case of increasing fuzziness in the model parameter, the degrees of influence are less reliable (Hanss, 2004a).
- iv. The present decomposition scheme for the general transformation method, in certain applications, produces recurring points which are dependent on the membership function. This might be a drawback in terms of practical applications, especially for complex systems that computation time is one of the main issues (Klimke, 2003).
- v. Also, a drawback concerning memory allocation must be considered. For instance, in the reduced transformation method, for each of the n fuzzy input parameters, $8n2^n$ bytes are required just to allocate the input arrays of the function when using double precision floating point numbers (Klimke, 2003).

Therefore, instead of adopting the transformation method in its standard form, in the next chapter, efficient alternatives that have been proposed by Klimke (2003, 2004ab) to improve some of the limitations discussed above will be addressed.

In this sense, the main idea is to provide an efficient and attractive method to be combined with any other structural dynamics deterministic method, such as the spectral element method, to address the influence of non-deterministic input parameters in the frequency response analysis.

2.7 Summary

In this Chapter, a review in the field of fuzzy set based methods and some words on probabilistic methods were presented. In this regard, one important point to emphasize is that in the case of more statistical information about the random variables, probabilistic methods are recommended. However, in the opposite side, i.e., little statistical information about random variables is available, fuzzy set based methods are better suited.

In this thesis, fuzzy set based is the chosen method, where one the main focus is to treat dynamic problems considering the initial design phase. In this context, the transformation method proposed by Hanss (2002b) is suggested to be combined with a deterministic method, which in this thesis, is the spectral element method (See Appendices A, B, C and D). In addition, the main advantages and disadvantages of the transformation method were pointed out.

Following this work, in the next chapter, an efficient and alternative proposal to be applied in the transformation method will be discussed.

Chapter 3

Efficient Fuzzy Set Based Methods to be Combined with SEM

In Chapter 2, a brief review of the field of probabilistic and fuzzy set based methods was presented. Basically, the main idea stressed was that when statistical information about the random variables is available, probabilistic methods are recommended. However, when little or no statistical information is available, fuzzy set based methods are better suited. In this thesis, the transformation method applied in the context of fuzzy set based methods, is used. In this chapter the main focus is to explore some possible alternative schemes that improve the original version of the transformation method and also to introduce the sparse grids approach as an efficient alternative.

3.1 Introduction

The use of fuzzy set methods applied in engineering problems has been extensively discussed in literature (Hanss (2004ab), Hanss (2002ab), Hanss (1999) and Klimke et al. (2004a)).

Recently, Nunes et al. (2004a) and Arruda et al. (2004) presented the application of the fuzzy set combined with the spectral element method. In both papers, the standard transformation method in its reduced form proposed by Hanss (2002b) is applied to estimate frequency response function envelopes.

In terms of practical applications, however, as discussed in Chapter 2, some improvements to the transformation method should be done. First, this can be focused in terms of an efficient implementation of the algorithm, which leads to less computation effort as whole. Second, the idea also provides a more compact algorithm that can be combined with deterministic approaches to address typical engineering problems. In this thesis, the spectral element

method has been chosen as our deterministic method. It is important to keep in mind that some characteristics described in Chapters 1 and 2 justified such a choice.

Considering the above, the transformation method proposed by Hanss (2002) has been shown to be a very interesting approach that can be combined with the spectral element method. Nevertheless, some improvements should be done for a possible, realistic application.

Therefore, in this chapter, some possible improvements to be applied to the transformation method will be discussed. Following that, a new approach based on a sparse grid interpolation algorithm is also introduced. This chapter is based on recent works published by Klimke (see for instance Klimke, 2004b) in the context of algorithm improvement for fuzzy set based methods application.

3.2 Transformation Method Removing Recurring Points

This section presents alternatives that improve the original version of the transformation method. Here, the general transformation method that eliminates recurring combinations is presented. Also, in the same context, Klimke (2003) proposed the use of a multi-dimensional array, instead of working with the original arrays proposed by Hanss (2002b). However, even with the multi-dimensional array alternative for the transformation method, there is also an important drawback that must be considered. For each of the n fuzzy input parameters, $8n2^n$ (reduced) and $8n(m+1)^n$ (general) bytes are required just to allocate the input arrays of the function when using double-precision floating point numbers. Therefore, further improvements are necessary to give a more efficient and general implementation. For example, the alternative of removing recurring points is suggested to cover some of the weak points presented in the transformation method.

In the general transformation method, it has been noted that the interior points of each fuzzy number interval of a given membership level are subsets of the next, lower level. In such a case, considering the decomposition scheme proposed in the general transformation method, it is found that this produces recurring points. Klimke (2003) also observed that this is a special case, which happens when fuzzy numbers are implemented using a symmetric triangular membership function. An alternative to remove recurring combinations from the evaluation procedure is the reuse of inner points described for any α -cut. See for instance Figure 3.1, where the recurring points are shown in detail.

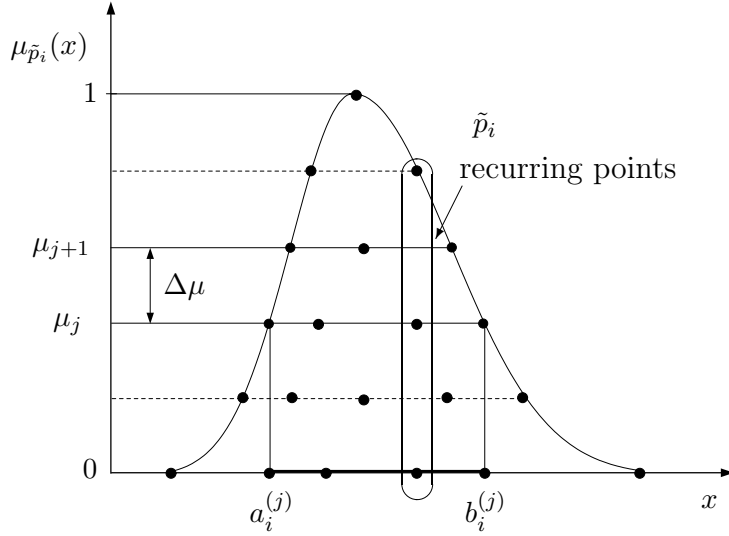


Figure 3.1: General transformation method and its recurring points (Klimke, 2003).

In this case, to compute the discretization points, instead of adopting the original Eq. (2.25) presented in Chapter 2, a new expression for the decomposition scheme is defined

$$c_{l,i}^{(j)} = \begin{cases} a_i^{(j)} & \text{for } l = 1 & \text{and } j = 0, 1, \dots, m, \\ c_{l-1,i}^{(j+2)} & \text{for } l = 2, 3, \dots, m - j & \text{and } j = 0, 1, \dots, m - 2, \\ b_i^{(j)} & \text{for } l = m - j + 1 & \text{and } j = 0, 1, \dots, m, \end{cases} \quad (3.1)$$

On the one hand, it can be found that, in terms of results, using the new step introduced in the general transformation method, a less accurate result can be found due to a smaller number of inner points. On the other hand, to avoid such a problem, the number of α -cuts should be increased to achieve better results.

For instance, as described in Klimke (2003), taking the original form for the general transformation method (*gtrm*) with dimension 2, one can say that with 100 α -cuts, a reduction number of function evaluation of a factor 17.1 is found using the proposed method (avoiding additional functions evaluations for recurring combinations) called *gtrmrecur*. For the same example, taking 10 α -cuts, a factor of 2.1 is found. Therefore, a general conclusion is that, in the case of large numbers of α -cuts compared with the number of uncertain parameters, better performance is found with the *gtrmrecur*. However, it is important to add that, in the case of less regular distribution of the inner points, results are less accurate. In this case, it is suggested to increase the number of α -cuts instead of keeping it constant as in the original version of the transformation method (Klimke, 2003).

Table 3.1: Comparison of the number of function evaluations in *gtrm* and in the *gtrmrecur* (Klimke, 2003).

α -cuts	parameters	<i>gtrm</i>	<i>gtrmrecur</i>
10	$n = 2$	385	181
100	$n = 2$	338350	19801
10	$n = 3$	3025	1729
100	$n = 3$	26 Million	2.0 Million
10	$n = 5$	22085	159049
100	$n = 5$	172 Billion	20 Billion

From Table 3.1 it can be noted that for a large number of α -cuts in comparison with the number of uncertain parameters n , the new scheme presents better performance in terms of functions evaluations.

Additionally, in Klimke (2003) the new scheme with the *gtrmrecur* is compared to the original algorithm for some specific test functions, in terms of convergence for three types of membership functions, the symmetric triangular, the non-symmetric triangular and the quasi-Gaussian. The results presented in that work show that for the symmetric triangular fuzzy numbers, the *gtrmrecur* requires less function evaluations than the original one, i.e, the *gtrm*. However, considering the case of small number of α -cuts, the new algorithm presents no regular distribution for the inner points of the non-symmetric and non-linear membership functions.

In terms of computation time, the new proposal offers the advantage that just the lowest α -cut of each part of all permutations is treated with the upper α -cuts defined automatically (Klimke, 2003).

In Nunes et al. (2004b), the new scheme is compared with the reduced transformation method *rtrm* algorithm and the fuzzy arithmetic using sparse grids interpolation for two test problems, which consist of a coupled rod and a reinforced plate model. Also, the SEM is combined with a Monte Carlo analysis and compared to the fuzzy set based methods proposed.

In the same context, the fuzzy arithmetic using sparse grids interpolation can also be considered an attractive approach when combined with the SEM. In the next section, a fuzzy set method using sparse grids interpolation will be introduced for further applications with the SEM.

3.3 Fuzzy Set Method using Sparse Grids Interpolation

Some possible improvements for the general transformation method were discussed in the former sections. In this section, the sparse grid interpolation approach, which has been the subject of intensive study by A. Klimke at the University of Stuttgart, Institute of Applied Analysis and Numerical Simulation, Germany (Klimke, 2004b), will be combined with the SEM in the context of fuzzy set based methods.

The sparse grid interpolation method is based on previous work by Smolyak (1963). In this area, most of the important developments are based on numerical data compression and image processing. Besides that, the sparse grids has also been applied to solve partial differential equations, which was addressed by Zenger (1991).

The main idea of the method is to compute a sparse grid interpolant of the objective function with sufficient accuracy for the d -dimensional box Ω_0 in Eq. 3.2, using only a small number of real-valued function evaluations. The number of support nodes of the sparse grid interpolant grows moderately with increasing problem dimension d (Klimke, 2004b). The hierarchical structure of the sparse grid interpolation scheme permits a subsequent increase to the interpolation depth until a sufficient estimated relative or absolute accuracy is reached.

Going further, the interpolant then replaces the objective function in the optimization problems in Eq. 3.2. The subsequent optimization problems are solved by suitable global optimization algorithms that take advantage of the known properties of the interpolant as described in Nunes et al. (2004b).

$$\begin{aligned} \tilde{B} &= \{(y, \mu_{\tilde{B}}(y)) \mid y \in Y\}, \text{ with} \\ \mu_{\tilde{B}}(y) &= \begin{cases} \sup\{\alpha \mid y \in B_\alpha\} & \text{if } y \in B_0, \\ 0 & \text{otherwise,} \end{cases} \\ B_\alpha &= \left[\min_{\mathbf{x} \in \Omega_\alpha} f(\mathbf{x}), \max_{\mathbf{x} \in \Omega_\alpha} f(\mathbf{x}) \right], \quad 0 \leq \alpha \leq 1. \end{aligned} \quad (3.2)$$

The computational complexity of the sparse grid approach cannot be expressed as simply as the other methods above, since it depends on the objective function itself. However, in the case of expensive objective functions, the evaluation of the model at the support nodes of the interpolant usually governs the overall computation time. Depending on the type of the sparse grid used, the number of support nodes varies.

From the mathematical point of view, the idea is to interpolate *smooth* functions with

$f : [0, 1]^d \rightarrow \mathbb{R}$ adopting a finite number of support nodes. Taking the interpolation case for one-dimensional problems, the following formula can be defined

$$U^i(f) = \sum_{j=1}^{m_i} a_j^i \cdot f(x_j^i) \quad (3.3)$$

with $i \in \mathbb{N}$, the basis function $a_j^i \in C([0, 1])$, $a_j^i(x_l^i) = \delta_{j,l}$, $l \in \mathbb{N}$, and the support nodes $x_j^i \in X^i = \{x_1^i, \dots, x_{m_i}^i\}$, $x_k^i \in [0, 1]$, $1 \leq k \leq m_i$.

In Klimke (2004b), the application for the multivariate case is introduced. In this case, a tensor product formula can be adopted. However, it requires a very high number of support nodes. In order to solve this problem, the Smolyak's algorithm is then applied to reduce the number of support nodes, with the important property that it maintains the approximation quality of the interpolation formula. The Smolyak interpolant $A_{q,d}(f)$ is given by

$$A_{q,d}(f) = \sum_{|\mathbf{i}| \leq q} (\Delta^{i_1} \otimes \dots \otimes \Delta^{i_d})(f) = A_{q-1,d}(f) + \underbrace{\sum_{|\mathbf{i}|=q} (\Delta^{i_1} \otimes \dots \otimes \Delta^{i_d})(f)}_{\Delta A_{q,d}(f)} \quad (3.4)$$

where the multi-index \mathbf{i} , with $|\mathbf{i}| = i_1 + \dots + i_d$ and $\mathbf{i} \in \mathbb{N}^d$. The parameter n , with $n = q - d$, $q \geq d$, $q \in \mathbb{N}$ indicates the depth of the hierarchical construction. One important thing to add is that, to assess the term $A_{q,d}$, we need just points defined at the sparse grid, which leads to

$$H_{q,d} = \bigcup_{q-d+1 \leq |\mathbf{i}| \leq q} (X^{i_1} \times \dots \times X^{i_d}) \quad (3.5)$$

and we might select the sets X^i in a way that $X^i \subset X^{i+1}$ to provide many recurring points increasing the parameter q . By doing so, with $X^0 = \emptyset$, $X_\Delta^i = X^i \setminus X^{i-1}$, Eq. (3.5) can be rewrite as

$$H_{q,d} = H_{q-1,d} \cup \bigcup_{|\mathbf{i}|=q} (X_\Delta^{i_1} \times \dots \times X_\Delta^{i_d}) \quad (3.6)$$

with $H_{q-d,d} = \emptyset$, which is more convenient in case of refinement of the grid with increasing q . In terms of comparison with the full grid $H_{full,n+d,d}^{CC}$, applying the full grid, the number of points in the sparse grid $H_{q,d}$ is given by

$$H_{full,q,d} = X^{q-d+1} \times \dots \times X^{q-d+1} \quad (3.7)$$

It is important to note that the sparse grid interpolation is based on a collection of points and that a *smooth* function can be approximated with an interpolation formula. In this context, different approaches based on sparse grids are needed in order to find a function that is suitable for the interpolation. In Klimke (2004b), three types of construction have been suggested: the classical maximum or simply L_2 -norm-based sparse grid H^M , the maximum-norm-based sparse grid denoted by H^{NB} and the Clenshaw-Curtis denoted by H^{CC} .

The set of support nodes X^i for the L_2 -norm based sparse grid including the boundary can be defined as follows

$$\begin{aligned} m_i &= 2^i + 1 \\ x_j^i &= (j - 1)/(m_i - 1) \quad \text{for } j = 1, \dots, m_i \text{ and } i \geq 1 \end{aligned}$$

The maximum-norm-based sparse denoted by H^{NB} , which excludes the points on the boundary is introduced with the following set of support nodes

$$\begin{aligned} m_i &= 2^i - 1, \\ x_j^i &= j/(m_i + 1) \quad \text{for } j = 1, \dots, m_i \end{aligned}$$

In the case of the Clenshaw-Curtis type sparse grid with equidistant nodes represented by H^{CC} , the following description is found in Klimke (2004b)

$$\begin{aligned} m_i &= \begin{cases} 1 & \text{if } i = 1 \\ 2^{i-1} + 1 & \text{if } i > 1 \end{cases} \\ x_j^i &= \begin{cases} (j - 1)/(m_i - 1) & \text{for } j = 1, \dots, m_i \text{ if } m_i > 1 \\ 0.5 & \text{for } j = 1 \text{ if } m_i = 1 \end{cases} \end{aligned}$$

In terms of basis functions a_j^i , we have the following piecewise linear basis functions

$$\begin{aligned} a_1^1(x) &= 1 \quad \text{for } i = 1, \text{ and} \\ a_j^i(x) &= \begin{cases} 1 - (m_i - 1) \cdot |x - x_j^i|, & \text{if } |x - x_j^i| < \frac{1}{(m_i - 1)}, \\ 0 & \text{otherwise,} \end{cases} \end{aligned}$$

for $i > 1$ and $j = 1, \dots, m_i$.

Figure 3.2 shows a 2D example for $H_{3,2}$ considering the Clenshaw-Curtis type sparse grid with univariate sets of nodes X^i .

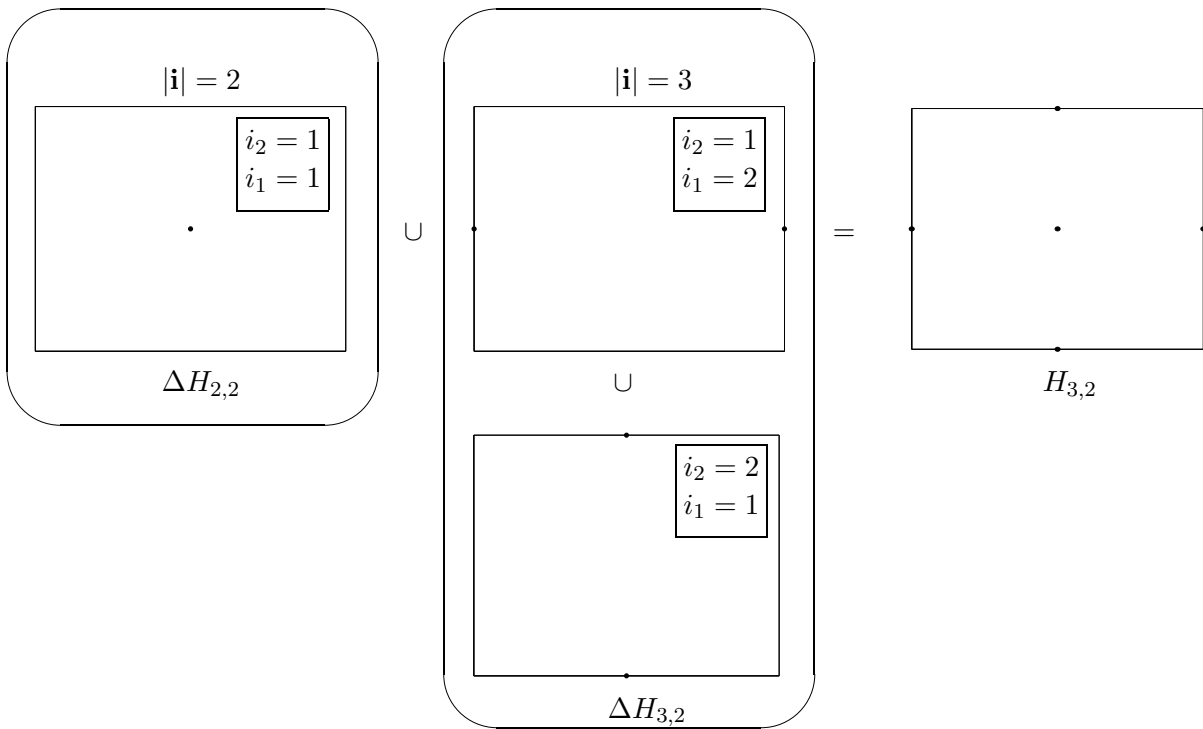


Figure 3.2: Sparse grid $H_{3,2}$ construction using Clenshaw-Curtis for 2D case.

In Klimke (2004b), the three sparse grids discussed above are presented with some discussion on how to evaluate the accuracy of the piecewise interpolation. In that work, he demonstrated, using simple numerical results, that the Clenshaw-Curtis grids is more attractive in terms of the grid size. On the other hand, other basis functions have been used, such as polynomial basis and wavelets (Bungartz and Griebel, 2004). In order to give an example, Figure 3.3 shows the grids for $H_{7,2}^M$, $H_{7,2}^{NB}$ and $H_{7,2}^{CC}$ in case of a problem with dimension $d = 2$. In this figure, it is important to note that the occurrence of the number of grid points increase for H^M , while the H^{CC} presents the lowest number of points.

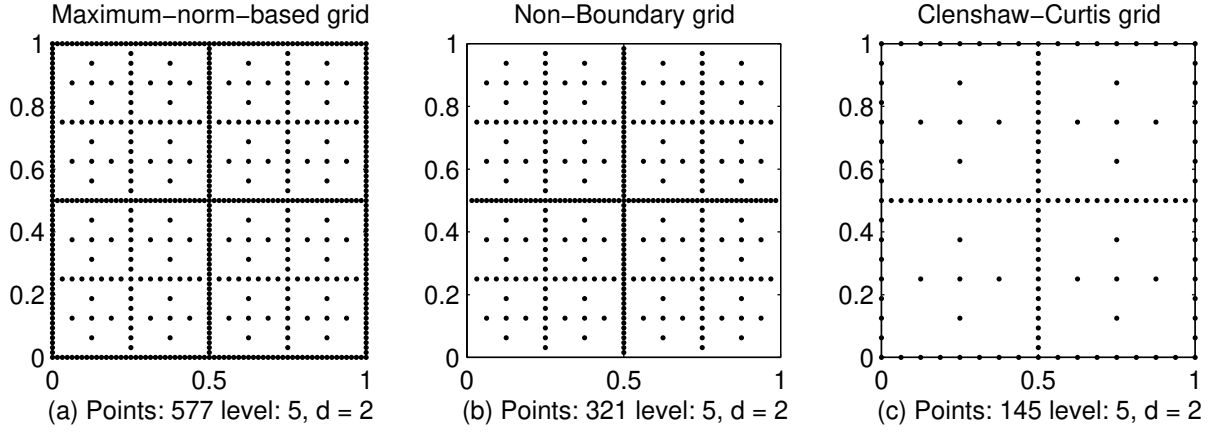


Figure 3.3: Comparison for sparse grids: (a) $H_{7,2}^M$, (b) $H_{7,2}^{NB}$ and (c) $H_{7,2}^{CC}$.

In addition, in Table 3.2, the Clenshaw-Curtis type sparse grid is compared with full grid interpolation, which shows some important advantages of the sparse grids method.

Table 3.2: Comparison of number of grid points for refinement level $n = q - d$ (Klimke, 2005).

n	full grid $H_{full,n+d,d}^{CC}$				sparse grid $H_{n+d,d}^{CC}$			
	$d = 2$	$d = 4$	$d = 8$	$d = 16$	$d = 2$	$d = 4$	$d = 8$	$d = 16$
1	9	81	6581	$4.3e7$	5	9	17	33
2	25	625	41553	$1.5e11$	13	41	145	545
3	81	6561	$4.3e7$	$1.9e15$	29	137	849	6049
4	289	83521	$7.0e9$	$4.9e19$	65	401	3937	51137
5	1089	$1.2e6$	$1.4e12$	$2.0e24$	145	1105	15713	$3.5e5$
6	4225	$1.8e7$	$3.2e14$	$1.0e29$	321	2561	31745	$2.1e6$
7	16641	$2.8e8$	$7.7e16$	$5.9e33$	705	7537	$1.9e5$	$1.1e7$

In Nunes et al. (2004b), the sparse grid with piecewise multilinear basis functions defined in Klimke (2004b) is adopted, where the number of function evaluations N is at most

$$N \leq 2^{n+1} \cdot \frac{(n+d-1)!}{n!(d-1)!}$$

where n denotes the depth of the sparse grid, $n \in \mathbf{N}$. The interpolant can be made arbitrarily accurate with increasing n .

According to Klimke (2005) the sparse interpolation has the following important characteristics:

- i. Number of support nodes is reduced in comparison to full grid (See Table 3.2);

- ii. Hierarchical structure (In this case, its is important to use this benefit to estimate the current approximation error);
- iii. A special tensor product construction can be used (Smolyak, 1963);
- iv. The most important property of the method is that the the asymptotic quadratic error decay of the full grid interpolation with increasing grid resolution is preserved up to a logarithmic factor. According to Barthelmann et al. (2000) the order of the interpolation error in the maximum norm is then given by

$$\|f - A_{q,d}(f)\|_\infty = \mathcal{O}(N^{-2} \cdot (\log_2 N)^{3 \cdot (d-1)}) \quad (3.8)$$

where N denotes the number of sparse grid points of $H_{q,d}$.

To give an example of the sparse grids approach, consider a two coupled rod system modelled via SEM with two non-deterministic input parameters, with nominal values for Young's modulus E equal to 2.71×10^9 N/m² and an internal loss factor η equal to 0.03. We assume a standard deviation for the parameter E of 10% and for η a value of 30%. In this example, the idea is to show for one specific frequency, namely at 5.4774×10^3 Hz, the interpolation surface response considering the range proposed for those uncertain parameters.

Figure 3.4 (a) shows the original surface and Figure 3.4 (b) the surface obtained using the sparse grid type $H_{7,2}^{CC}$ with piecewise linear basis functions. See also Figure 3.3 (c). For more detail about the two coupled rod set-up, i.e., point forces, material and geometrical details, please refer to the Chapter 4, where the main results for some test problems using the SEM and fuzzy set based method are discussed.

For the proposed case, adopting $d = 2$ with Clenshaw-Curtis type sparse grid, just 321 points were used for the interpolation process showing similar results compared with the original function.

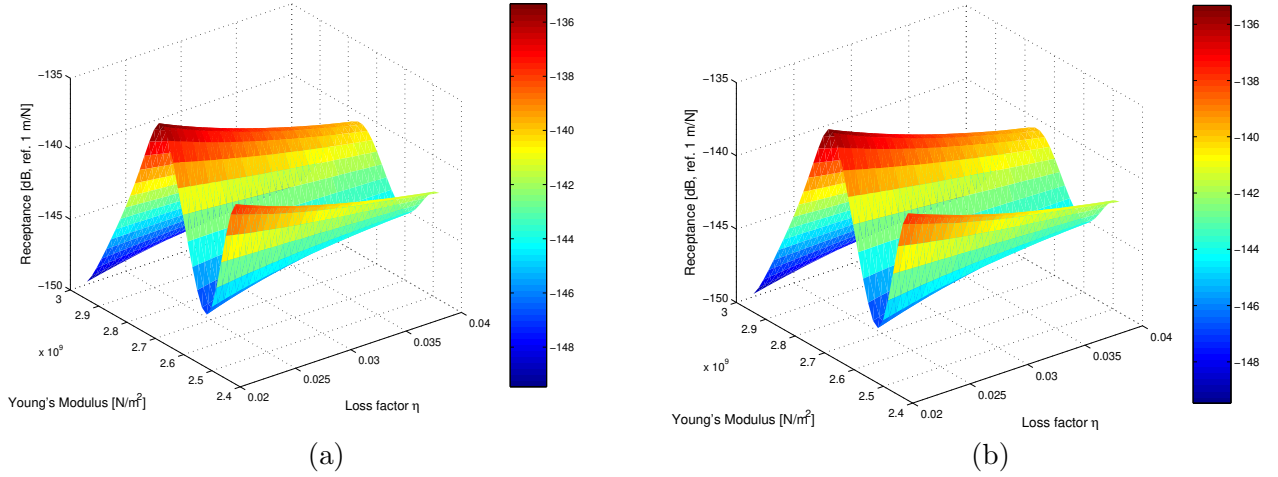


Figure 3.4: Sparse grids method: (a) original surface and (b) result using the interpolation.

3.4 Estimating of Envelopes for FRF using SEM and Fuzzy Set Based Methods

In this section, the main idea is to present a *step-by-step* implementation of SEM combined with fuzzy set based methods in order to obtain an approximate solution of the dynamic response envelopes. As described in Nunes et al. (2004b), this can be done by a three-step procedure:

Step 1: Discretization process. First, the objective frequency range $[f_0, f_1]$ is divided into $s - 1$ *logarithmically* spaced steps, giving s discrete frequencies f_i , $i = 1, \dots, s$. It is advisable to compute the frequency response function for a crisp set of input parameters first to select an adequate resolution, i.e., capable of clearly resolving the resonance frequencies. The d uncertain input parameters $\tilde{p}_1, \dots, \tilde{p}_d$ are discretized into N discrete parameter vectors \mathbf{p}_j , $j = 1, \dots, N$, $\mathbf{p}_j \in \Omega_0$ according to the chosen implementation of the extension principle, i.e., in this work the transformation and its variants and the sparse grid interpolation method, and also Ω_0 as in Eq. 3.2. In case of the reduced and the general transformation method, N is determined by the number of α -cuts m chosen for the fuzzy number discretization. For the sparse grid approach, it requires the interpolation depth parameter n .

Step 2: Model evaluation. In the next step, the $\text{FRF}(f_i, \mathbf{p}_j)$ is computed for all $s \cdot N$ permutations. In this regard, using the MATLAB software, an efficient implementation may vectorize the calls to the SEM model to treat multiple discrete frequencies, or alternatively,

several sets of parameter permutations at once.

Step 3: FRF envelope construction. In case of the reduced and the general transformation method, the resulting discrete frequency responses $\text{FRF}(f_i, \mathbf{p}_j)$ can be used directly to compute an approximate envelope. For each α -cut $\in [0, 1]$ (where α must match the cuts selected for the discretization), that means one can be done as follows $\text{FRF}_\alpha(f_i) = [\text{FRF}_{\alpha, \min}(f_i), \text{FRF}_{\alpha, \max}(f_i)]$, with

$$\text{FRF}_{\alpha, \min}(f_i) = \min_{\mathbf{p}_j \in \Omega_\alpha} \text{FRF}(f_i, \mathbf{p}_j) \quad \text{and} \quad (3.9)$$

$$\text{FRF}_{\alpha, \max}(f_i) = \max_{\mathbf{p}_j \in \Omega_\alpha} \text{FRF}(f_i, \mathbf{p}_j). \quad (3.10)$$

In case of sparse grid-based fuzzy arithmetic, the discrete frequency responses $\text{FRF}(f_i, \mathbf{p}_j)$, $i = 1, \dots, s$, $j = 1, \dots, N$, are used to construct s sparse grid interpolants $A_{n+d,d}(\text{FRF}(f_i))$ that approximate the frequency response function at each discrete frequency f_i in the parameter domain Ω_0 . In Klimke (2004a) a detailed description of constructing these sparse grid interpolants can be found. Then, to obtain the frequency response envelope, a suitable global optimization algorithm is used to compute, according to

$$\text{FRF}_{\alpha, \min}(f_i) = \min_{\mathbf{p} \in \Omega_\alpha} A_{n+d,d}(\text{FRF}(f_i))(\mathbf{p}) \quad \text{and} \quad (3.11)$$

$$\text{FRF}_{\alpha, \max}(f_i) = \max_{\mathbf{p} \in \Omega_\alpha} A_{n+d,d}(\text{FRF}(f_i))(\mathbf{p}). \quad (3.12)$$

Additionally, any set of α levels can be chosen for the optimization part. For the sparse grid-based approach, however, it requires more computational effort to compute the envelope as whole. On the other hand, often much fewer evaluations of the SEM model are required to compute an accurate approximation of the response envelope. In real world applications, for more complex, expensive to evaluate models, this can result in enormous time savings.

On important to note is that to obtain plausible results using the sparse grid-based approach, it is recommended to perform FRF function values in *logarithmic* scale, i.e., use $\log(\text{FRF}(f_i, \mathbf{p}_j))$ to build the interpolant. This is necessary, since the underlying multilinear interpolation scheme will produce more appropriate interpolated values.

At the end of the process, the fuzzy-valued frequency response at any given frequency f_i can be composed from the α -level sets $\text{FRF}(f_i)_\alpha$. Furthermore, the response function envelopes for a given interval of confidence α are easily obtained by plotting the two curves of the minimum and the maximum FRF values $\text{FRF}_{\alpha, \min}(f_i)$ and $\text{FRF}_{\alpha, \max}(f_i)$, respectively, over the frequencies f_i , $i \in [f_0, f_1]$. In practical applications, for instance, the *maximum* curve

can be set up as a *target* or a *safety* value to be achieved during the development process of some structural dynamic system.

3.5 Summary

In this chapter, some alternatives to improve the original version of the transformation method were presented. Basically, for an efficient implementation of the transformation method combined with the SEM, the proposed method of considering recurring permutations (*gtrmrecur*) with a multi-dimensional array was recommended. Also, the sparse grids interpolation was introduced. It can be used to reduce the computational effort in computing real-valued function evaluations in the fuzzy set based methods. At the end of this chapter, a *step-by-step* procedure to estimate the envelopes for FRF using the SEM and fuzzy set based methods was proposed.

Chapter 4

Numerical Applications using the SEM Combined with Fuzzy Set Based Methods

In this Chapter, the spectral element method is combined with a special implementation of fuzzy arithmetic that avoids the well-know effect of overestimation in interval computations. In this context, the transformation method and the sparse grid approach combined with fuzzy sets are proposed. The proposed methods are used to build the envelopes for frequency response function and the results are compared with Monte Carlo simulation. In addition, the SEM is combined with a fuzzy set based method to estimate SEA coupling loss factors under the influence of non-deterministic input parameters.

4.1 Coupled Rods System

In this chapter, numerical examples are proposed in order to show the applicability of the SEM combined with fuzzy set-based methods. In the Appendices A, B, C and D, the SEM formulation is presented for rod, beam and plate elements. Also, some numerical examples using SEM and FEM are discussed.

The first example is the main part of the work proposed by Nunes et al. (2004b), which investigates a coupled rod system (see Figure 4.1). In this case, it is assumed that there are two non-deterministic input parameters, the Young's Modulus E and the loss factor η . Table 4.1 summarizes the physical properties for rod 1 and rod 2 used in the numerical model with description of uncertain parameters. In addition, free-free condition was adopted in the numerical model. In this set-up, one important feature is that rod 2 has a much higher modal density than rod 1, which, in other words, means that rod 2 acts as fuzzy attachment to

rod 1 providing additional damping to the modes of rod 1. In addition, as the frequency increases, the modal overlap of rod 2 exceeds unity and the effect of individual modes is no longer visible (Langley and Bremner, 1999).

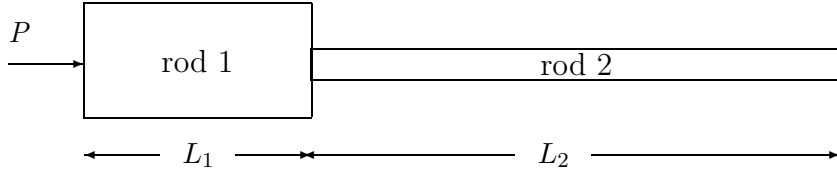


Figure 4.1: Schematic of the coupled rods system.

Table 4.1: Physical and geometrical properties of the coupled rods system.

parameter	mean value \bar{m}	standard deviation σ	dimension
$E_{1/2}$	2.71×10^9	10 % \bar{m}	N/m ²
$\rho_{1/2}$	1140	0	kg/m ³
$\eta_{1/2}$	1.0×10^{-2}	10 % \bar{m}	—
A_1	1.735×10^{-3}	0	m ²
A_2	1.862×10^{-4}	0	m ²
L_1	0.20	0	m
L_2	2.46	0	m

4.2 Plate with Reinforcements

In the second case, also described in Nunes et al. (2004b), a simply supported plate in the yz -plane and free-free in the xz -plane is adopted. See Figure 4.2. The plate is assumed to have the following properties described in Table 4.2. The uncertain parameters assumed are the Young's modulus E and the thickness h . The FRF deterministic curve is carried out at the driving point located at position $(x, y) = (333.4, 160.0)$ mm.

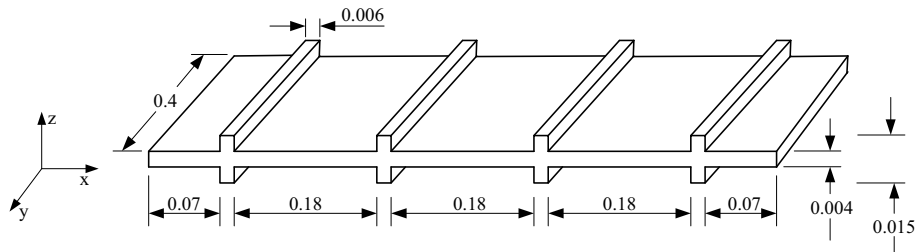


Figure 4.2: Schematic diagram of the stiffened plate (units in meters).

Table 4.2: Physical properties of the plate with non-deterministic input parameters.

parameter	mean value \bar{m}	standard deviation	dimension
E	69×10^9	5%	N/m ²
ρ	2700	0	kg/m ³
ν	0.3	0	—
L_x	0.400	0	m
L_y	0.704	0	m
h	0.004	10 %	m

4.2.1 Envelopes for FRF: coupled rods system

In this section, we present some results using envelopes for frequency response function (FRF) variations. Note that the choice of the envelopes for FRF is due to the possibility to obtain *maximum* and *minimum* amplitude values for the dynamic system to be analyzed. In terms of engineering application, such a choice can be very helpful during design phase.

In order to obtain envelopes for frequency response function variations, the following methods are combined with SEM: the reduced transformation method (*rtrm*), the general transformation method considering recurring permutations (*gtrmrecur*) and the sparse grid approach (*sparse grids*). Also, the SEM is combined with Monte Carlo analysis (SEM/MC) in order to give a reference value.

In this context, it is important to note that the comparison of each method with the MC is done using the same deterministic method, i.e., without any other influence. In this example, the SEM/MC is applied using uniform distribution instead of Gaussian one. Here, it is important to emphasize that such a choice is based on preliminary tests that indicates better results using uniform distribution instead of applying Gaussian distribution.

In the first numerical example presented in Fig. 4.3, just rod 1 is presented. In the second, shown in Fig. 4.4, rods 1 and 2 are presented to form the coupled systems.

In case of SEM combined with fuzzy set based methods, the influence of the number of α -cuts m is also presented. For the SEM/MC, instead of m , the number of samples N is used for comparison. Also, for the uncoupled case, a *zoom* between 7.0 kHz and 8.5 kHz is presented. For the coupled case, a *zoom* between 3 kHz and 5 kHz is shown.

In what follows, the results for the uncoupled and coupled cases are presented for the methods proposed above.

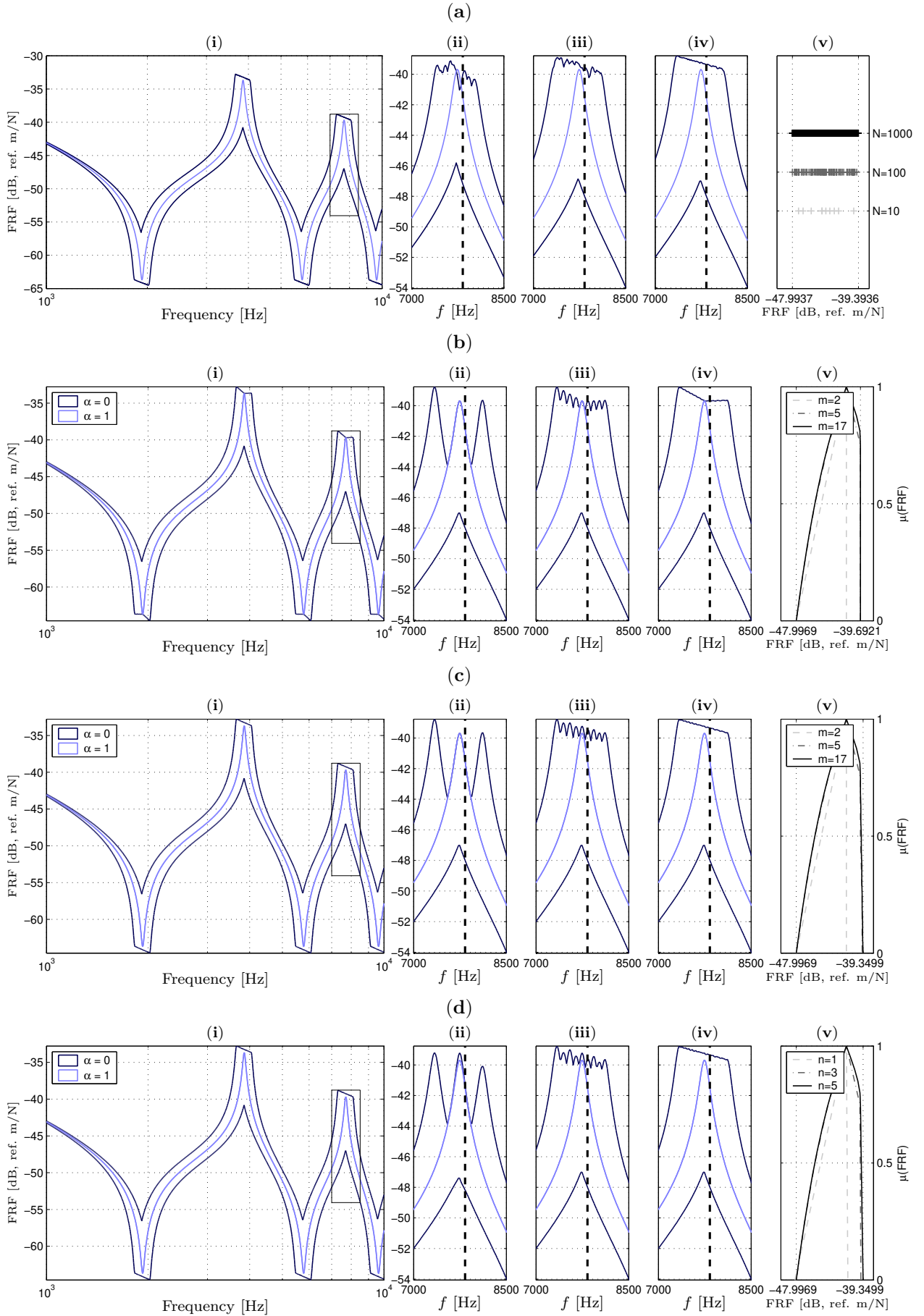


Figure 4.3: Envelopes for FRF for the uncoupled rod system. (a) MC, (b) *rtrm*, (c) *gtrm-recur*, (d) *sparse grid*; (i) full spectrum, (a,ii–iv) zoom for $N = 10, 100, 1000$, (b–c,ii–iv) zoom for $m = 2, 5, 17$ α -cuts, (d,ii–iv) zoom for level $n = 1, 3, 5$; (a,v) range of MC results depending on N at $f_{892} = 7796.4$ Hz, (b–d,v) fuzzy-valued result at f_{892} depending on m, n .

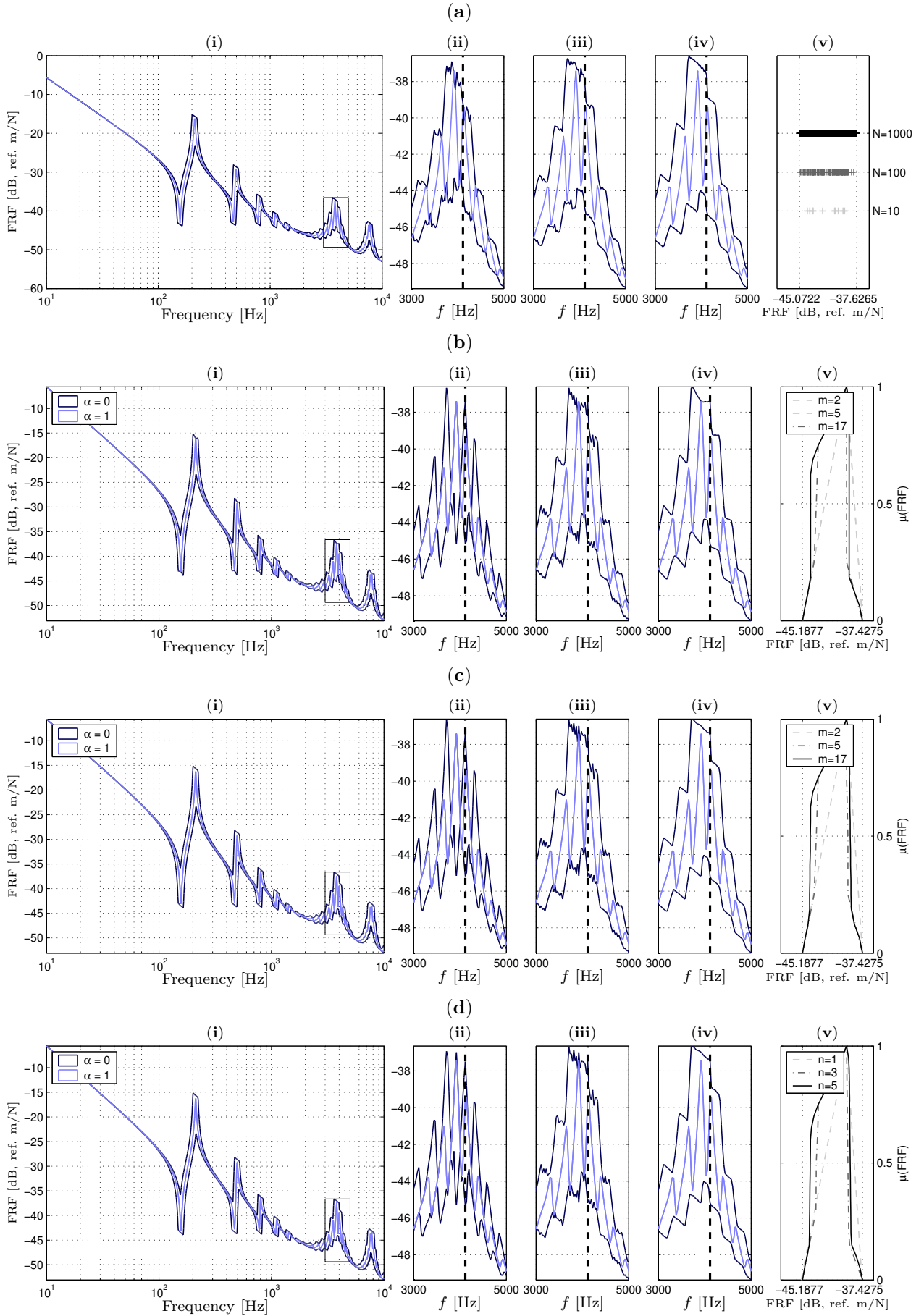


Figure 4.4: Envelopes for FRF for the coupled rod system. (a) MC, (b) *rtrm*, (c) *gtrm*-*recur*, (d) sparse grid; (i) full spectrum, (a,ii-iv) zoom for $N = 10, 100, 1000$, (b-c,ii-iv) zoom for $m = 2, 5, 17$ α -cuts, (d,ii-iv) zoom for level $n = 1, 3, 5$; (a,v) range of MC results depending on N at $f_{867} = 3986.6$ Hz, (b-d,v) fuzzy-valued result at f_{867} depending on m, n .

4.2.2 Envelopes for FRF: plate model

In Fig. 4.5, assuming the same procedure adopted to the rod setup, the results for the plate model are presented for three different fuzzy set based methods and MC. For each method proposed, a SEM model is used as a determinist one.

4.2.3 Error plots

In general, the output of the fuzzy set methods are just discrete fuzzy numbers, i.e., a set of intervals which, in other words, is only an approximation of the exact solution.

In this context, one important thing is to determine a way to measure the error of the result. According to Giachetti and Young (1997a), error measures were given by comparing the approximation and the actual result separately for the left and right segment of the fuzzy numbers for a given α level $\alpha \in [0, 1]$.

Here, to conduct an error analysis and to assess the quality of the computed results, the reference solutions R_{\min} and R_{\max} at $\alpha = 0$ were obtained numerically with a highly accurate sparse grid interpolant using an interpolation depth of $n = 9$, which resulted in $N = 3329$ support nodes per frequency. The maximum error e_{\max} and the average error e_{avg} of the frequency response function envelopes were computed according to the following formulae

$$e_{\max} = \max_{i=1, \dots, s} [| \text{FRF}_{0, \min}(f_i) - R_{\min}(f_i) | + | \text{FRF}_{0, \max}(f_i) - R_{\max}(f_i) |] \quad (4.1)$$

$$e_{\text{avg}} = \left[\sum_{i=1}^s (| \text{FRF}_{0, \min}(f_i) - R_{\min}(f_i) | + | \text{FRF}_{0, \max}(f_i) - R_{\max}(f_i) |) \right] \cdot s^{-1} \quad (4.2)$$

In case of a Monte Carlo analysis (MC), the following number of samples were performed with $N = 10, 100, \text{ and } 1000$. The samples were uniformly distributed in Ω_0 , generated by the pseudo-random number generator **RAND** of **MATLAB**.

To summarize, the error plots are displayed in Fig. 4.6 for the two rod cases and also for the plate set-up. In addition, a summary for the discretization and accuracy of each method is displayed in Table 4.3.

In order to obtain more information about the results found, in the next section, a summary with interpretation of the main results found is presented. The idea is to cover all

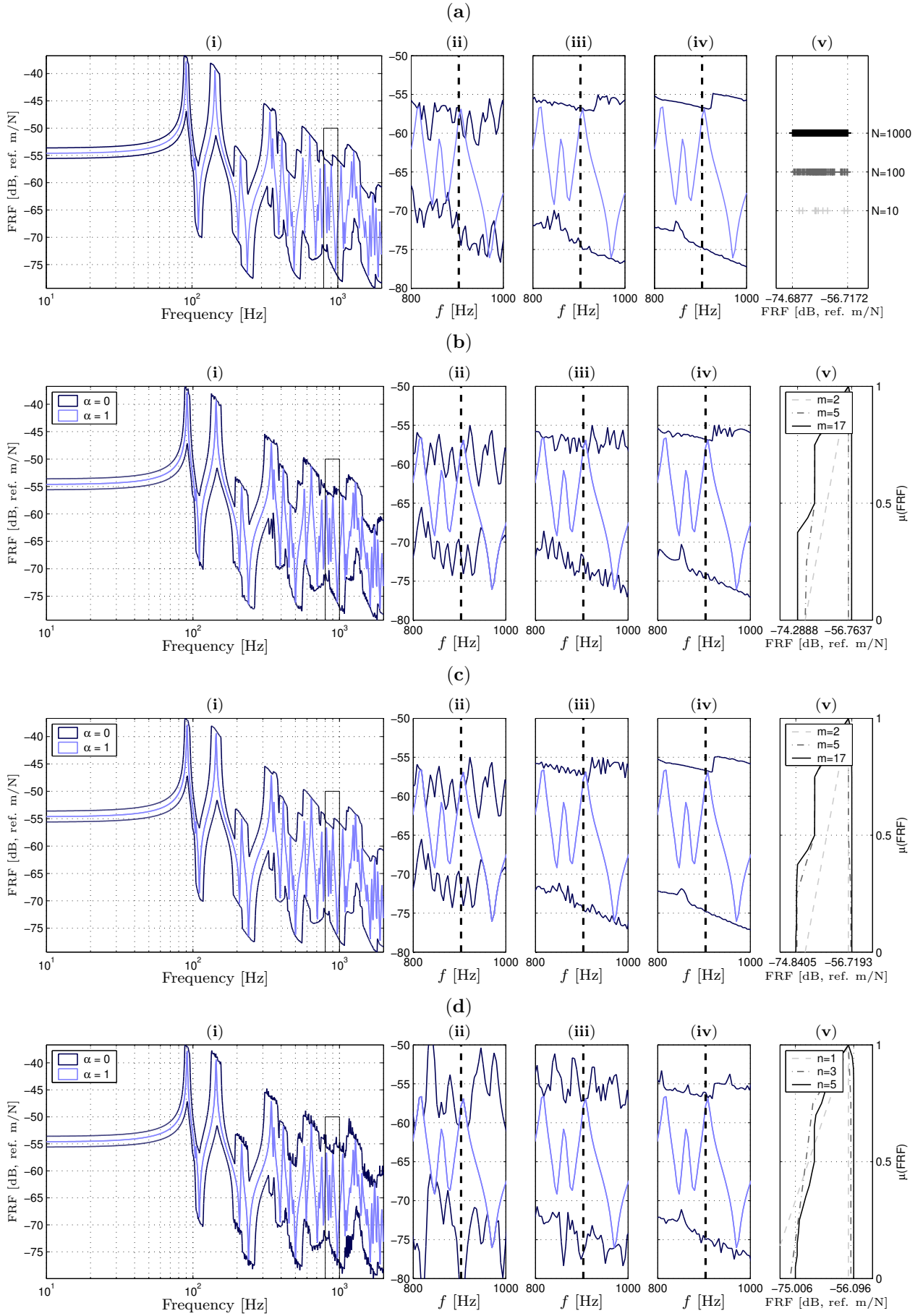


Figure 4.5: Envelopes for FRF for the plate system. (a) MC, (b) *rtrm*, (c) *gtrmrecur*, (d) *sparse grid*; (i) full spectrum, (a,ii–iv) zoom for $N = 10, 100, 1000$, (b–c,ii–iv) zoom for $m = 2, 5, 17$ α -cuts, (d,ii–iv) zoom for level $n = 1, 3, 5$; (a,v) range of MC results depending on N at $f_{849} = 897.90$ Hz, (b–d,v) fuzzy-valued result at f_{849} depending on m, n .

advantages and disadvantages of each method discussed. Therefore, to avoid simple conclusions based on just elapsed time, the results will be discussed in terms of performance, accuracy and scalability.

Table 4.3: Discretization parameters and approximation error for the simulation runs.

<i>method</i>	<i>m</i>	<i>n</i>	<i>N</i>	uncoupled rod		coupled rod		plate	
				e_{max}	e_{avg}	e_{max}	e_{avg}	e_{max}	e_{avg}
MC	–	–	10	4.6	1.3	7.4	0.57	14	3.3
	–	–	100	0.73	0.15	0.85	0.083	6.5	0.86
	–	–	1000	0.30	0.037	0.38	0.024	2.3	0.22
rtrm	2	–	5	5.0	0.52	7.0	0.37	14	3.0
	5	–	17	1.1	0.11	1.8	0.092	8.6	1.2
	17	–	65	0.49	0.054	0.58	0.042	3.9	0.33
	33	–	129	0.46	0.051	0.54	0.039	3.8	0.23
gtrmrecur	5	–	41	1.0	0.078	1.6	0.069	5.2	0.56
	17	–	545	0.085	0.0076	0.14	0.0068	0.55	0.059
	33	–	2113	0.028	0.0026	0.042	0.0023	-	-
sparse	21	1	5	5.0	0.56	7.2	0.39	15	3.0
	21	3	29	1.0	0.090	1.6	0.082	11	1.0
	21	5	145	0.096	0.0089	0.15	0.0080	5.2	0.27
	21	6	321	0.027	0.0023	0.036	0.0020	2.1	0.13

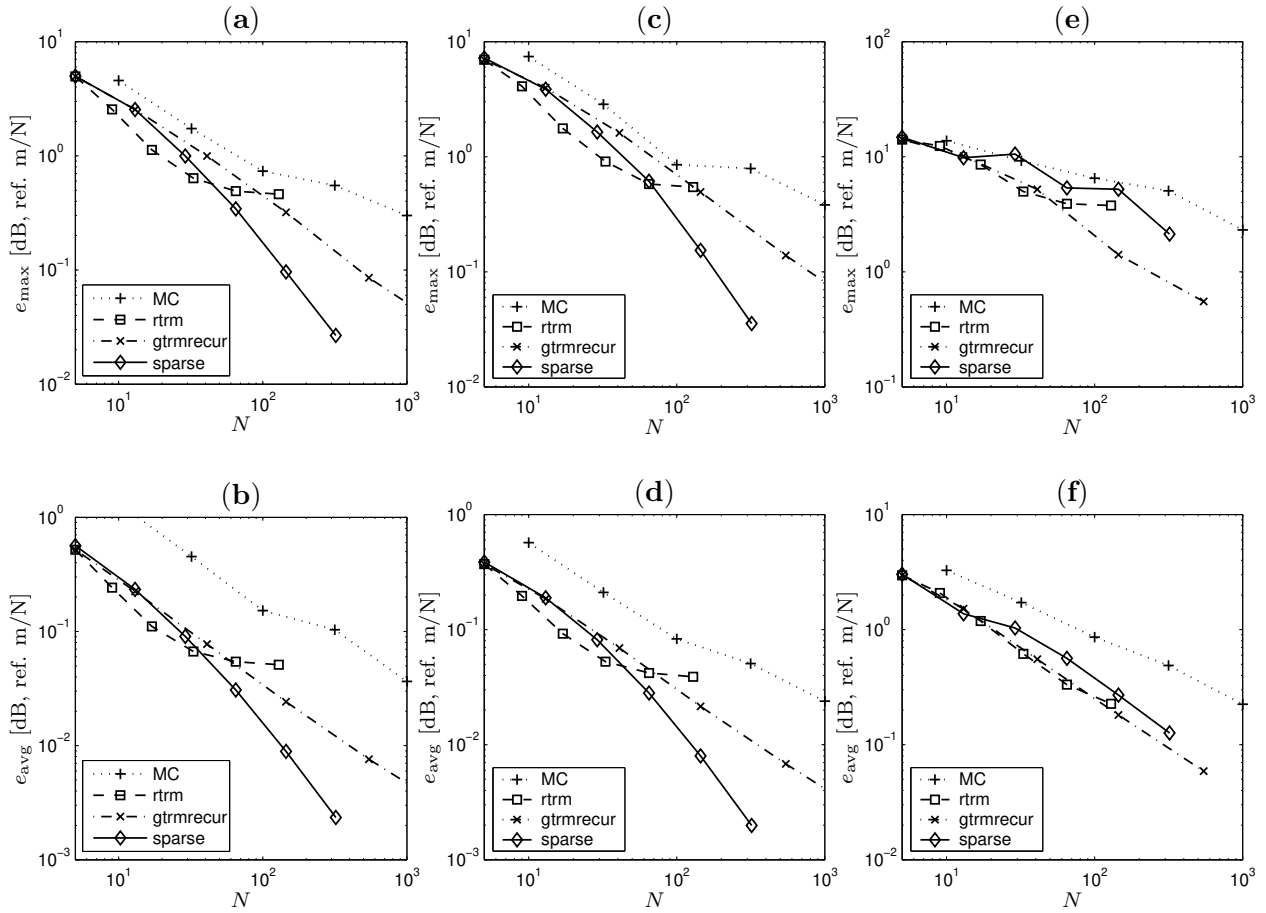


Figure 4.6: Error plots for the SEM combined with fuzzy set based methods and with MC: (a-b) uncoupled rod (c-d) coupled rod (e-f) plate case.

4.2.4 Interpretation of the results

Accuracy

All of the deterministic fuzzy set-based methods significantly outperformed the Monte Carlo analysis in terms of achieved accuracy vs. the number of required function evaluations. This is no surprise, since unlike in problems such as integration, where pure Monte Carlo methods provide the attractive convergence order of $1/\sqrt{N}$ due to the central limit theorem independently of the problem dimension, the convergence order decreases exponentially with the dimension. We emphasize that the MC method was only used here to verify the correctness of the fuzzy-set based results.

Both transformation method variants sample the corner points of the domain of the uncertain parameters, which are the relevant points when monotonicity is present. In proximity of the resonance frequencies, the response function is non-monotonic, and the sampled inner points become relevant. The reduced transformation method only samples the diagonals of the parameter domain hypercube, and is thus not guaranteed to converge to the correct result. This can be observed in the sub-plots (**b,ii-iv**) of the Figs. 4.3 and 4.4, where the envelope curve shows a kink near to the peak, which is not present in case of the other methods (**a,c,d,ii-iv**).

The sparse grid-based approach showed mixed results. In the rod case, the performance was very good. Compared to the general transformation method, a significantly better asymptotic convergence rate was achieved (see Fig. 4.6), as was shown to hold in Klimkle (2004b) for smooth functions. However, for the plate example, the encountered oscillations were too strong to be correctly resolved by an interpolant with a small number of nodes.

In summary, considering the error plot of Fig. 4.6, we suggest to use the reduced transformation method if only a *crude* approximation of the envelope is needed. For frequency response functions that do not exhibit a highly oscillatory behavior in the objective frequency domain, we suggest to use sparse-grid based approach. Otherwise, the general transformation method is most suitable.

Performance

In this section, the performance of each method will be discussed. In practice, it is of great importance to obtain simulation results quickly. We therefore give performance results of the discussed SEM combined with fuzzy set based methods in the following. All numerical tests

were carried out using MATLAB V6.5 running on a Linux i686 1.6 GHz PC.

The evaluation of the coupled rod SEM model at 1000 discrete frequencies took $t_{\text{rod}} = 0.55$ seconds. The evaluation of the plate SEM model at 1000 discrete frequencies took $t_{\text{plate}} = 24$ seconds. The overhead of the transformation method variants was negligible in all runs (i.e., less than 0.1 % of the overall computation time). The sparse grid-based approach required additional computing time depending on m and n ; this took about $t_{\text{sp}} = 25 - 40$ seconds for the considered parameters $m = 21$ and $n = 1, \dots, 5$. In case of the plate model, this overhead was insignificant due to the expensive model evaluations. The approximate overall run times can be obtained by multiplying t_{rod} and t_{plate} by N from Table 4.3, and adding t_{sp} in case of the sparse grid-based method.

Scalability

The scalability is the most important parameter to be checked. For these first examples, only problems with two uncertain parameters were addressed. In that case a maximum of about 1000 model evaluations per frequency is feasible in practice. The applicability of the reduced transformation is then limited to about $d = 8$ uncertain parameters if five α -cuts are used. For the general transformation method scaling is significantly worse, since its complexity grows with $\mathcal{O}(m^d)$. Better results than with the reduced transformation method were only achieved for more than 10 α -cuts. Therefore, only models with up to three uncertain parameters are feasible. For $d = 4$, a sparse grid interpolant of level $n = 5$ requires 1105 function evaluations. For $d = 9$, a level 3 interpolant requires 1177 evaluations, which may be still suffice depending on the smoothness of the FRF curve. Of course, it is quite needless to say that a Monte Carlo simulation would require significantly more than 1000 samples to produce reliable results in higher dimensions.

4.3 SEA Coupling Loss Factors Estimation

In this section, the general transformation method without recurring permutations, i.e., *gtrmrecur* presented in Chapter 3 is applied to the estimation of the SEA coupling loss factors (CLFs) under influence of the uncertain parameters. The CLFs can be considered an important parameter when building and solving Statistical Energy Analysis (SEA) models. In Chapter 1, a review for SEA was presented. In addition, some alternatives based on deterministic approaches to assess the CLFs were also discussed. Finite element models have been used by many authors to provide accurate estimations of CLFs. See the following works by (Simmons (1991), Steel and Craik (1994), Fredö (1997), Maxit and Guyader (2001ab), Gagliardini et al. (2003)). Also, Ahmida and Arruda (2003a) presented an efficient alternative based on the SEM to assess these parameter. Although much progress in this area has been achieved, little attention has been paid to the influence of the uncertain parameters in the deterministic model used to estimate these factors. In this context, a fuzzy method is proposed as an alternative to compute coupling loss factors. The proposed technique is applied to a coupled rod system and to a frame-type structure.

4.3.1 Case 1: Estimation of SEA CLFs for two coupled rods

For the first case, the same setup applied in Section 4.1 is used. In this simple case, two subsystems with just longitudinal waves are considered, leads to

- η_{12} : CLF between longitudinal waves incident at rod 1 and longitudinal waves transmitted to rod 2.
- η_{21} : CLF between longitudinal waves incident at rod 2 and longitudinal waves transmitted to rod 1.

In order to build a SEA model for the two coupled rod system, a formulation presented in Lyon and DeJong (1995) is reviewed. Note that, in Chapter 1, the SEA was discussed in more details and here just the main equations necessary to assess the CLFs will be reviewed.

We begin with definition of the modal density of rod, which leads to

$$n_i = 2L\sqrt{\frac{\rho_i}{E_i}} \quad (4.3)$$

where the modal density (n) of each rod is defined respectively for its physical parameters. In this case, the sub-indices i, j refer to the subsystem i for rod 1 and j for 2, respectively.

The modal overlap factor m is defined as follows

$$m_i = \omega \eta_i n_i \quad (4.4)$$

For the transmission coefficient between two rods, the rod impedance is needed, which can be defined as infinite rod impedance

$$Z_i = 2\rho_i A_i \sqrt{\frac{\rho_i}{E_i}} \quad (4.5)$$

and for the transmission coefficient, we have the following

$$\tau_{ij} = \frac{4R_i R_j}{|Z_i Z_j|^2} \quad (4.6)$$

Note that, the term R means the real part of the impedance, and for the particular case of a semi-infinite rod, the half value of the infinite one is required.

The next step is to develop a way to assess the CLFs. This can be done as follows

$$\beta_i = \frac{2m_i}{\pi} \quad (4.7)$$

$$\beta_{corr} = \frac{1}{[1 + (\frac{1}{2\pi(\beta_i + \beta_j)})^8]^{\frac{1}{4}}} \quad (4.8)$$

Going further, the CLFs is found using the following expression

$$\eta_{ij} = \sqrt{\frac{E_i}{\rho_i}} \frac{1}{2\pi f L_i} \beta_{corr} \frac{\tau_{ij}}{2 - \tau_{ij}} \quad (4.9)$$

and using the reciprocity relation

$$\eta_{ji} = \frac{n_i}{n_j} \eta_{ij} \quad (4.10)$$

In order to determine the energies values, it is necessary to assess the input power from a excitation point, which can be found using the following relation

$$P_i = \frac{(P_0)^2}{Z_i} \quad (4.11)$$

With the coupling loss factor defined and the input power found, the energies can be estimated using the matrix system defined as

$$\begin{Bmatrix} E_i(\omega) \\ E_j(\omega) \end{Bmatrix} = \frac{1}{\omega} \begin{bmatrix} \eta_i(\omega) + \eta_{ij}(\omega) & -\eta_{ji}(\omega) \\ -\eta_{ij}(\omega) & \eta_j(\omega) + \eta_{ji}(\omega) \end{bmatrix}^{-1} \begin{Bmatrix} P_i(\omega) \\ P_j(\omega) \end{Bmatrix} \quad (4.12)$$

It is important to note that with the above expression for the energies values, the energy level performed by the standard SEA equals $M\langle v^2 \rangle$, with M defined as the subsystem mass and $\langle v^2 \rangle$ the mean-squared velocity. On the other hand, to find out the total vibration energy with spectral and finite elements, the average kinetic energy is multiplied per two.

Now, with the short review presented, the energies and the CLFs can be easily estimated either by standard SEA equations or by SEM. In addition, it is interesting to also present a comparison with the energies performed with the SEM combined with the fuzzy method-*gtrmrecur*. This can be done and instead of one curve carried out, the envelope energy responses are found.

Figure 4.7 presents the results considering both, the SEA and the SEM as nominal energy responses. In this case, it is important to emphasize that for the energy of rod 1, the coupling with rod 2 is not considered, which clarified the poor results presented by standard SEA. The results for the CLFs using the standard SEA analytical expressions combined with the *gtrmrecur* are shown in Fig. 4.8. Here, it is also clear that the influence of non-deterministic input parameters for rods 1 and 2 play an important role in the CLFs estimation. Finally, Figure 4.9 show the energies estimated with the SEM combined with fuzzy method-*gtrmrecur*, which in this case are compared with the mean energy performed with the standard SEA for rods 1 and 2.

4.3.2 Case 2: Estimation of SEA CLFs for frame-type structures

In order to show the applicability of the SEM combined with a fuzzy set based method-*gtrmrecur* for estimation of the SEA CLFs of frame-type junction, an example proposed in Figure 4.10 is presented. This example is the main part of the work proposed by Nunes et al.(2005).

Table 4.4 shows the physical properties for the beams 1 and 2 with mean values and standard deviation for each non-deterministic input parameter. In this regard, it is important to emphasize that different parameterization schemes may be used for the frame junction

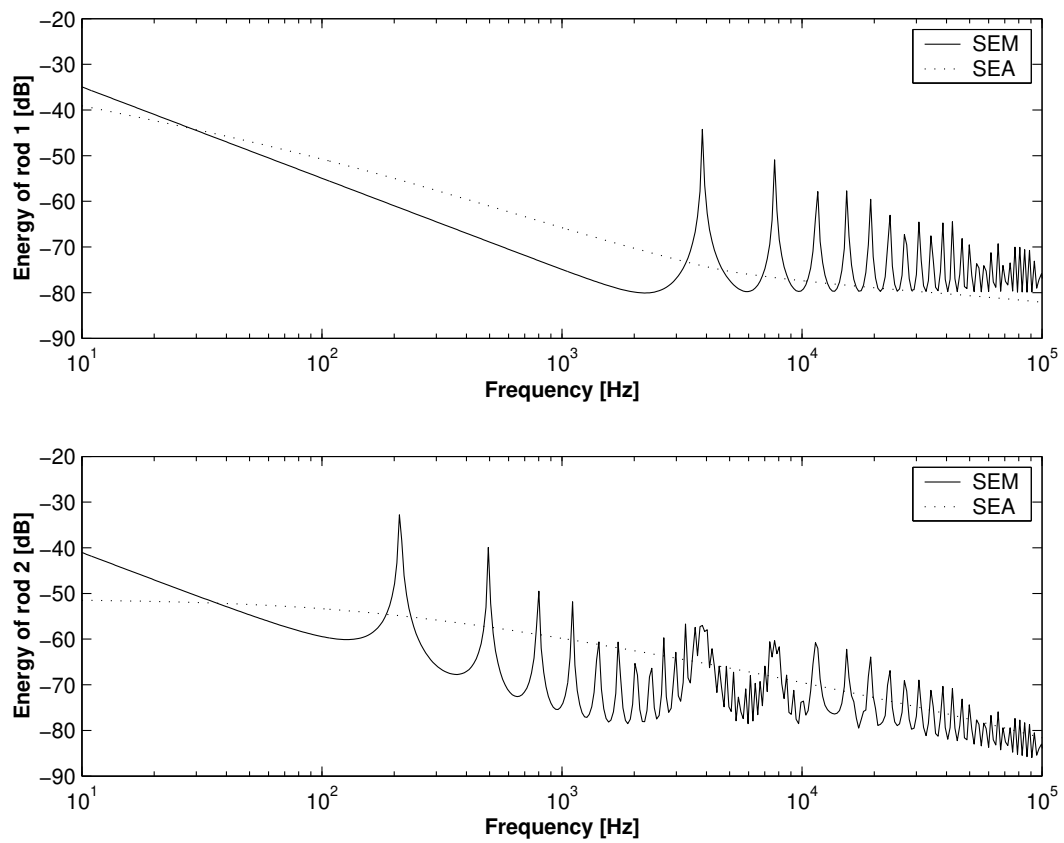


Figure 4.7: Energies for rods 1 and 2 performed by standard SEA and SEM.

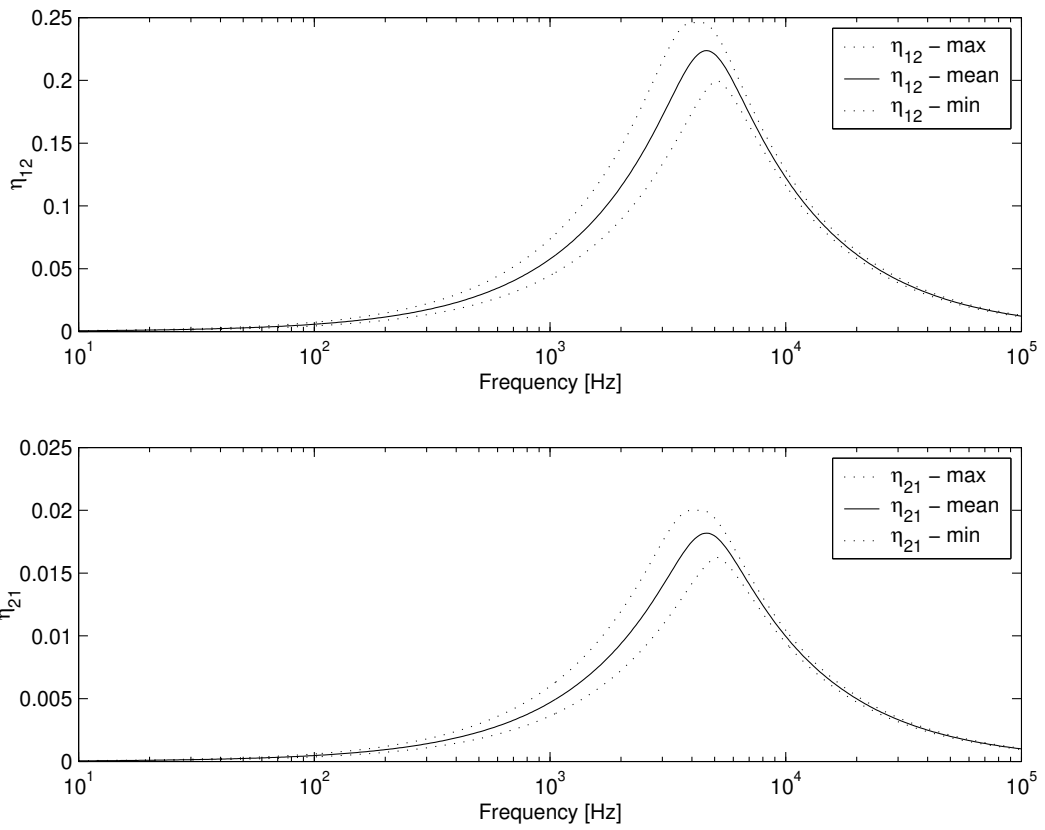


Figure 4.8: CLFs performed by standard SEA and analytical expressions with Fuzzy - *gtrmrecur*.

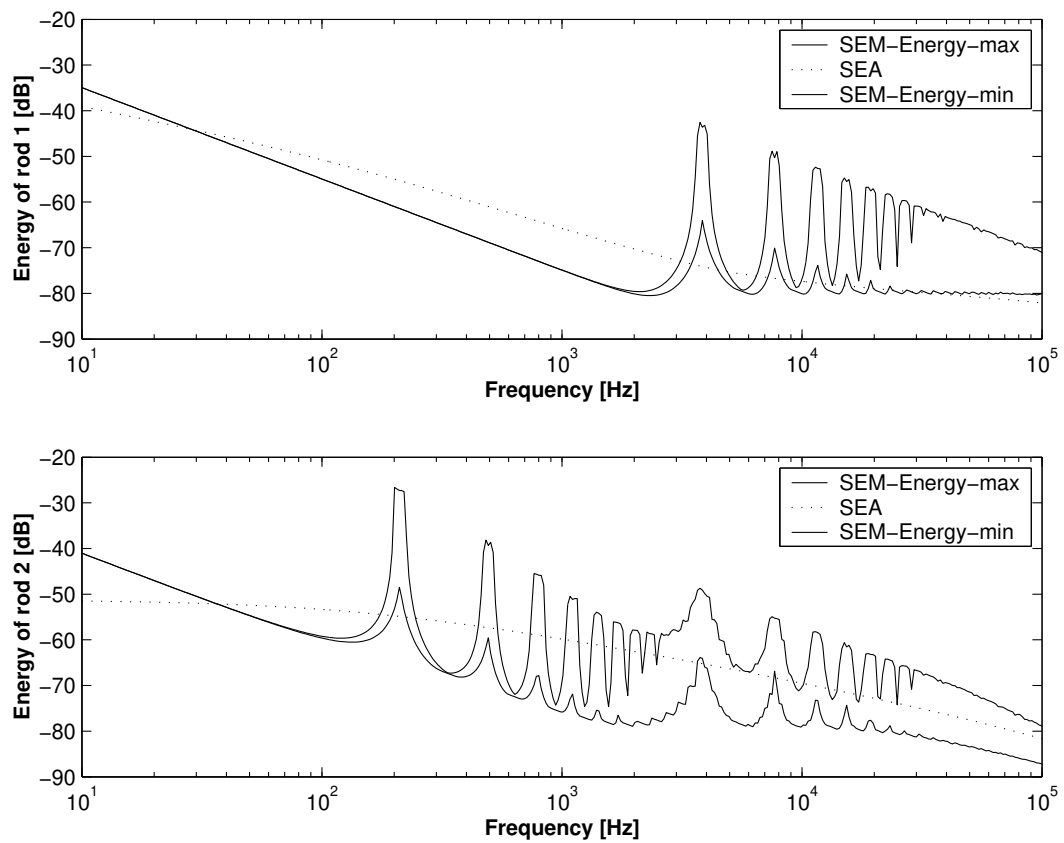


Figure 4.9: Nominal energy performed via standard SEA and energies by SEM combined with the fuzzy set based method-*gtrmrecur*.

depending on the physics of the problem at hand.

For the proposed example, the Young's modulus \tilde{E} , mass density $\tilde{\rho}$ and moment of inertia in z direction \tilde{I}_z are treated as uncertain parameters. Also, it is important to note that in this simulation, $\tilde{E}_{1,2}, \tilde{\rho}_{1,2}$ and $\tilde{I}_{z1,2}$ are not independent, i.e., $\tilde{E}_1 = \tilde{E}_2 = \tilde{E}$, $\tilde{\rho}_1 = \tilde{\rho}_2 = \tilde{\rho}$ and $\tilde{I}_{z1} = \tilde{I}_{z2} = \tilde{I}_z$. For the length of the beams $L_{1,2}$ and the cross-section areas $A_{1,2}$, the mean values are assumed. In this study a simple, and not very realistic, uncertainty model was used only for the sake of illustrating the proposed procedure. The L-beam model shown in Figure 4.10 (a) consists of two semi-infinite beams, respectively, beam 1 and beam 2 connected at an arbitrary angle θ . In this example an angle of 60° is assumed. However, it is important to stress that it is straightforward to address arbitrary angles and arbitrary number of beams converging to the junction with the SE model described here.

Table 4.4: Physical properties: beams with non-deterministic input parameters.

parameter	mean value \bar{m}	standard deviation	dimension
$E_{1,2}$	2.62×10^9	10%	N/m ²
$\rho_{1,2}$	1280	10%	kg/m ³
$A_{1,2}$	1×10^{-4}	0	m ²
$I_{z1,z2}$	8.33×10^{-10}	1%	m ⁴
$L_{1,2}$	100	0	m

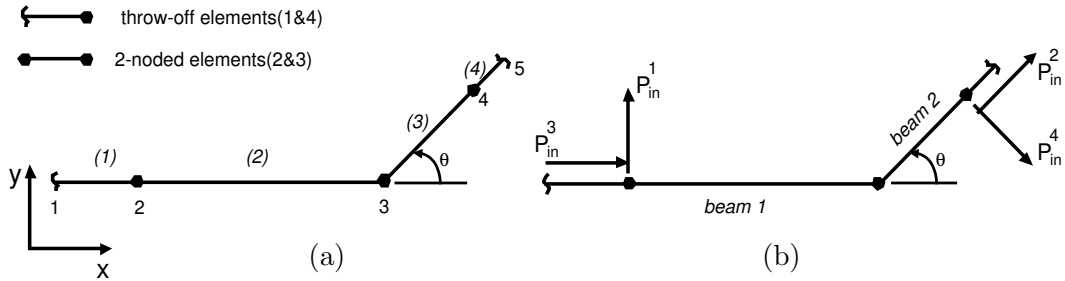


Figure 4.10: SE model for connected beams with arbitrary angle.

The SE model is composed of two 2-noded and two throw-off spectral elements as presented in Figure 4.10 (a). Using SEA methodology, four subsystems are set-up: two for longitudinal waves and another two for the flexural waves in the x - y plane. To assess the total energy in each subsystem using SEM, power is input into each subsystem and then the energy is found one at a time. See Figure 4.10 (b). The CLFs for these subsystems are defined as follows

- η_{B1B2} : CLF between flexural waves incident at *beam 1* and flexural waves transmitted to *beam 2*.

- η_{B1L2} : CLF between flexural waves incident at *beam* 1 and longitudinal waves transmitted to *beam* 2.
- η_{L1B2} : CLF between longitudinal waves incident at *beam* 1 and flexural waves transmitted to *beam* 2.
- η_{L1L2} : CLF between longitudinal waves incident at *beam* 1 and longitudinal waves transmitted to *beam* 2.

As discussed in Ahmida and Arruda (2003a), in terms of deterministic response, a good agreement with the CLFs was obtained using the SEM with the simplified expressions of Stimpson and Lalor (S&L) (1991) and using the analytical expressions of Cremer and Heckel (1988).

In the next section, the SEA CLFs will be estimated using the proposed SEM combined with the fuzzy set based method-*gtrmrecur* with the simplified expression defined in Stimpson and Lalor (1991) so that a more robust estimation of the SEA CLFs can be expected, instead of just obtaining a deterministic one.

4.3.3 Estimation of CLFs using the SEM combined with the fuzzy method-*gtrmrecur*

In this section, the CLFs estimated via the SEM combined with the fuzzy method-*gtrmrecur* are presented. Robust CLFs by means of confidence limits are provided in order to be used in SEA models. A frequency range is setup from 1 Hz to 5kHz using 1/3-octave bands.

In addition, for each frequency band analyzed, the mean square energy values were computed over 10 frequency lines. Figures 4.11 and 4.12 show the main results found using the Stimpson and Lalor approximation with the SEM combined with the fuzzy method-*gtrmrecur*.

The energies for bending and longitudinal waves in beams 1 and 2 were computed from the spectral element solution using the methodology explained in (Ahmida and Arruda, 2003b).

With an internal loss factor of $\eta = 0.001$ in each beam the energy in the throw-off elements could be neglected due to the length of the two-noded elements, i.e., equal to 100 m. For the fuzzy method combined with SEM, 7 α -cuts and a membership functions of type quasi-Gaussian shaped, clipped at plus and minus 3 standard deviations. The results include the *mean*, *maximum* and *minimum* values for the CLFs found for beam 1 and beam 2 plotted versus *Average Modal Overlap (AMO)*. In order to compute the *AMO*, the following expressions

defined in (Lyon and DeJong, 1995) are adopted

$$m = \omega\eta n \quad (4.13)$$

where m is defined as the modal overlap factor, η is the loss factor and n is the total modal density of the L-beam system, which is composed by modal densities for the longitudinal and transversal waves.

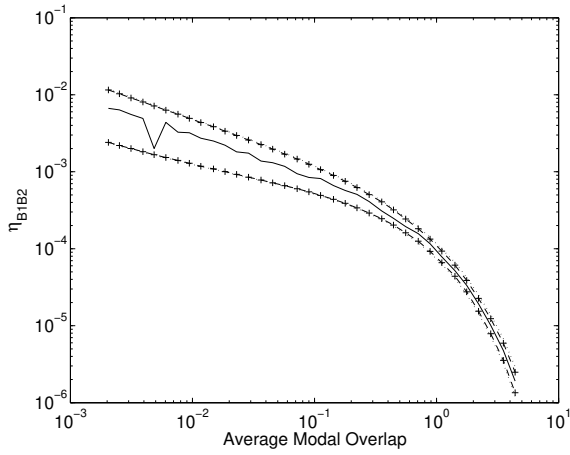
To assess the *AMO*, a central frequency band is considered. As discussed above, for each frequency band analyzed, the mean values were computed over 10 frequency lines.

Also, a Monte Carlo analysis (MC) was conducted to check the results found using the SEM combined with a fuzzy set based method. For the MC analysis considering the same uncertain parameters defined in Table 4.4, Gaussian normal distributions, but also clipped at 3σ -bounds, were adopted. They were generated by the pseudo-random number generator of MATLAB. In addition, to determine the required sample size, the following expression, suggested in Maglaras et al. (1997) was adopted

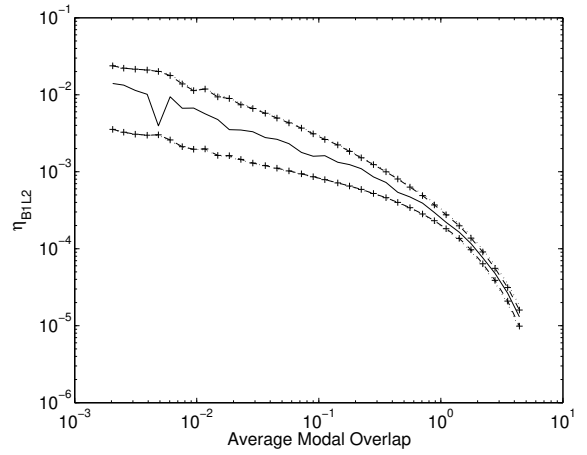
$$N = \frac{1 - P}{P - COV_P^2} \quad (4.14)$$

with P defined as the anticipated probability of failure and COV_P the desired coefficient of variation of probability of failure. The coefficient of variation is defined as the standard deviation divided by the mean. For instance, taking a probability of failure of 0.1 and a coefficient of variation of 0.1, we find, substituting these values, a minimum required N of 900. In our case, just for simplicity, we assume a sample size of $N = 1000$.

In what follows, the estimation of the SEA coupling loss factors for the two beams shown in Figure 4.10 are presented for SEM combined with the fuzzy set based method-*gtrmrecur* and the SEM combined with MC approach.

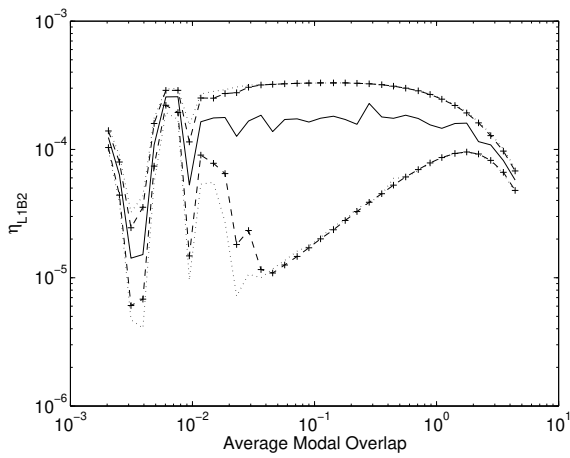


(a)

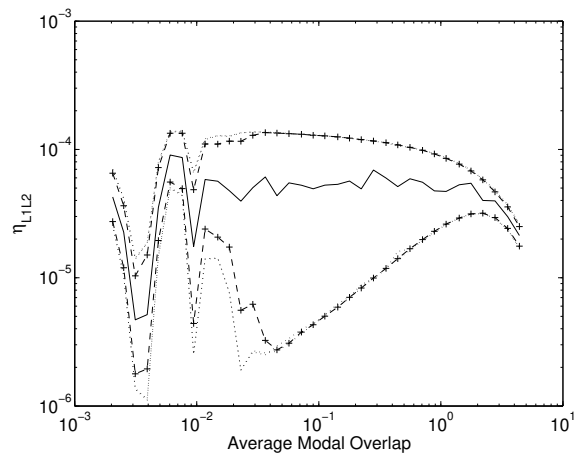


(b)

Figure 4.11: Estimation of CLFs using S&L approximation and their envelopes: (a) η_{B1B2} and (b) η_{B1L2} . SEM-nominal (solid), SEM with the fuzzy method-*gtrmrecur* (dotted-line) and SEM with MC (dashed +)



(a)



(b)

Figure 4.12: Estimation of CLFs using S&L approximation and their envelopes: (a) η_{L1B2} and (b) η_{L1L2} . SEM-nominal (solid), SEM with the fuzzy method-*gtrmrecur* (dotted-line) and SEM with MC (dashed +)

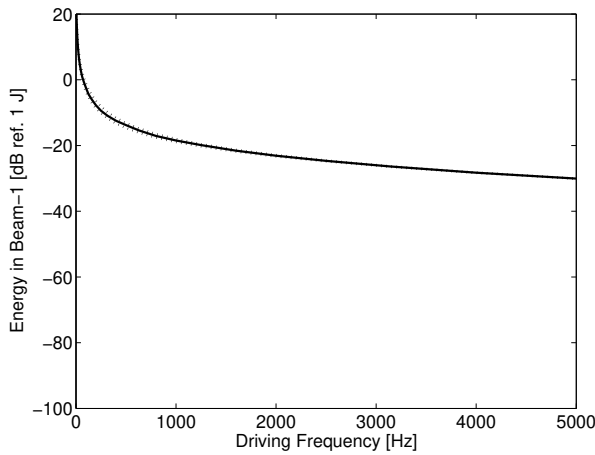
In general, Figures 4.11 and 4.12 show that the SEM combined with the fuzzy set based method-*gtrmrecur* and the SEM with MC yielded quite similar results, specially for higher *Average Modal Overlap*. However, in Figure 4.12 (a) and (b), for the longitudinal waves, some difference in the anti-resonance can be observed for the SEM with fuzzy set based method-*gtrmrecur* and SEM with MC results. In this context, it is important to add that on the basis of the transformation method, the overestimation effect is avoided.

In the next section, where the main proposal is to find the energy envelopes using the robust CLFs obtained in Figures 4.11 and 4.12, we have used just the CLFs found with the SEM with fuzzy set based method-*gtrmrecur*. In order to assess the energy levels for the 4 sub-systems described above, conventional SEA is adopted in this process.

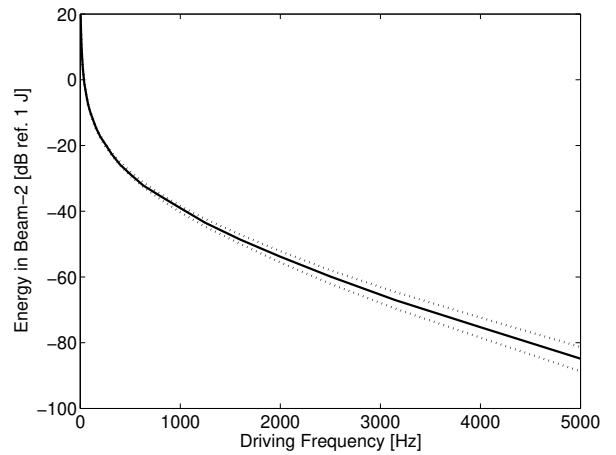
4.3.4 Estimation of energies using the SEM with the fuzzy method-*gtrmrecur*

Basically, in this section, two examples are proposed to estimate the energies levels. In the first one, the CLFs obtained with the SEM combined with the fuzzy set based method-*gtrmrecur* are adopted with a unit power to the subsystem associated with transverse waves on beam 1 to assess the energy levels, i.e., *maximum*, *mean* and *minimum* values. In the second, the same CLFs obtained above, instead, are combined with the power input envelopes of each subsystem in order to build the confidence energy limits. The second example is proposed in order to show that uncertainty in the input power plays an important role in SEA analysis. See for example the recent paper presented by Davis (2004), where the uncertainty in the predictions are presented as three separate problems. The first concern is due to uncertainty in the input power, which is demonstrated as the major issue. The second is regard to uncertainty in the transfer functions, and finally uncertainty due to the definition of SEA model and its subsystems. Here, the two examples proposed are mainly focus on two of those concerns, which means, uncertainty in the input power and transfer functions addressed to the influence of the input physical parameters.

Figures 4.13 and 4.14 show the results for the transversal and longitudinal energies for beams 1 and 2 for the first case, i.e., the energies were computed for a unit power input to the subsystem associated with transverse waves on beam 1. In this first example, it is important to add that the effects of uncertain parameters increase when the central frequency increase, which is clearly presented in Figures 4.13(b) and 4.14(a).

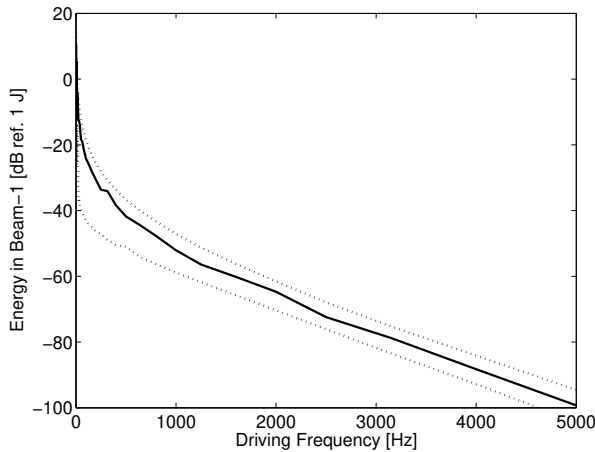


(a)

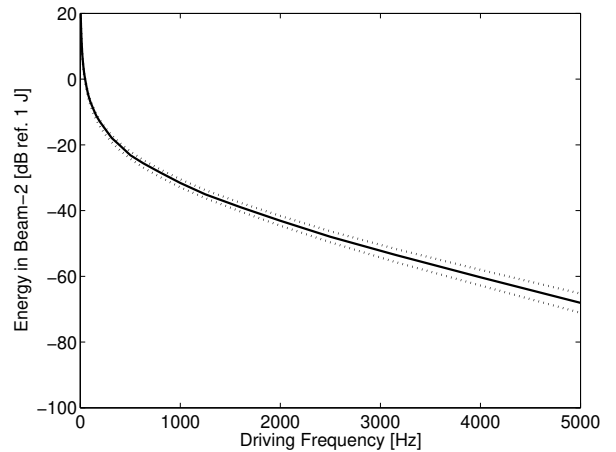


(b)

Figure 4.13: Energy levels for the beams 1 and 2 using CLFs estimated with SEM combined with fuzzy method-*gtrmrecur*: (a) Transversal energy in beam 1 and (b) Transversal energy in beam 2. *Max* and *Min* energies (dotted-line) and nominal energy (solid)



(a)



(b)

Figure 4.14: Energy levels for the beams 1 and 2 using CLFs estimated with SEM combined with the fuzzy method-*gtrmrecur*: (a) Longitudinal energy in beam 1 and (b) Longitudinal energy in beam 2. *Max* and *Min* energies (dotted-line) and nominal energy (solid)

In the second example, the energy limits are performed using the same CLFs, however, including the respective envelopes obtained with the input powers, i.e., input powers *max*, *min* and *mean*. To assess those values of input power, for each point mobility, the respective force and velocity are assessed using the following expression

$$P_{in} = \frac{1}{2} \Re(F \cdot v^*) \quad (4.15)$$

where F is the affecting point force, in this example simulated with 1 N, \Re is the real number specified under simulation and v^* is the complex conjugate velocity at the same point where the force acts. In the case of displacement u assessment, velocity is defined as $v = i\omega u$, which leads to $P_{in}/\omega = -(F \cdot \Im(u))/2$. In this regard, the imaginary part (\Im) of displacement at the node where the force is applied is always negative and the input power is always positive.

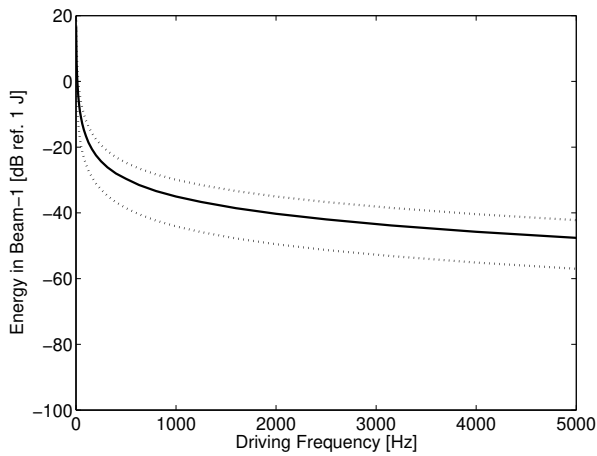
Figures 4.15 and 4.16 shown those plots. Basically, note that the envelope energies found considering the power input for each subsystem have greater influence in the estimation final result as a whole.

To summarize, both examples show that, using the SEM with the fuzzy set based method-*gtrmrecur*, it is possible to take into account the influence of the uncertain input parameters into a SEA model. In addition, one important fact to add from example 2 is that in terms of input power, it is recommended that such envelope might be considered in this analysis. This is clarified based on results presented in Figures 4.13 (a) and 4.15 (b). Thus, either CLFs and input powers envelopes can be well estimated via SEM with the fuzzy set based method-*gtrmrecur* and more robust energy levels can be found.

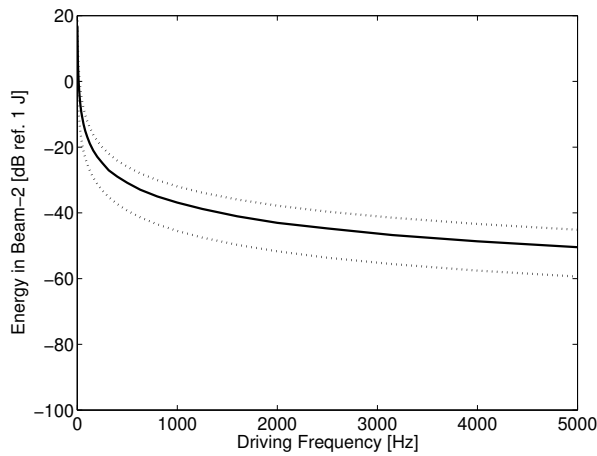
In terms of the scope proposed, both examples assumed that some of the input parameters contain uncertainty, which can be considered for the specialist that those hypotheses are taken as *possible* to occur.

For a new projects, not much information is available and uncertainty is predicted based upon the experience in former projects. On the one hand, as the development cycle evolves and more experimental data becomes available, a more accurate parameter variation prediction can be made. The pressure to develop new products in shorter time means, in most cases, that there is no time to set up many experiments to provide power density functions (PDF) of model parameters. However, in the case for which input data with PDF are available, more accurate models can be obtained combining both theories, i.e., *possibility* and *probability*.

Therefore, for an initial estimation of the influence of non-deterministic input parameters, the SEM combined with fuzzy set based methods proposed here can be helpful to address uncertainty in frame-type structures.

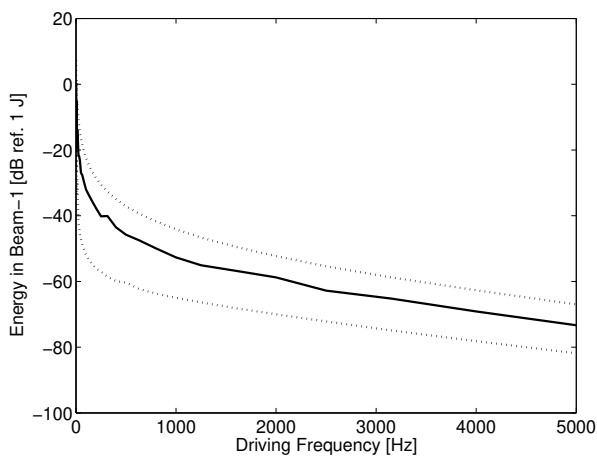


(a)

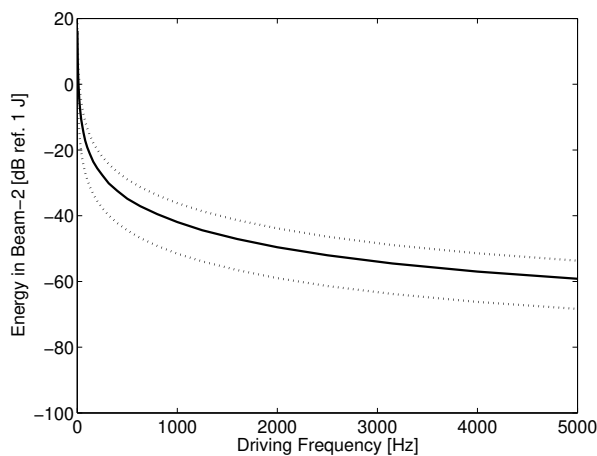


(b)

Figure 4.15: Energy levels for the beams 1 and 2 using CLFs and power input estimated with the SEM combined with the fuzzy method-*grmrecur*: (a) Transversal energy in beam 1 and (b) Transversal energy in beam 2. *Max* and *Min* energies (dotted-line) and nominal energy (solid)



(a)



(b)

Figure 4.16: Energy levels for the beams 1 and 2 using CLFs and power input estimated with the SEM combined with the fuzzy method-*grmrecur*: (a) Longitudinal energy in beam 1 and (b) Longitudinal energy in beam 2. *Max* and *Min* energies (dotted-line) and nominal energy (solid)

4.4 Summary

In this chapter, a spectral element method combined with fuzzy set methods was proposed to perform frequency response function envelopes for structures under uncertain input parameters. Initially, to discuss in more details the different application of the extension principle, two different test problems were presented. Although those test problems considered only two simple examples, very important conclusions were made in terms of different alternatives of implementation of the extension principle compared with the Monte Carlo simulation. One important conclusion is that the SEM combined with the fuzzy method using the *rtrm* is suggested to get a first approximate solution with just few function evaluations. In the case of FRFs that are sufficiently smooth, which was the case of the rod example, the sparse grid method performs better. For FRFs that have very high curvature, i.e., for example the plate case set-up, the sparse grid method did perform better than the other fuzzy set methods proposed. The SEM combined with MC is significantly inferior to the SEM combined with fuzzy set based methods proposed, specially in terms of function evaluations and error plot. Additionally, the SEM with fuzzy set based method was also adopted to estimate the SEA coupling loss factors (CLFs), which is another important area to be covered with this approach. Finally, two test problems were selected to show the applicability of the SEM combined with fuzzy set based methods for CLFs estimation.

Chapter 5

Initial Design Phase Considering a Non-Deterministic Dynamic Analysis

This chapter provides a numerical example using a fuzzy set based method in the initial design phase of a new engineering project. Based on the fundamental ideas presented in former chapters, the main focus here is to give more insight on how to apply the concepts of the methodology proposed. Our chosen example consists of an automotive application, where the use of reinforced panels is proposed.

5.1 Describing our Example Problem

In the present stage of industrial development, the characteristics of new materials become one of the main issues. Important industries, such as the automotive, aerospace and naval industries, require less weight and more resistance for new material applications, and one attractive alternative is the use of composite materials. In this sense, the main idea is to have materials with high mechanical resistance combined with weightlessness. However, composite materials are not suitable in applications where there is a high temperature or an aggressive environment (Agarwal and Broutman, 1990).

Considering the above, one alternative applied in the industry is to adopt reinforced panels, which in general are composed of panels reinforced with beams. In those applications, the idea is to add local stiffness, without adding excessive weight to the structure. In terms of dynamic behavior, as discussed in previous chapters, this presents some important modelling challenges, since panels generally have a much higher modal density than reinforcement beams. To give an example, Figure 5.1 shows a floor area applied in the automotive industry, where transversal and longitudinal beams are added to the main panel to provide local stiffness.

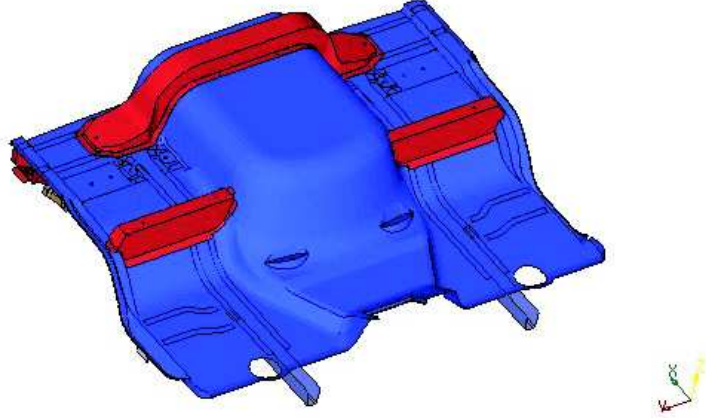


Figure 5.1: Floor area with reinforcement applied in the automotive industry.

In this context, we would like to provide in this chapter a numerical example using the concepts presented in the former chapters using a fuzzy set based method. The numerical example used here is the same discussed in Chapter 4, Figure 4.2. It consists of a simply supported plate with reinforcement beams.

Before presenting the main results found using the concepts of fuzzy set based methods, the plate model is discussed and some important considerations and limitations using the present methodology are presented.

5.2 Dynamic Modelling of the Example Structure

5.2.1 Finite element model

Considering a reinforced plate model with a thickness equal to $h = 2$ mm, the wave number using the Kirchhoff theory is given by $k = 1.3347\sqrt{f}$, where f is the frequency in Hz. The wavelength is then equal to $\lambda = 4.707/\sqrt{f}$. Considering a maximum dimension, $Lx = 0.70$ m, and assuming the *rule-of-thumb*, which recommends that 6 to 10 linear elements per wavelength are necessary to correctly describe the dynamic behavior. Now, assume the expression suggested by Langley (1998), which says that the number of nodes necessary to model a structure with length L and wavelength λ is computed by $(8L/\lambda)^r$, where r is defined for plates as $r = 2$. Thus, we have for this example a total of $1.41f$ nodes, i.e., consider that in a 3D analysis we have 6 DOFs per node, for a frequency range of up to 1kHz, it leads to 8460 DOFs to perform such an analysis. In addition, in Appendix D of this thesis, the

FEM and the SEM for a reinforced plate are compared for frequency response function (FRF) analysis.

For the present simple case, the number of DOFs, considering typical computers adopted in CAE developments, a low computational effort is required. However, in a more realistic scenery, if we change the present dimension to $L = 10$ m, which is a typical size in aerospace applications, we should have a model with approximately 2 million DOFs. For the present development stage of commercial FE codes and computers, such a number of DOFs is computationally expensive, but still feasible in terms of dynamic analysis. However, if we intend to treat problems considering non-deterministic input parameters and to increase the frequency range of applicability, much more computational effort is required. This is the situation where methods such as the SEM might be suggested.

5.2.2 Spectral element model

The SE model for the reinforced plate example is shown in Figure 5.2 (a). Also, to give an example comparing with FEM, in Figure 5.2 (b) the respective reinforced plate is presented. For the FE model, HEXA elements consisting of 6806 nodes and 3280 elements were used to describe the reinforced plate model.

In the context above, the biggest advantage of the SEM compared with FEM is that the number of elements needed to model the reinforced plate with the SEM is only 6 elements. For the present SE model, the response is obtained with 10 propagation modes for the frequency range DC-2 kHz.

On one hand, the SEM demands less computation effort than FEM, which, for the mid-high frequency range is an important factor. On the other hand, the negative point for the SEM is that in its present stage, this technique is quite limited with respect to the geometries that can be treated (see Appendix D).

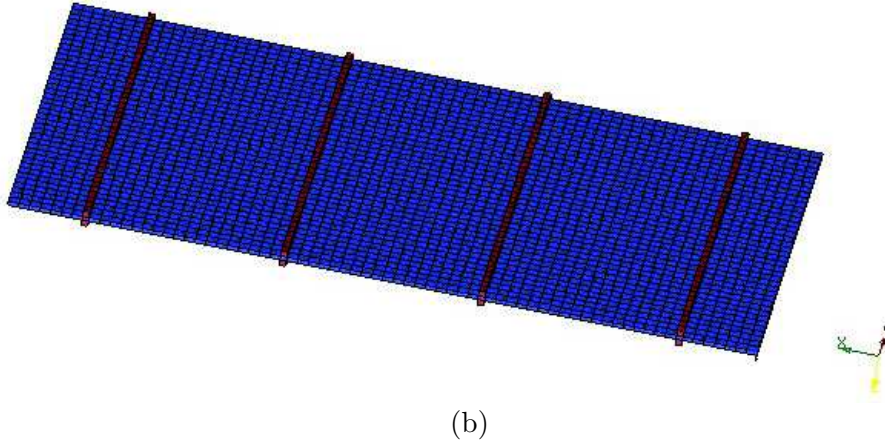
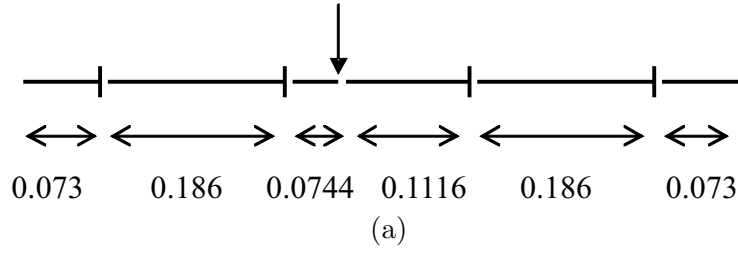


Figure 5.2: Scheme for the spectral element and finite element mesh for the reinforced plate: (a) SEM and (b) FEM.

5.3 Non-Deterministic Input Data

5.3.1 *Uncertainty, variability and error*

In this section, using the definitions proposed in Chapter 2 for *uncertainty, variability, error* and their extensions, we first select our input data according to these definitions.

Initially, we begin with the analysis of the *variability*. Considering our plate model, material properties and manufacturing tolerances should be considered with this definition. This include the following data: Young's modulus $E = 69$ GPa, Poisson's ratio $\nu = 0.3$, mass density $\rho = 2700$ kg/m³ and the geometrical dimensions, such as $Lx = 0.70$ m and $Ly = 0.40$ m. For the reinforcements of the plate with a beam rectangular section, we will just consider the moment of inertia $Ib = 1.687 \times 10^9$ m⁴.

Furthermore, as suggested by Moens and Vandepitte (2004), the term *variability* could also be limited to lack of knowledge, where the information on the likelihood is missing or simply no information of the possible bounds are available. In this case, they suggest the

concept of *uncertain variability*, because there is a lack of knowledge.

For this first group of uncertain parameters, we have found additional information from experimental results obtained for the thickness h , which will be considered in our project. An experiment was conducted considering only one prototype plate system, where the thickness of the plate was measured for a grid of 209 points. The measurement uncertainty was $10 \mu\text{m}$ for a confidence level of 95 %. The temperature was 20°C . For the sample considered, a mean value of the thickness equal to $h = 4.128 \text{ mm}$ with a standard deviation equal to $\sigma_h = 6.93\%$ was found.

Note that, if we consider that such an experiment is representative of the ensemble of produced panels, the initial definition of the source on non-determinism applied to the parameter h should be changed to *certain variability*, because the variability range and the likelihood would be known.

Although we know that for one sample such a measurement is not representative of the ensemble, for our plate model, only to illustrate the concepts discussed above, we assume that the h is classified as *certain variability*. In Figure 5.3, a histogram for the thickness value with the symmetric quasi-Gaussian membership function clipped at 3σ -bounds are adopted to represent it.

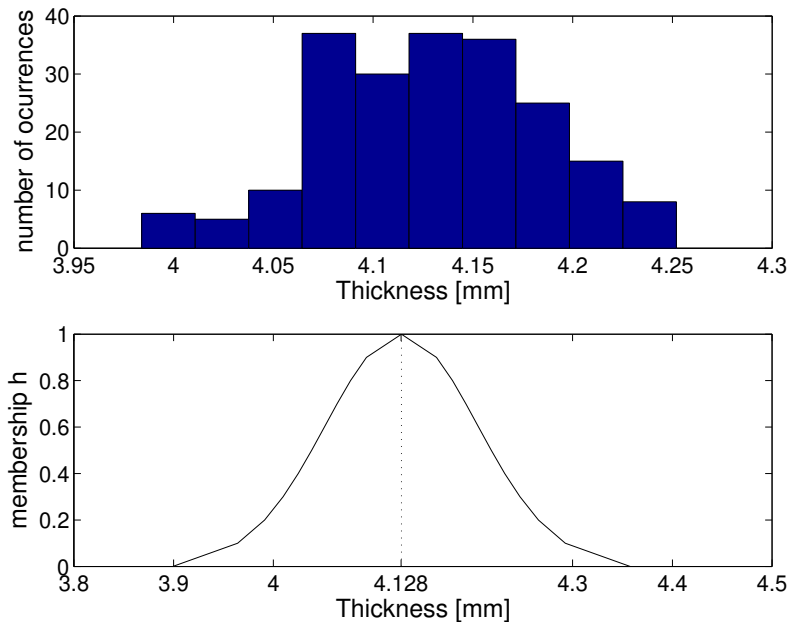


Figure 5.3: Experimental data for the thickness h with respective histogram and quasi-Gaussian approximation adopted for membership function.

Considering the term *invariable uncertainty*, in our plate model, this can refer to the damping, the input force and also the boundary conditions, which are generally assumed constant in numerical models. In our plate model, the boundary conditions are considered constant, but in real problems they can be a major source of uncertainty. Also, based on experimental results discussed in Albuquerque et al. (2004), for the internal loss factor, a mean value equal to $\eta = 0.001$ and a standard deviation of $\sigma_\eta = 5.56\%$ are adopted.

Again, it is important to emphasize that, for the η measured value, the result only considered one sample structure, i.e., without any selection of a representative statistical group of the same type of structure. In practical terms, this would mean building and testing many nominally plates and measuring the effects of non-deterministic input data (Maglaras et al., 1997). In terms of a realistic application, in general, it is impractical or simply too difficult to have such a group of measurements.

Additionally, for some practical applications in the aerospace industry, e.g. in Marczyk (2004), it is found that the coefficient of variation (CV) for a dynamic load P around 20%. Although in our case the reinforced plate is applied to the automotive industry, the idea to add the dynamic load as *invariable uncertainty* is quite convenient.

Therefore, for the initial design phase, the type of load and their amplitudes can also be important issues, and are generally considered deterministic in FE analysis. Thus, based on test results presented in Marczyk (2004), the dynamic load P in our plate problem assumed non-deterministic and represent by a membership function.

In Figures 5.4 (a,b), the triangular shape membership functions for the η and P adopted to represent the non-deterministic input parameters are shown.

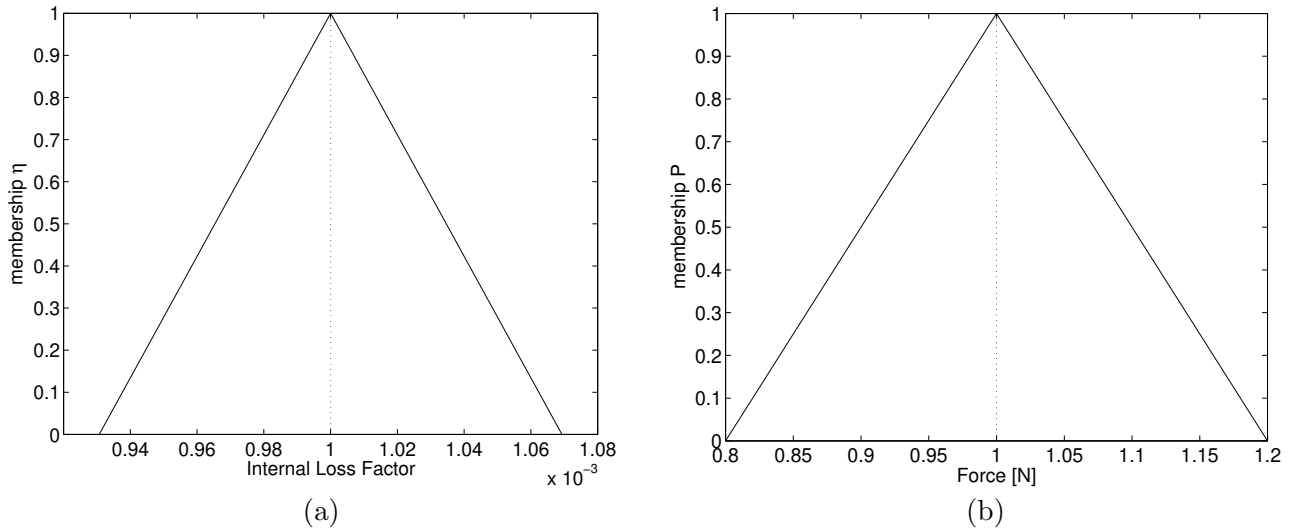


Figure 5.4: Uncertain parameter for the (a) internal loss factor $\tilde{\eta}$ and (b) force \tilde{P} for the reinforced plate model.

In terms of the *error* concept, which can be applied to modelling assumptions, the limits based on the Euler-Bernoulli beam theory and the Kirchhoff model for plates might also be considered. In this context, if we take the FE plate model discussed in Section 5.2.1, and if we don't have such a discretization, our result might be a poor estimate and an *error* may be introduced in our model.

Going one step further, we can select in our plate model each parameter separately, according to its definition. Table 5.1 summarizes the mean and standard deviation values proposed. Also, for each non-deterministic parameter we add two extra information, which consist of the type of membership function selected and type of non-determinism in our numerical modelling. Here, we select only fuzzy numbers represented by symmetric membership functions. The reason for such a choice is that for the fuzzy set based method to be used, the General Transformation Method avoiding recurring permutations (*gtrmrecur*) using symmetric membership functions require significantly less function evaluations than the original version of the General Transformation Method (*gtrm*) algorithm. The alternative *gtrmrecur* algorithm was treated in Chapter 3.

Table 5.1: Plate properties with non-deterministic input parameters.

input parameter	mean value \bar{m}	standard deviation σ	dimension adopted	membership function	source of non-determinism
E	69×10^9	5%	N/m ²	triangular	<i>uncertain variability</i>
ρ	2700	5%	kg/m ³	triangular	<i>uncertain variability</i>
ν	0.3	5%	—	triangular	<i>uncertain variability</i>
Lx	0.400	1%	m	triangular	<i>uncertain variability</i>
Ly	0.704	1%	m	triangular	<i>uncertain variability</i>
h	0.004	6.93%	m	quasi-Gaussian	<i>certain variability</i>
Ib	1.687×10^9	1%	m ⁴	triangular	<i>uncertain variability</i>
η	0.001	5.56%	—	triangular	<i>invariable uncertain</i>
P	1	20%	N	triangular	<i>invariable uncertain</i>

In the next Section, a sensitivity analysis will be done for the plate model with the non-deterministic input parameters described in Table 5.1. The main idea is to obtain the degree of influence of each parameter in the response envelope.

5.4 Sensitivity Analysis: Degree of Influence of the Non-Deterministic Input Parameters

We initially perform a sensitivity analysis in order to check the degree of influence of each non-deterministic parameter separately. After selecting the most important parameters that contribute to the response of our dynamic system, we perform a new analysis adopting just the parameters selected. To perform the sensitivity analysis, we adopt the procedure described in Hanss and Klimke (2004a). In that work, the degree of influence provided by the transformation method is compared to the classical one derived from differential calculus.

In order to give a brief description of the procedure, the idea is to adopt the total differential df of the model function $f(p_1, p_2, \dots, p_n)$ to assess the degree of influence of each parameter $p_i, i = 1, 2, \dots, n$, where n are the uncertain parameters. The total differential at the point $\bar{P} = (\bar{x}_1, \bar{x}_2, \dots, n)$ is given by

$$df = \sum_{i=1}^n \frac{\partial f}{\partial x_i}(\bar{P}) dx_i \quad (5.1)$$

where df is an approximation of the overall change rate of the function value $f(\bar{P})$. This is the case when the input parameters x_i are changed by dx_i around \bar{x}_i . In this expression, we can interpret that for each input change dx_i , a separate contribution by $(df)_i$ to the overall change rate df can be determined. If assuming that the change rate dx_i of the i th input

parameter is constant percentage c of its corresponding value \bar{x}_i , then the following can be done

$$df = \sum_{i=1}^n (df)_i = c \sum_{i=1}^n \bar{x}_i \frac{\partial f}{\partial x_i}(\bar{P}) \quad (5.2)$$

where dx_i in Eq. 5.1 is replaced by $c\bar{x}_i$.

Going further, a relative degree of influence can be determined in terms of the normalized change rates ρ_i^* of each parameter as follows

$$\rho_i^* = \frac{|(df)_i|}{\sum_{q=1}^n |(df)_q|} = \frac{|\bar{x}_i \frac{\partial f}{\partial x_i}(\bar{P})|}{\sum_{q=1}^n |\bar{x}_q \frac{\partial f}{\partial x_q}(\bar{P})|} \quad (5.3)$$

also satisfying the consistency condition

$$\sum_{q=1}^n \rho_q^* = 1 \quad (5.4)$$

However, in terms of a realistic application, the total differential procedure can only be determined for a model function f described in analytical form. In this regard, a common procedure adopted in practical engineering is replacing the derivative by a finite difference approximation

$$\frac{\partial f}{\partial x_i}(\bar{P}) \cong \frac{f(x_1^0, \dots, x_i^0, \dots, x_n^0) - f(x_1^0, \dots, x_i^0 - h_i, \dots, x_n^0)}{h_i} \quad (5.5)$$

where h_i is defined as the mean value of the *upper* and *lower* bounds of the interval X_i^0 at the membership level α_0 (see Eq. (2.27) defined in Chapter 2).

5.4.1 Results using a sensitivity analysis

Next, we present the main results found using the sensitivity analysis for the plate with non-deterministic input parameters. The results are presented for different frequency ranges in order to give more detail about the most important parameters to be selected.

In conducting a sensitivity analysis, the degree of influence of all input data can be found and the most important parameters that contribute to the response of the dynamic system can be selected.

Considering Figure 5.5, we can select from our original group of non-deterministic input parameters, four parameters with a higher contribution: Lx , h , E and ρ .

Therefore, taking only these four parameters selected, we can avoid extra computational effort by taking into account only the parameters that have more influence in the dynamic behavior of our plate model. Basically, for the present reinforced plate model, the effects of manufacturing tolerances and material properties uncertainty are responsible for the non-deterministic behavior in our numerical model. In the next section, we introduce the concept of *target* applied in the initial design phase. Also, the effects of non-deterministic input parameters are discussed.

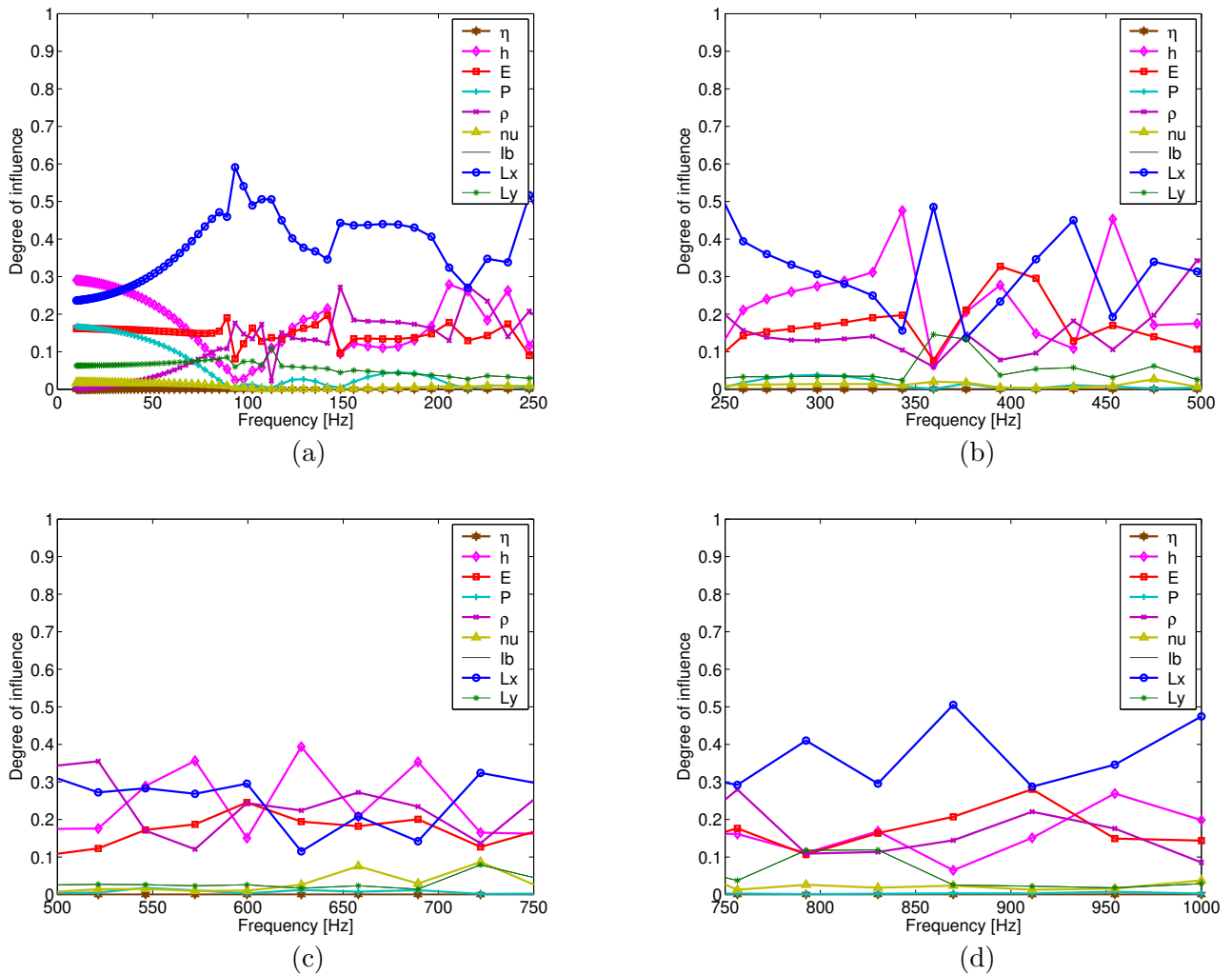


Figure 5.5: Degree of influence for the non-deterministic input parameters of the reinforced plate model.

5.5 *Targets* during the initial design phase

In the automotive industry, during the initial design phase, it is quite common practice to work with CAE models to give some initial information, for instance, on vibration and acoustic comfort. At this point, FE models are built to provide a possible way to check the new concepts. When using numerical models whilst considering vibration and acoustic applications, the dynamic behavior is verified and some possible changes are suggested. This can be a concern with respect to receptance responses, mobility points, sound pressure levels at the driver's ear, vibration comfort (mounts, suspension and so on) and the dynamic stiffness. In this context, another practice is to adopt initial *limits* also called *targets* based on former projects. The concept of the *target* is defined as a *limit* that can be used to have an initial idea about the behavior (vibration and acoustic) of the new structure. During the development phase, it is also common practice that as more data becomes available, new *targets* or *limits* are proposed. The important concept to have in mind is that the initial *target* is helpful to give an initial idea about the virtual CAE project.

In the situation presented above, a question arises as to how to take into account the influence of the non-deterministic input parameters in this initial design phase. In order to address this problem, one idea is to apply the concepts discussed in this work, where fuzzy set based methods have been suggested. Here it is also important to emphasize that other alternatives have been discussed in the literature, such as the probabilistic framework. However, we decide that the available data is neither representative nor applicable in terms of probabilistic concepts. For this reason, we select, in this initial design phase, the use of a fuzzy set based method.

In the next section, the dynamic behavior of the reinforced plate model taking into account the influence of the non-deterministic input parameters and the concept of the *target* value will be presented.

5.6 Dynamic Behavior of the Reinforced Plate Model

5.6.1 Initial design requirements

We assume that, in the present set-up, just one drive point is required in our dynamic response analysis. In terms of SE modelling, if we add more points, additional elements must be considered. For the boundary conditions, the reinforced plate is simply supported

in the yz -plane and free-free in the xz -plane. The drive point is taken at position $(x, y) = (333.4, 160)$ mm. Here, the drive point location is chosen based on previous results presented by Albuquerque et al. (2004). However, in a more realistic situation, such as in the automotive application, such a choice might be, for instance, based upon mounts locations, points located at suspension areas, chassis and so on. To assess the frequency response function (FRF), a frequency range up to 1 kHz is chosen.

In addition, an *upper limit* on the receptance at the drive point on the structure is set as equal to 10^{-4} m/N for a fixed damping, i.e., constant internal loss factor equal to $\eta = 0.001$. Note that, in our plate model, such a *target* is suggested only between 250 Hz to 1kHz, which can be justified in terms of the high dependence of the damping value in the low frequency range, i.e., up to 250 Hz.

Therefore, in this initial design phase, our reinforced plate system *fails* if the receptance response exceeds this *limit* for the frequency range up to 250 Hz. It is important to add that, in the present setup, such a *limit* is not available from experimental data. Thus, this *limit* is *assumed* in our problem based on a preliminary study from a *similar structure*. In additional, during the initial design phase, such an assumption is generally based on former projects, which is a common practice adopted in the automotive industry.

5.6.2 Deterministic receptance response and *target*

Figure 5.6 shows the vibration *limit* proposed, where the reinforced plate model in this initial phase *fails* if the receptance response is above this *limit* or *target*.

It is again important to emphasize that a nominal damping equal to $\eta = 0.001$ is selected, which leads to say that the vibration peaks observed above 250 Hz in our present case study must lie within this *target*, which is the case for the deterministic response.

For some other general application, i.e., without any initial information about damping, the peak values are much dependent on the damping adopted, which in our example is very low due to the simplicity of the reinforced plate model adopted.

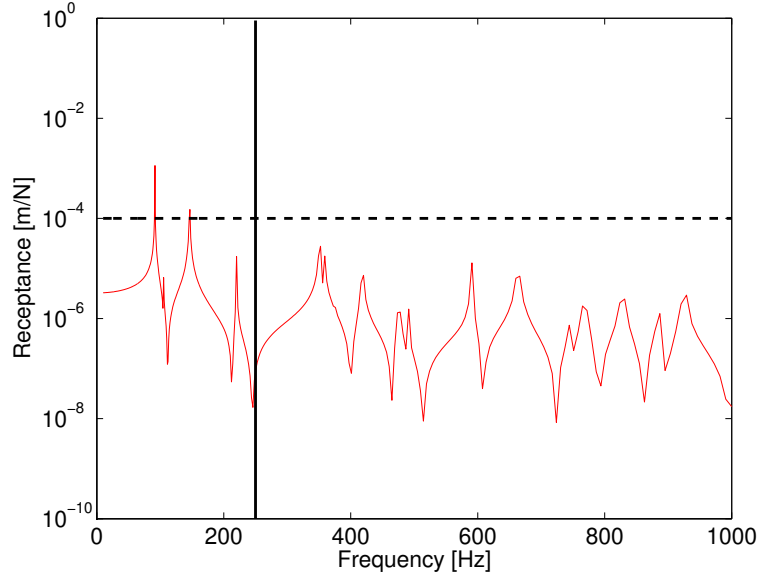


Figure 5.6: Deterministic receptance response (solid line) at the drive point with the *target* (dashed line) proposed.

In the next section, the vibration behavior of the reinforced plate model considering the effects of non-deterministic input data will be considered. At this stage, a fuzzy set based method might be a good alternative to check this effect, which means computing the envelopes for frequency response function, i.e., the *max* and the *min* receptances.

5.6.3 Envelopes for the Receptance

The fuzzy based method called *gtrmrecur* (see Chapter 3) is used to assess the envelopes for the panel receptance. Even when applying the *gtrmrecur* algorithm proposed by Klimke (2003) which removes recurring combinations from the evaluation by reusing the inner points of the α -cuts and thus, reduces the number of real function evaluations, it is important to emphasize that a preliminary sensitivity analysis, such as the one presented in Section 5.4.1, is recommended in practical applications to avoid excessive computational effort.

To assess the envelopes for the receptance curve, the number of α -cuts used in the *gtrmrecur* is chosen to be $m = 3$, $m = 5$ and $m = 9$. Figures 5.7, 5.8 and 5.9 show the results for different numbers of α -cuts and the *target*. Note that the main difference observed in Figures 5.7, 5.8 and 5.9 is that increasing the number of α -cuts, the envelopes become more *smooth* in the peaks and anti-resonances. In Chapter 4, for the same plate model, 17 α -cuts were used with very *smooth* envelopes found.

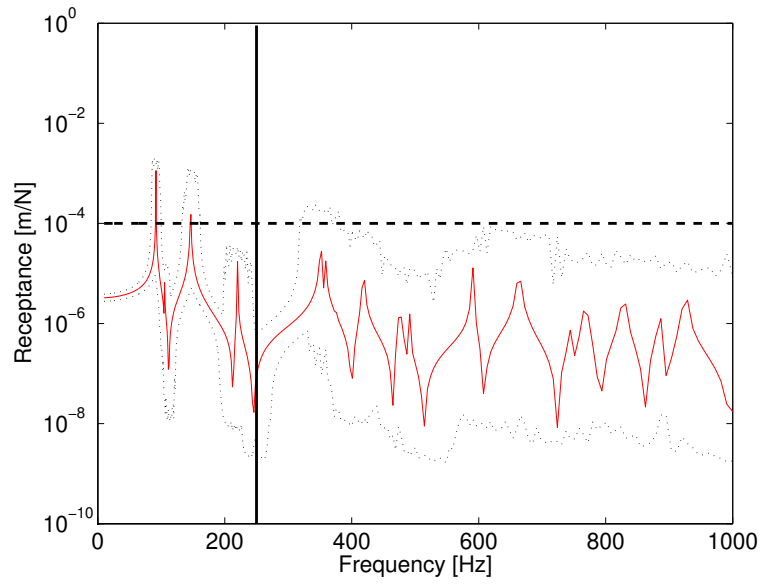


Figure 5.7: SEM-*deterministic* (solid), SEM combined with *gtrmrecur* using 3 α -cuts: envelopes (dotted line) and *target* value (dashed line).

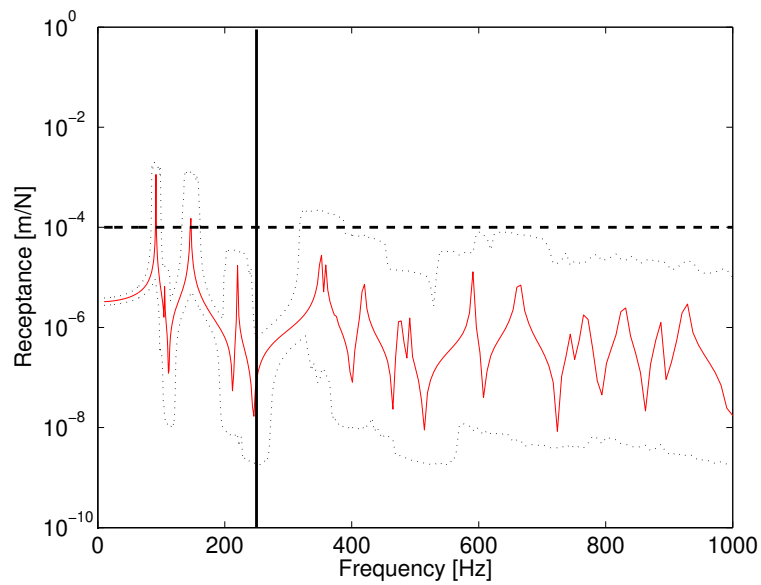


Figure 5.8: SEM-*deterministic* (solid), SEM combined with *gtrmrecur* using 5 α -cuts: envelopes (dotted line) and *target* value (dashed line).

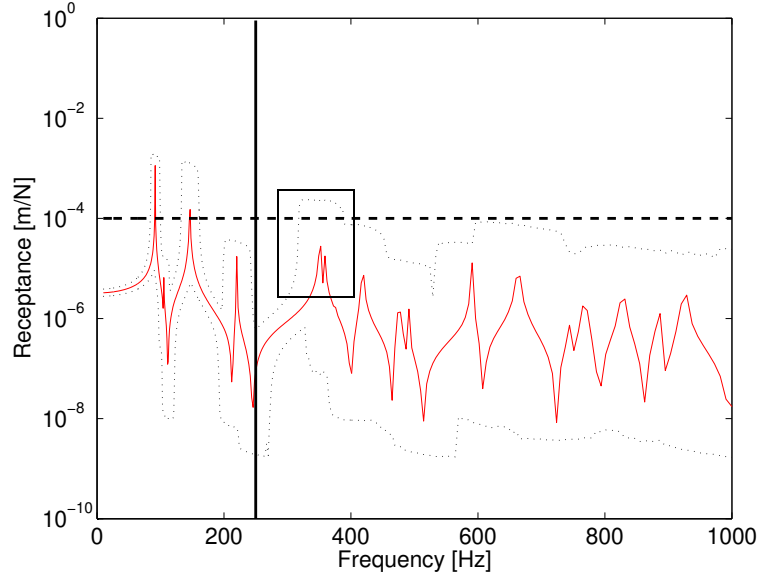


Figure 5.9: SEM-*deterministic* (solid), SEM combined with *gtrmrecur* using 9 α -cuts: envelopes (dotted line) and *target* value (dashed line).

In addition, we have also selected here a fuzzy-valued result at 84 Hz and 304 Hz. Figure 5.10 (a) and (b) shown results obtained for three different α -cuts, $m = 3$, $m = 5$ and $m = 9$, respectively.

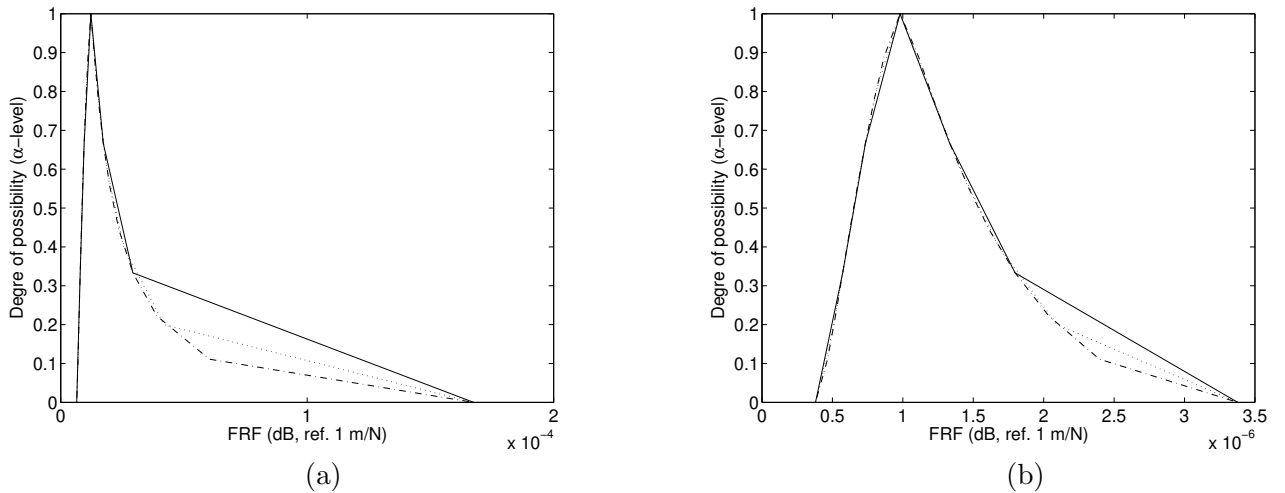


Figure 5.10: Fuzzy-valued results for different number of α -cuts: at 84 Hz (a) and at 304 Hz (b) with 3 α -cuts (solid line), 5 α -cuts (dotted line) and 9 α -cuts (dash dot line).

For the frequency range of interest, i.e., above 250 Hz, we note that in Figure 5.9 the *max* receptance response is found above the *target* proposed between 330 Hz and 370 Hz.

In this case, we suggest to change the original plate thickness $h = 4$ mm to $h = 5.5$ mm. Conducting a deterministic analysis, we found a suitable reduction for the frequency range of interesse, especially for the two peaks observed in the baseline model. Figure 5.11 shows this effect comparing with the original value of $h = 4.0$ mm. In addition, in Figure 5.12 the envelopes for the receptance considering a mean thickness value equal to $h = 5.5$ mm are presented. In terms of project recommendation, such an example give us an idea that with the new thickness value, deterministic and the envelopes for receptance response lie within the *target* proposed.

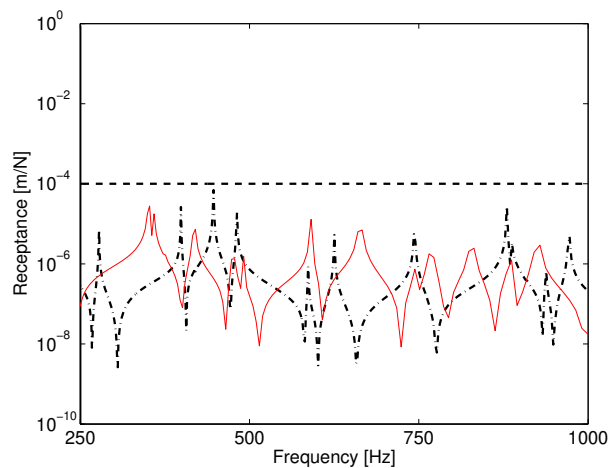


Figure 5.11: SEM-*deterministic* (solid), *target* value (dashed line) and the improved version with $h = 5.5$ mm (dotted line).

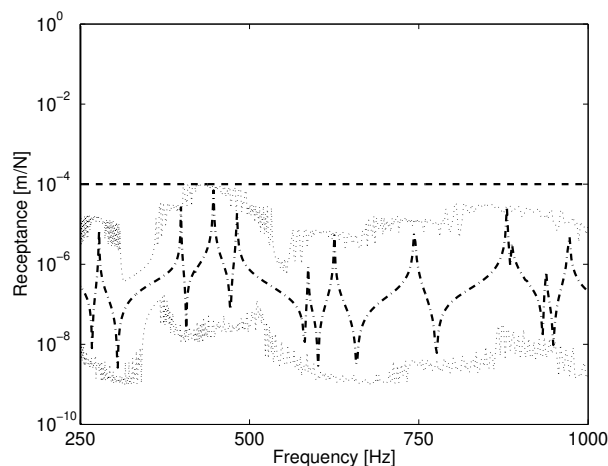


Figure 5.12: SEM-*deterministic* improved version with $h = 5.5$ mm (dotted line), *target* value (dashed line) and the envelopes with 3 α -cuts (dash dot line).

5.6.4 Interpretation of the results

With the results presented in Section 5.6.3, the main goal was to provide a design scenario where a fuzzy set based method could be well applied. With the envelope curves obtained, the analysis can be very helpful during the initial design phase. It gives information about the effects of uncertain parameters in the dynamic response. If we take the *max* receptance while taking into account the influence of uncertain parameters, and such receptance lies within this *limit*, then a more *safe* design would be achieved. In addition, in conducting a sensitivity analysis, the degree of influence of all input data can be found and the most important parameters that contribute to the response of the dynamic system can be selected.

5.7 Summary

This chapter shows the application of a fuzzy set based method considering a non-deterministic dynamic analysis of a reinforced plate in the context of an automotive application. Typical considerations were treated and the main steps to conduct such an analysis were pointed out. In conclusion, within the above context, fuzzy set based methods can be used to address structural dynamic problems under the influence of non-deterministic input parameters.

Chapter 6

Concluding Remarks

In this thesis, some important issues concerning the dynamic analysis of structures in the mid-frequency range were discussed. In this sense, a SEM combined with fuzzy set based methods was proposed. Frequency response function envelopes were presented to cover the *maximum* and *minimum* responses under the influence of the uncertain input parameters.

In the first part of this work, a review of different techniques for addressing the mid-frequency range were presented. Some of the most important areas were covered, including the Hybrid FEA/SEA methods, the Virtual/Experimental SEA, the Energy Influence Coefficient (EIC) and also the Wave Based Method (WBM).

In Chapter 2, the effects of dynamic analysis of structures taking into account the influence of the non-deterministic input parameters were addressed. In this chapter, a special implementation of the extension principle called the transformation method was introduced. In addition, a brief introduction to probabilistic methods was also presented. The main idea was to show how we select the fuzzy set based methods to be combined with the SEM. In this sense, it was recommended that, in the presence of few statistical data, fuzzy set based methods are better suited than probabilistic techniques.

In Chapter 3, before implementing the SEM combined with fuzzy set based methods, some possible efficient alternatives to the fuzzy set based methods were discussed, including the transformation method using multi-dimensional arrays and its variant avoiding recurring permutations. The sparse grid interpolation method was also introduced as an attractive alternative.

In Chapter 4, some test problems were presented to show the applicability of the proposed SEM combined with fuzzy set based methods. Three main problems were shown: a simple coupled rods system, a reinforced plate and a frame-type model. In this chapter, applications

to Statistical Energy Analysis (SEA) were also addressed.

In Chapter 5, an example is presented to give more insight into the proposed methodology in the context of a practical engineering application. Some important aspects covering the design process, such as possible initial data available, *targets*, statistical information type of non-determinism were discussed.

Additionally, a review of the spectral element method for rod, beam and plate elements is given in appendices A, B, C and D.

6.1 Main contributions

The main contributions of this thesis can be summarized as follows:

- i. Definition of an alternative method to address the mid-frequency range problems considering the effect of the dynamic response of structures under uncertainty. The SEM combined with fuzzy set methods is proposed. With this approach, two main weak points found in the traditional Finite Element Analysis (FEA) are addressed: the limitation of the frequency range of application and the influence of the non-deterministic input parameters in the predicted dynamic response.
- ii. Description of an efficient implementation of the fuzzy set based methods to be combined with the SEM.
- iii. A new scheme to provide accurate estimation of the SEA coupling loss factors (CLFs), covering the confidence limits using the SEM combined with fuzzy set based methods.
- iv. More accurate explanation of how to combine the fuzzy set based methods with an efficient deterministic approach, showing the main advantages and disadvantages of each method.

6.2 Discussion for further research

In this thesis, two main areas might be considered subject for further research: considering more realistic applications, it is necessary to develop a more general spectral element approach with flexible choice of boundary conditions. The SEM, in general, can be considered a powerful tool to be applied in the mid frequencies range for structural dynamic problems. However,

in terms of practical and possible future industrial applications, a more general library of elements should be developed for different kinds of structural elements and boundary conditions. In this regard, reinforced shell elements with more general boundary conditions should be an interesting area to be explored. Likewise, hybrid methods combining finite elements and also statistical energy analysis should be a very interesting area of research.

Regarding fuzzy set based methods, the first topic to be subject of further development is algorithm implementation. In this area, more research seems to be necessary to make the method more attractive for practical engineering applications. For instance, the transformation method without recurring permutation has shown some advantages in this context. Despite this, for the case of more than ten uncertain parameters, for example, even with such improvements achieved, the complexity increases substantially. The sparse grids interpolation seems to be absolutely necessary in such cases. However, to obtain results more efficiently, it still depends on the *smoothness* of the surfaces representing response as a function of structural parameters.

Another important area for future research is related to how to select the main non-deterministic input parameters during the development process. This subject was already introduced by Hanss (2003) and Hanss and Klimke (2004) for some simple functions. For complex functions, it requires more investigation, specially for the case of increasing *fuzziness* of the model parameters. Considering the above, it seems also to be very interesting to combine a deterministic method with fuzzy sets in a commercial finite element code. For more simple problems, the SEM can be adopted to extend the frequency range of applicability, covering some limitations found with traditional FEA.

6.3 List of Publications

During development of this thesis, the following manuscripts have been submitted to journals:

Nunes, R. F., Ahmida, K. M. and Arruda, J. R. F. Applying a Fuzzy Set Based Method for Robust Estimation of the Coupling Loss Factors. *Submitted to the Journal of Sound and Vibration, 2005.*

Nunes, R. F., Klimke, A. and Arruda, J. R. F. On estimating frequency response function envelopes using the spectral element method and fuzzy sets. *Accepted to be published in the Journal of Sound and Vibration, 2005.*

Also, the following paperwork have been published:

Nunes, R. F., Ahmida, K. M. and Arruda, J. R. F. A SEM/Fuzzy Method for the Estimation of the SEA Coupling Loss Factors. *Proceedings of the NOVEM 2005*, Saint Raphael, France, paper 52, 2005.

Nunes, R. F., Klimke, A. and Arruda, J. R. F. *On estimating frequency response function envelopes using the spectral element method and fuzzy sets.* IANS report 2004/020, Tech. rep., University of Stuttgart, 2004, URL <http://preprints.ians.uni-stuttgart.de>. 09/11/2004.

Arruda, J. R. F., Donadon, L. **Nunes**, R. F. and Albuquerque, E. On the modeling of reinforced plates in the mid-frequency range, *Proceedings of the ISMA2004*, Leuven, Belgium, paper number 308, 2004.

Nunes, R. F., Oexl, S. and Arruda, J. R. F. Taking uncertainties into account in spectral element modeling of structures, *Proceedings of the Inter-Noise 2004*, Prague, Czech Republic, paper number 436, 2004.

Bibliography

- Agarwal, B. D. and Broutman, L. J. *Analysis of performance of fiber composite*. John Wiley and Sons Inc., New York, 2nd edition, 1990.
- Ahmida, M. K. and Arruda, J. R. F. Estimation of the SEA coupling loss factors by means of spectral element modeling, *Journal Brazilian Society Mechanical Science*, V25(3), pp. 259-263, ISBN 0100-7386, 2003.
- Ahmida, K. M. and Arruda, J. R. F. Exact modeling of Kinetic Energy in Truss-type Members. *Journal of Sound and Vibration*, V267(1), pp. 167–177, 2003.
- Ahmida, M. K. *Dynamic analysis of truss-type structures in medium and high frequencies*, Doctorate dissertation, University of Campinas, Brazil, 1998 (in Portuguese).
- Albuquerque, E., Arruda, J., R., F. and Donadon, L., V. Dynamic analysis of reinforced panel, *Cobem 2004*, paper number 56027, Brazil, 2004.
- Alefeld, G. and Herzberger, J. *Introduction to interval computations*. Academic Press, New York, 1983.
- Arruda, J. R. F., Donadon, L., Nunes, R. F. and Albuquerque, E. On the modeling of reinforced plates in the mid-frequency range, *Proceedings of ISMA2004*, Leuven, Belgium, paper number 308, 2004.
- Arruda, J. R. F. and Ahmida, K. M. The structural dynamics mid-frequency challenge: Bridging the gap between FEA and SEA, *Proceedings of the X International Symposium on Dynamic Problems of Mechanics (DINAME)*, ABCM, Ubatuba, SP, Brazil, pp. 159-164, 2003.
- AutoSEA-X. *User guide Manual*, InterAC Sarl, Version 1.3, 1999.

- Babuska, I., Szabo, B. A. and Katz, I. N. The p-version of the finite element method, *Journal on Numerical Analysis*, SIAM, V18(3), pp. 515–545, 1981.
- Barthelmann, V., Novak, E. and Ritter, K. High dimensional polynomial interpolation on sparse grids. *Adv. Comput. Math.*, V12, pp. 273–288, 2000.
- Bathe, K. J. *Finite element procedures*. Prentice Hall, Upper Saddle River, New Jersey 07458, 1996.
- Battil, S. M., Renaud, J. E. and Gu, X. Modeling and simulation uncertainty in multidisciplinary design optimization, *AIAA Journal*, IAA-2000-4803, 2000.
- Bies, D. A. and Hamid, S. In situ determination of loss and coupling loss factors by power injection method, *Journal of Sound and Vibration*, V70(2), pp. 187–204, 1980.
- Bungartz, H. J., Griebel, M. Sparse Grids, *Acta Numerica*, V13, pp. 147–269, 2004.
- Chen, S. Q. *Comparing probabilistic and fuzzy set approaches for design in the presence of uncertainty*, Ph.D. Thesis, Virginia Polytechnic Institute and State University, Blacksburg, Virginia USA, 2000.
- Cimerman, B., Bharj, T. and Borello, G. Overview of the experimental approach to statistical energy analysis, *Proceedings of the SAE Noise and Vibration Conference*, Traverse City, Michigan, USA, 1997.
- Clarkson, B. L. and Pope, R. J. Experimental determination of modal densities and loss factors of flat plates and cylinders, *Journal of Sound and Vibration*, V77, pp. 535–549, 1981.
- Craig, R. R. Jr. Coupling of Substructures for Dynamic Analyses: An Overview, *AIAA Journal*, Paper No. 2000-1573, AIAA Dynamics Specialists Conference, Atlanta, GA, April 5, 2000.
- Craig, R. R. Jr. Substructure methods in vibration, *Journal of Vibration and Acoustics*, Transactions of ASME, V117 (50th Anniversary o Design Issue), pp. 207–213, 1995.
- Craig, R. R. Jr. *Structural dynamics: An introduction to computer methods*, Wiley, New York, 1981.

- Craig, R. R. Jr. and Bampton, M. C. Coupling of substructures for dynamic analysis, *AIAA Journal*, V6(7), pp. 1313–1319, 1968.
- Cremer, L. and Heckl, M. *Structure-borne sound*, Springer Verlag, 2nd edition, 1988.
- Davis, E. B. By air by SEA, *Proceedings of the NOISE-CON 2004*, Baltimore, Maryland, USA, 2004.
- Desmet, W. Mid-frequency vibro-acoustic modelling: challenges and potential solutions, *Proceedings of ISMA2002*, Leuven, Belgium, 2002.
- Donadon, L., Albuquerque, E. L. and Arruda, J. R. F. Modeling reinforced plates using the spectral element method, *Proceedings of the InterNoise 2004*, Prague, Czech Republic, 2004.
- Dong, W. and Shah, H. C. Vertex method for computing functions of fuzzy variables, *Fuzzy Sets and Systems*, V24, 65–78, 1987.
- Dong, W. M. and Wong, F. S. Fuzzy weighted averages and implementation of the extension principle, *Fuzzy Sets and Systems*, V21, 183–199, 1987.
- Doyle, J. F. *Wave propagation in structures: spectral analysis using fast discrete Fourier transforms*, 2nd ed., Springer-Verlag, 1997.
- Dubois, D. and Prade, H. *Fuzzy sets and systems, theory and applications*, V144 of Mathematics in Science and Engineering, Academic Press, Inc., New York, 1980.
- Elishakoff, I. and Ren, Y. *Finite element methods for structures with large stochastic variations*, Oxford University Press, Oxford, Great Britain, 2003.
- Fahy, F. J. Statistical energy analysis: a critical overview, *Phil. Trans. Royal Society of London a Mathematical and Physical Sciences*, V346, n. 1681, pp. 431–447, 1994.
- Fahy, F. J. Statistical Energy Analysis: a wolf in sheep's clothing ?, *Proceedings Inter-Noise 93*, Leuven, Belgium, pp. 13–36, 1993.
- Fredö, C. SEA-like approach for the derivation of energy flow coefficients with finite element model, *Journal of Sound and Vibration*, V199, pp. 645–666, 1997.

- Gagliardini, L., Houillon, L., Petrinelli, L. and Borello, G. Virtual SEA: Mid-frequency structure-borne noise modeling based on Finite Element Analysis, *Proceedings of the SAE Noise and Vibration Conference*, Traverse City, Michigan, USA, 2003.
- Gautier, F., Moulet, M. H. and Pascal, J. C. Scattering matrix of a stiffener elastically connected to a plate, *Proceedings of the International Conference on Recent Advances in Structural Dynamics*, Southampton, UK, 2003.
- Giachetti, R. E. and Young, R. E. Analysis of the error in the standard approximation used for multiplication of triangular and trapezoidal fuzzy numbers and the development of a new approximation, *Fuzzy Sets and Systems*, V91(2), 1–13, 1997.
- Giachetti, R. E. and Young, R. E. A parametric representation of fuzzy numbers and their arithmetic operators, *Fuzzy Sets and Systems*, V91(2), 185–202, 1997.
- Ghanem, R. G. and Spanos, P. D. *Stochastic finite elements: a spectral approach*, Springer Verlag, Berlin, Germany, Revised Edition, 2003.
- Hal, B. V., Vanmaele, C. and Desmet, W. Hybrid finite element – wave based method for steady-state acoustic analysis. *Proceedings of ISMA2004*, Leuven, Belgium, paper number 411, 2004.
- Hansen, E. H. *Global optimization using interval analysis*, Marcel Dekker, New York, NY, 1992.
- Hanns, M. *Applied Fuzzy Arithmetic: An introduction with engineering applications*, Springer-Verlag, Berlin, 256 pp., 2004.
- Hanns, M. and Klimke, A. On the reability of the influence measure in the transformation method of fuzzy arithmetic, *Fuzzy Sets and Systems*, V143, pp.371–290, 2004.
- Hanns, M. The extended transformation method for the simulation and analysis fo fuzzy-parameterized models, *International Journal of Uncertainty, Fuzziness and Knowledge-Based Systems*, V11, pp. 711–727, 2003.
- Hanns, M., Oexl, S. and Gaul, L. Identification of a bolted-joint model with fuzzy parameters loaded normal to the contact interface, *Mechanics Research Communications*, V29(2-3), pp. 177–187, 2002a.

- Hanss, M. The transformation method for the simulation and analysis of systems with uncertain parameters, *Fuzzy Sets and Systems*, V130(3), pp. 277–289, 2002b.
- Hanss, M., Oexl, S. and Gaul, L. Simulation and analysis of structural joint models with uncertainties, *Proceedings of the Int. Conference on Structural Dynamics Modelling*. Madeira, Portugal, 2002c.
- Hanss, M. A nearly strict fuzzy arithmetic for solving problems with uncertainties, *Proceedings of the 19th International Conference of the North American Fuzzy Information Processing Society - NAFIPS 2000*. Atlanta, GA, USA, pp. 439–443, 2000.
- Hanss, M. On the implementation of fuzzy arithmetical operations for engineering problems, *Proceedings of the 18th International Conference of the North American Fuzzy Information Processing Society - NAFIPS 1999*. New York, USA, pp. 462–466, 1999.
- Hanss, M. and Willner, K. On using fuzzy arithmetic to solve problems with uncertain model parameters operations for engineering problems, *Proceedings of the Euromech 405 Colloquim*. Valenciennes, France, pp. 85–92, 1999.
- Hepberger, A., Pribsch, H. H., Desmet, W., van Hal, B., Pluymers, B. and Sas, P. Application of the wave based method for the steady-state acoustic response prediction of a car cavity in mid-frequency range, *Proceedings of ISMA2002*, Leuven, Belgium, 2002.
- Huber, T. *Monte Carlo Simulation*, Physics Department, Gustavus Adolphus College, 1997, URL <http://physics.gac.edu/huber/envision/instruct/montecar.htm>. 12/05/2004.
- Hurty, W. C. Dynamic analysis of structural systems using component modes, *AIAA Journal*, V3(4), pp. 678–685, 1965.
- Kaufmann, A. and Gupta, M. M. *Introduction to fuzzy arithmetic*, Van Nostrand Reinhold, New York, 1991.
- Keese, A. *A review of recent developments in the numerical solution of stochastic partial differential equations (Stochastic Finite Elements)*, Informatikbericht Nr.:2003/06, Technical University Braunschweig, Brunswick, Germany, URL <http://opus.tu-bs.de/opus/volltexte/2003/470/>. 15/04/2004.

- Kleiber, M. and Hien, T. D., *The stochastic finite element method*, West Sussex, John Wiley and Sons, 1992.
- Klimke, A. *On barycentric Lagrangian interpolation, dimension-adaptive sparse grids, and their application to fuzzy arithmetic*, Internal Presentation at the University of Stuttgart, Institute of Applied Analysis and Numerical Simulation, Stuttgart, 2005.
- Klimke, A., Willner, K. and Wohlmuth, B. Uncertainty modeling using efficient fuzzy arithmetic based on sparse grids: applications to dynamic systems, *International Journal of Uncertainty, Fuzziness and Knowledge-Based Systems*, V12(6), pp. 745–759, 2004.
- Klimke, A. Algorithm: SPINTERP: Piecewise multilinear sparse grid interpolation in MATLAB, *ACM Transactions on Mathematical Software*, 2004 [in press].
- Klimke, A. and Wohlmuth, B. *Computing expensive multivariate functions of fuzzy numbers using sparse grids*, IANS report 2004/002, Tech. rep., University of Stuttgart, 2004, URL <http://preprints.ians.uni-stuttgart.de.18/08/2004>.
- Klimke, A. An efficient implementation of the transformation method of fuzzy arithmetic, E. Walker (Ed.), *Proceedings of NASFIPS 2003*, Chicago, IL, pp.468–473, 2003.
- Klir, C. J. Fuzzy arithmetic with requisite constraints, *Fuzzy Sets and Systems*, V91, pp. 165–175, 1997.
- Kompella, M. S. and Bernhard, R. J. Measurement of statistical variational of structural-acoustic characteristics of automotive vehicles, *Proceedings of the SAE Noise and Vibration Conference*, Traverse City, Michigan, USA, SAE paper 931272, 1993.
- Langley, R. S. and Cotoni, V. Variance prediction in SEA, *Proceedings of the 10th International Congress of Sound and Vibration - ICSV10*, Stockholm, Sweden, 2003.
- Langley, R. S., Cotoni, V. and Kidner, M. Response statistics and variance for a single SEA subsystem: Theory and experiment, *Proceedings of the Vibro-Acoustic Users Conference*, Leuven, Belgium, 2003.
- Langley, R. S. and Brown, A. W. M. Natural frequency statistics and response variance prediction, *Proceedings of the Second International AutoSEA Users Conference*, Troy, Michigan, USA, 2002.

- Langley, R. S. and Bremner, P. A hybrid method for the vibration analysis of complex structural-acoustic systems, *Journal of the Acoustical Society of America*, V105, pp. 1657–1671, 1999.
- Langley, R. S. and Bardell, N. S. A review of current analysis capabilities to high frequency vibration prediction of aerospace structures, *Aeronautical Journal*, pp. 287–297, 1998.
- Langley, R. S. A derivation of the coupling loss factors used in statistical energy analysis equations for coupled dynamic systems, *Journal of Sound and Vibration*, V141(2), pp. 207–219, 1990.
- Langley, R. S. A general derivation of statistical energy analysis equations for coupled dynamic systems, *Journal of Sound and Vibration*, V135(3), pp. 499–508, 1989.
- Lee, L. and Lee, J. Spectral-element method for Levy-type plates subjected to dynamic loads, *Journal of Engineering Mechanics*, February, pp. 243–247, 1999.
- Leung, A. Y. T. and Chan, J. K. W. Fourier p-element for the analysis of beams and plates, *Journal of Sound and Vibration*, V212(1) pp. 179–185, 1998.
- Lyon, R. H. and DeJong, R. G., *Theory and application of statistical energy analysis*, 2nd ed., Butterwoth-Heinemann, Boston, 1995.
- Lyon, R. H. and Eichler, E. Random vibration of connected structures, *Journal of the Acoustical Society of America*, V36(7), pp. 1344–1354, 1964.
- Lyon, R. H. and Maidanik, G. Power flow between linearly coupled oscillators, *Journal of the Acoustical Society of America*, V34(5), pp. 623–639, 1962.
- Mace, B. R. and Shorter, P. J. Energy flow models from finite element analysis, *Journal of Sound and Vibration*, V233(3), pp. 369–389, 2000.
- Mace, B. R. On the statistical energy analysis hypotesis of coupling power proportionality and some implications of its failure, *Journal of Sound and Vibration*, V178(1), pp. 95–112, 1994.
- Mace, B. R. The statistical energy analysis of two continuos one-dimensional subsystems, *Journal of Sound and Vibration*, V166(3), pp. 429–461, 1993.

- Mace, B. R. Power flow between two continuous one-dimensional subsystems: a wave solution, *Journal of Sound and Vibration*, V154(2), pp. 289–319, 1992.
- Maglaras, G., Nikolaidis, E., Haftka, R. and Cudney, H. H. Experimental comparison of probabilistic methods and fuzzy set based methods for designing under uncertainty, *Uncertainty Modelling in Vibration and Fuzzy Analysis of Structural Systems*, V10, pp. 253–318, 1997.
- Manohar, C. S. and Gupta, S. Modeling and evaluation of structural reliability: current status and future directions, *In Golden Jubilee publications of Department of Civil Engineering*, IISc, Bangalore, 2002.
- Manohar, C. S. and Ibrahim, R. A. Progress in structural dynamics with stochastic parameter variations 1987-1998, *ASME Applied Mechanics Reviews*, V52(5), pp. 177–197, 1999.
- Marczyk, J. Does optimal mean best ?, *Proceedings of Virtual Product Development - VPD Conference and MSC.Software User Meeting 2004*, Munich, 2004.
- Matthies, H., Brenner, C. E., Bucher, C. G. and Soares, C. G. Uncertainties in probabilistic numerical analysis of structures and solids - Stochastic finite elements, *Structural Safety*, V19(3) pp. 283–336, 1997.
- Maxit, L. and Guyader, J. L. Estimation of SEA coupling loss factors using a dual formulation and FEM modal information, part I: Theory, *Journal of Sound and Vibration*, V239(5) pp. 907–930, 2001.
- Maxit, L. and Guyader, J. L. Estimation of SEA coupling loss factors using a dual formulation and FEM modal information, part II: Numerical Applications, *Journal of Sound and Vibration*, V239(5) pp. 931–948, 2001.
- Meirovitch, L. and Baruh, H. On the inclusion principle of the hierarchical finite element method, *International Journal for Numerical Methods in Engineering*, V19, pp. 281–291, 1983.
- Meirovitch, L. *Elements of vibration analysis*, 2nd edition, McGraw-Hill, New York, 1986.
- Miller, I. and Freund, J. *Probability and statistics for engineers*, Prentice Hall, Englewood Cliffs, 1985.

- Moens, D. and Vandepitte, D. Non-probabilistic approaches for non-deterministic dynamic FE analysis of imprecisely defined structures. *Proceedings of ISMA2004*, Leuven, Belgium, 2004.
- MSC.Nastran Software. *Release guide 2004*, The Macneal-Schwindler Corporation, Santa Ana, California 92707, USA, 2004.
- MSC.Nastran Software. *Quick reference guide 2004*, VII, The Macneal-Schwindler Corporation, Santa Ana, California 92707, USA, 2004.
- Norton, M. P. and Greenhalgh, R. On the estimation of loss factors in lightly damped pipeline systems: some measurements techniques and their limitations, *Journal of Sound and Vibration*, V105, pp. 397–423, 1986.
- Nunes, R. F., Ahmida, K. M. and Arruda, J. R. F. A SEM/Fuzzy Method for the Estimation of the SEA Coupling Loss Factors. *Proceedings of the NOVEM 2005*, Saint Raphael, France, paper 52, 2005.
- Nunes, R. F., Klimke, A. and Arruda, J. R. F. *On estimating frequency response function envelopes using the spectral element method and fuzzy sets*, IANS technical report 2004/20, University of Stuttgart, 2004. (URL: <http://preprints.ians.uni-stuttgart.de/downloads/2004/2004-020.pdf>).
- Nunes, R. F., Oexl, S. and Arruda, J. R. F. Taking uncertainties into account in spectral element modeling of structures, *Proceedings of Internoise 2004*, Prague, Czech Republic, paper number 436, 2004.
- Oexl, S., Hanss, M. and Gaul, L. Identification of a normally-loaded joint model with fuzzy parameters, *Proceedings of the Int. Conference on Structural Dynamics Modelling*. Madeira, Portugal, 2002.
- Papoulis, A. *Probability, random variables and stochastic processes*, McGraw-Hill, New York, USA, 1965.
- Pavic, G. Hybrid vibration modelling of structures using analytical formulations, *Proceedings of the XVII International Congress of Acoustics*, Rome, Italy, 8 pp., 2001.

- Ponslet, E. *Analytical and experimental comparison of probabilistic deterministic optimization*, Ph.D. Thesis, Virginia Polytechnic Institute and State University, Blacksburg, Virginia USA, 1995.
- Savage, L. J. *The foundation of statistics*, 2nd rev.edition, Dover, New York, 1972.
- Scharton, T. D. and Lyon, R. H. Power flow and energy sharing in random vibration, *Journal of the Acoustical Society of America*, V43(6), pp. 1332–1343, 1968.
- Shorter, P. J. and Langley, R. Numerical and experimental validation of hybrid FE-SEA method, *Proceedings of the NOISE-CON 2004*, Baltimore, Maryland, USA, 2004.
- Shorter, P. J., Gardner, B. K., Parret, A. V. and Zhang, Q. Full-spectrum structural-acoustic response predictions using the RESOUND approach to the mid-frequency problem, *Proceedings of the InterNoise 2002*, Dearborn, MI, USA, 2002.
- Shorter, P. J., Parret, A. V. and Gardner, B. K. Experimental validation of the RESOUND Full-spectrum method: acoustic radiation, *Proceedings of the Second International AutoSEA Users Conference 2002*, Troy, MI, USA, 2002.
- Shorter, P. J. *Combining finite elements and statistical energy analysis*, Ph.D. Thesis, University of Auckland, New Zealand, 1998.
- Siddall, J. N. *Probabilistic engineering design: Principles and applications*, Marcel Dekker Inc., New York, 1983.
- Simmons, C. Structure-borne sound transmission through plate junctions and estimates of SEA coupling loss factors using the FE method, *Journal of Sound and Vibration*, V144, pp. 215–227, 1991.
- Smolyak, S. A. *Quadrature and interpolation formulas for tensor products of certain classes of functions*, Sovietic Mathematic Dokl., V4, pp. 240–243, 1963.
- Steel, J. A. and Craik, R. J. M. Statistical energy analysis of structure-borne sound transmission by finite element methods, *Journal of Sound and Vibration*, V178, pp.553–561, 1994.
- Stimpson, G. and Lalor, N. Practical Noise Modelling of a car body structures using energy flow methods, *Proceedings of the InterNoise-1991*, pp. 1233–1236, 1991.

- Ugural, A. C., *Stress in plates and shells*, McGraw-Hill, New York, 1981.
- Ungar, E. E. Transmission of plate flexural waves through reinforcing beams; dynamic stress concentrations, *Journal of the Acoustical Society of America*, V33, pp. 633-639, 1961.
- Van Hal, B., Desmet, W. Vandepitte and Sas, P. Application of the efficient wave based technique for the steady-state analysis prediction of flat plates, *Proceedings of ISMA2002*, Leuven, Belgium, 2002.
- West, L. J., Bardell, N. S., Dundon, J. M. and Loasby, P. M. Some limitations associated with the use of L-orthogonal polynomials in hierarquical versions of the finite element method, *Proceedings of the 6th International Conference on Recent Advances Structural Dynamics*, V1, pp. 217–227, 1997.
- Wood, K. L., Otto, K. N. and Antonsson, E. K. Engineering design calculations with fuzzy parameters, *Fuzzy Sets and Systems*, V52(1), pp. 1–20, 1992.
- Zadeh, L. A. Fuzzy sets, *Information and Control*, V(8), pp. 338–353, 1965.
- Zenger, C. Sparse Grids, Parallel Algorithms for partial differential equations, *V31 of Notes Numerical Fluid Mechanical*, Vieweg, Braunschweig, pp. 241–251, 1991.
- Zhang, Q., Wang, C., Wang, D., Qian, M., Nack, W. and Pamidi, P. Energy flow method for mid-frequency vibration analysis, *Proceedings of the SAE Noise and Vibration Conference*, Traverse City, Michigan, USA, 2003.
- Zienkiewicz, O. C. Achievements and some unsolved problems of the finite element method, *International Journal for Numerical Methods in Engineering*, V47, pp. 9–28, 2000.
- Zienkiewicz, O. C. and Taylor, R. L. *The finite element method*, V1, 4th edition, McGraw-Hill, New York, 1989.
- Zienkiewicz, O. C., Cago, F. E. and Kelly, D. W. The hierarquical concept in finite element analysis, *Computer and Structures*, V16, pp. 53–65, 1983.

Appendix A

The Spectral Element Method

The Spectral Element Method (SEM) was proposed by Doyle (1997), although its basic formulation was already widely known and currently used in the context of wave propagation solutions. In the SEM, the main idea is to combine the advantages of analytical spectral analysis with the efficiency and organization of the Finite Element Method (FEM). The major advantage of the SEM in comparison with the FEM is due to the spectral element dynamic stiffness matrix which is computed in the frequency domain, which allows the stiffness and inertia of the distributed system to be described exactly. Thus it is not necessary to refine the mesh as the wavelength becomes smaller (Doyle, 1997).

The SEM is formulated based on two types of elements, *two-noded* and *single-noded*, or *throw-off* elements. The latter is adopted when the member extends to infinity and is connected at a single point (or line). The major drawback of SEM is that the elements may only be assembled in one dimension, the solution along the orthogonal dimensions having to be found analytically, which is only possible for simple geometries. Doyle (1997) proposes a more general approach, which consists of using image sources to enforce arbitrary boundary conditions, but the approach still requires an *ad hoc* solution, which is not always existing.

Considering the discussion above, in the following Appendices, the SEM is presented in its application to rod, beam and plate elements with development of the dynamic stiffness matrix. The SEM is introduced, and some numerical tests are compared with the FEM. The main part of this review is based on Doyle (1997) and Ahmida (1998).

Appendix B

The Spectral Element applied to Rods

In order to introduce the SEM, the so-called low-order rod element is presented. The most simple rod theory is described by the following equation of motion

$$\frac{\partial}{\partial x} \left[EA \frac{\partial u}{\partial x} \right] = \rho A \frac{\partial^2 u}{\partial t^2} - q \quad (\text{B.1})$$

where q is the distribute force, EA is the uniform axial stiffness and ρA is the mass density per unit length of the rod. Following that, the solution of Eq. (B.1) considering a general longitudinal displacement for a rod, in the spectral analysis, the solution can be represented as

$$\hat{u}(x, \omega) = \mathbf{A}e^{-ikx} + \mathbf{B}e^{-ik(L-x)} \quad (\text{B.2})$$

where \mathbf{A} and \mathbf{B} are the amplitudes at each frequency and L is the length of the rod element. It is understood that all quantities inside the summation (\mathbf{A} , \mathbf{B} , k , etc) could depend on the frequency ω . In addition, considering the undamped case for the wave number k , we have the following expression

$$k = \pm \omega \sqrt{\frac{\rho A}{E A}} \quad (\text{B.3})$$

Note that, for shorthand, here, the following representation is assumed

$$u(x, y, t) \implies \hat{u}_n(x, y, \omega_n), \quad \hat{u}(x, y, \omega) \quad \text{or simply} \quad \hat{u}.$$

The displacement end conditions for the two-noded element, can be found using

$$\hat{u}(0) \equiv \hat{u}_1 = \mathbf{A} + \mathbf{B}e^{-ikL}, \quad \hat{u}(L) \equiv \hat{u}_2 = \mathbf{A}e^{-ikL} + \mathbf{B} \quad (\text{B.4})$$

In this case, \hat{u}_1 and \hat{u}_2 are referred as *nodal* displacements or simply degrees of freedom.

Going further, after solving for \mathbf{A} and \mathbf{B} terms of the nodal displacements, the longitudinal displacement at an arbitrary point in a finite rod can then be defined as

$$\hat{u}(x) = \hat{g}_1(x)\hat{u}_1 + \hat{g}_2(x)\hat{u}_2 \quad (\text{B.5})$$

where $\hat{g}_1(x)$ and $\hat{g}_2(x)$ are the frequency dependent rod shape functions which have the following relations

$$\hat{g}_1(x) = \frac{e^{-ikx} - e^{-ik(2L-x)}}{1 - e^{-i2kL}} \quad (\text{B.6})$$

and

$$\hat{g}_2(x) = \frac{-e^{-ik(L+x)} + e^{-ik(L-x)}}{1 - e^{-i2kL}} \quad (\text{B.7})$$

Further, the significance of the shape functions is that the complete description of the element is captured in the two nodal degrees of freedom \hat{u}_1 and \hat{u}_2 .

Now, applying boundary conditions to a uniform wave-guide at each end of the rod, the forces are obtained as follows

$$\begin{aligned} \hat{F}_1 &= -\hat{F}(0) = -EA[\hat{g}'_1(0)\hat{u}_1 + \hat{g}'_2(0)\hat{u}_2 \\ \hat{F}_2 &= -\hat{F}(L) = -EA[\hat{g}'_1(L)\hat{u}_1 + \hat{g}'_2(L)\hat{u}_2 \end{aligned} \quad (\text{B.8})$$

Following that, the symmetric matrix can be obtained as

$$\begin{Bmatrix} \hat{F}_1 \\ \hat{F}_2 \end{Bmatrix} = \frac{EA}{L} \frac{ik_L L}{(1 - e^{-i2k_L L})} \begin{bmatrix} 1 + e^{-i2k_L L} & -2e^{-ik_L L} \\ -2e^{-ik_L L} & 1 + e^{-i2k_L L} \end{bmatrix} \begin{Bmatrix} \hat{u}_1 \\ \hat{u}_2 \end{Bmatrix} = [\hat{k}_e] \{\hat{u}\} \quad (\text{B.9})$$

where \hat{k}_e is defined as complex dynamic stiffness matrix for the rod element, \hat{F} is the complex amplitude of applied force, \hat{u} is the vector of the complex amplitudes of the node displacements and, finally, k_L is the wave number, which for rod is defined as

$$k_L = \sqrt{\frac{\omega^2 \rho}{E}} \quad (\text{B.10})$$

Also, in case of dispersion relation, the following definition for constant phase and group speed is given

$$c = \frac{\omega}{k} = \sqrt{\frac{EA}{\rho A}} = c_o \quad (\text{B.11})$$

and

$$c_g = \frac{d\omega}{dk} = \sqrt{\frac{EA}{\rho A}} = c_o \quad (\text{B.12})$$

The relations described in Eqs. (B.11) and (B.12) shown that the phase and group speeds are constant considering low order rod elements.

For taking into account structural damping, an internal loss factor η can be applied by just using a complex Young's modulus \hat{E} defined as

$$\hat{E} \rightarrow E(1 + i\eta) \quad (\text{B.13})$$

which in this case has the following relation with viscous damping defined as $\eta = 2\xi$, with ξ defined as the viscous damping fraction.

Thus, with the dynamic stiffness matrix of each element \hat{k}_e , it is straightforward to assemble a global stiffness matrix \hat{k} using the direct stiffness method. The solution is found by solving a linear system of equations of the type $\{\hat{F}\} = [\hat{k}]\{\hat{u}\}$.

In case of energy application, the following expression can be used to define the average kinetic energy of a rod

$$T_{kinetic} = \frac{1}{4}\omega^2\rho A \int_0^L \Re\{u \cdot u^*\}dx \quad (\text{B.14})$$

According to Lyon and DeJong (1995), considering the displacement and velocity, which repeat themselves in a period defined as $1/f_0$, the average of the kinetic and the potential energies over such period is found equal to the value of half of the total vibration energy T . This leads to both energies equal each other. Therefore, the total energy of vibration can be calculated using just the Eq. (B.14) defined for the average kinetic energy.

In case of rod application, the integral defined in Eq. (B.14) is calculated using Eq. (B.5) as follows

$$\int_0^L \text{Re}\{u \cdot u^*\} dx = u_1 \cdot u_1^* \int_0^L (g_1 \cdot g_1^*) dx + u_2 \cdot u_2^* \int_0^L (g_2 \cdot g_2^*) dx + u_1 \cdot u_2^* \int_0^L (g_1 \cdot g_2^*) dx + u_2 \cdot u_1^* \int_0^L (g_2 \cdot g_1^*) dx \quad (\text{B.15})$$

Thus, with the displacements u_1 and u_2 found in Eq. (B.9) and the frequency dependent rod functions defined in Eqs. (B.6) and (B.7), the average kinetic energy is given.

B.0.1 Dynamic stiffness matrix of a *throw-off* element

In order to develop a *throw-off* element, the term \mathbf{B} defined in Eq. (B.2) is neglected. This can be done since there are no reflections. Thus, we replace the coefficient \mathbf{A} with nodal information by using the end condition as follows

$$\hat{u}(0) \equiv \hat{u}_1 \quad (\text{B.16})$$

where \hat{u} is the single nodal displacement. Also, the displacement at an arbitrary point in a semi-infinite rod can be written as

$$\hat{u}(x) = \hat{g}_1(x) \hat{u}_1 \quad (\text{B.17})$$

and

$$\hat{g}_1(x) \equiv e^{-ikx} \quad (\text{B.18})$$

Finally, the stiffness matrix relation is given by the following expression

$$\{\hat{F}_1\} = E A[ik] \{\hat{u}_1\} = [\hat{k}] \{\hat{u}\} \quad (\text{B.19})$$

with the shape function $\hat{g}_1(x)$ complex and frequency dependent even in the simple rod case with no damping. This means, the *throw-off* elements dissipate energy out of the system.

B.0.2 Application to two coupled rods

In this Section, the SEM is applied to two test problems, which consisting of two connected rods. Additionally, for the examples proposed, the SEM is compared with Finite Element

Method (FEM) considering just longitudinal waves. Table B.1 summarizes the physical properties of rod 1 and rod 2 adopted for both numerical examples. In both cases, the free-free condition was also considered.

Table B.1: Physical properties for rods 1 and 2.

parameter	mean value \bar{m}	dimension
$E_{1/2}$	2.71×10^9	N/m ²
$\rho_{1,2}$	1140	kg/m ³
$\eta_{1,2}$	2.0×10^{-2}	—
A_1	1.735×10^{-3}	m ²
A_2	1.862×10^{-4}	m ²
L_1	0.20	m
L_2	2.46	m

B.0.3 Numerical results: case 1

In the first example, an axial force P is applied to the free end of rod 1 as shown in Figure B.1. In order to do this investigation, the SEM for rod elements was implemented in MATLAB software. The FEM analyzes were performed in MSC.NASTRAN commercial code using the ROD element defined in (Nastran, 2004b). Figure B.2 shows the respective SE model which adopt two *2-noded* spectral elements.

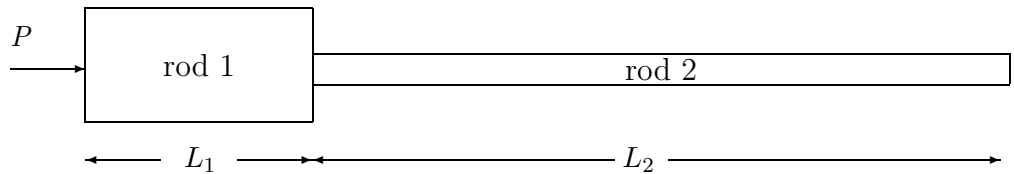


Figure B.1: Coupled rods system with axial force P applied to free end of uncoupled rod 1.



Figure B.2: SE model for the coupled rods applied to case 1.

Figures B.3 and B.4 present the results respectively for the FRF uncoupled rod, i.e., just rod 1 present, and coupled rods 1 and 2 using SEM and FEM.

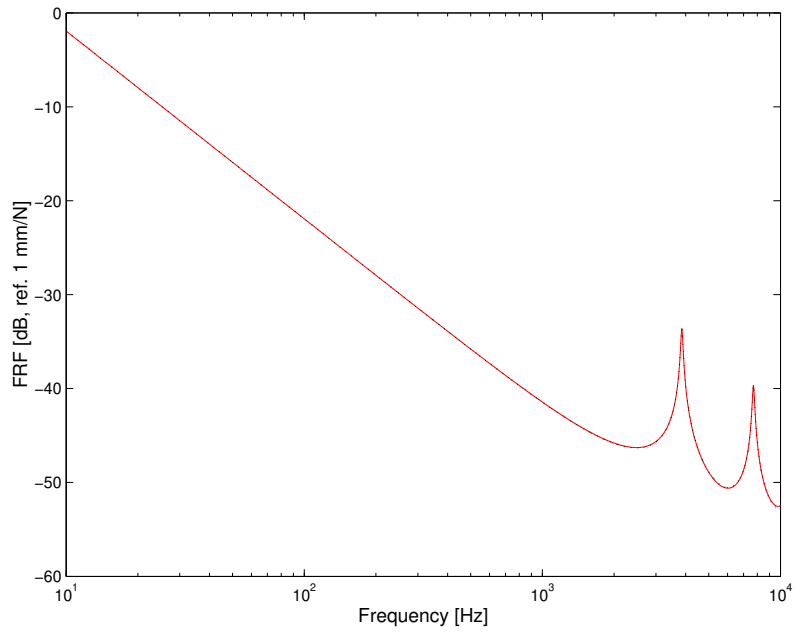


Figure B.3: FRFs for the uncoupled rod 1: comparison of FEM (dashed) and SEM (continuous).

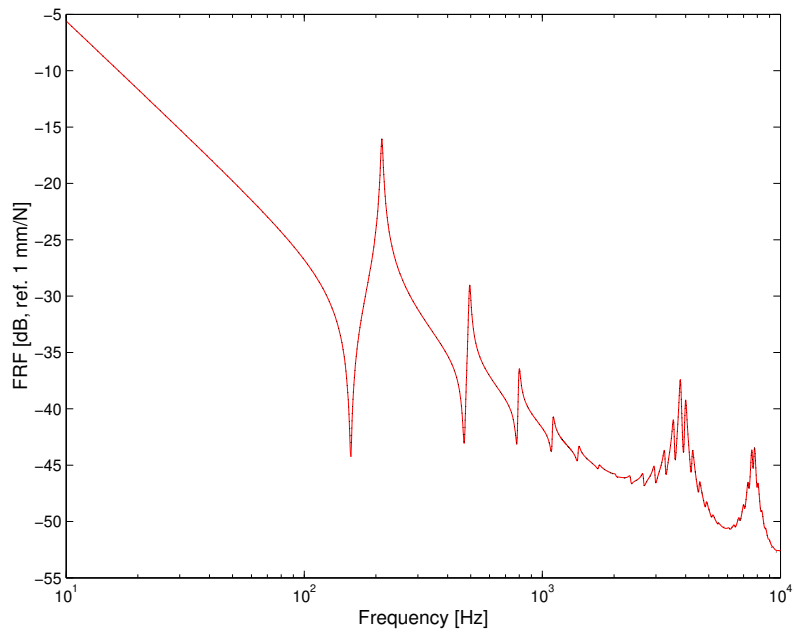


Figure B.4: FRFs for the coupled rods 1 and 2: comparison of FEM (dashed) and SEM (continuous).

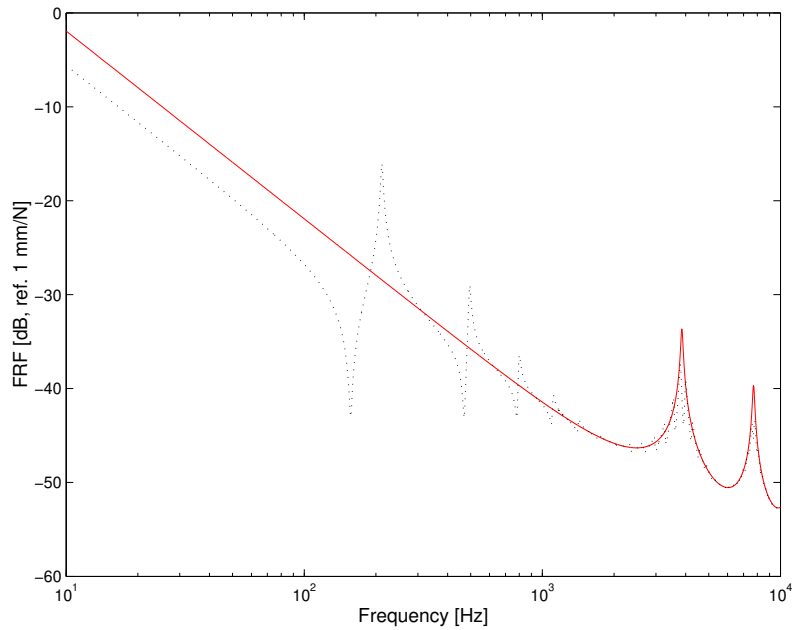


Figure B.5: Comparison for the uncoupled rod 1 (continuous) and coupled rods 1 and 2 (dashed) using SEM.

Considering the frequency range from 0 to 10 kHz, similar results for SEM and FEM are found. One important feature of this simple numerical example is that rod 2 has a much higher modal density than rod 1, which, in other words, means that rod 2 acts as fuzzy attachment to rod 1 (Langley and Bremner, 1999). In Figure B.5 it is clear that rod 2 provides additional damping to the modes of rod 1. In addition, as the frequency increases, the modal overlap of rod 2 exceeds unity and the effect of individual modes is no longer visible (Langley and Bremner, 1999).

B.0.4 Numerical and experimental results

In this section, results obtained via experimental measurements for the coupled rods case will be presented. Correspondingly, in the experimental setup, the rods were suspended as a pendulum.

Figure B.6 shows the experimental set-up used to obtain the FRFs. In the first one, the FRF of the single rod 1 was measured. In the second, shown in Figure B.6, the measurements were made on the coupled rods. The excitation signal was a white noise with the frequency range 0 to 12.8 kHz, 3200 frequency lines, total time window of 0.25 seconds, and Hanning window to avoid leakage. Also, in the second set-up, two accelerometers were used at the

junction of the two rods, and the sum signal was used to minimize the effects of undesirable flexural vibration as, in this investigation, only longitudinal waves are considered. Figure B.7 shows in details the accelerometers and the shaker position.

Finally, a comparison between numerical and experimental results for the uncoupled and coupled rods adopting the SEM were made. The connected point between rods 1 and 2 is used for comparison with experimental results. Figures B.8 and B.9 shown the results for the numerical and experimental cases. As a whole, a good agreement between numerical and experimental results is found. Some small differences can be explained about the influence of the flexural waves, which was not considered in the numerical model.



Figure B.6: Coupled rods experimental set-up.

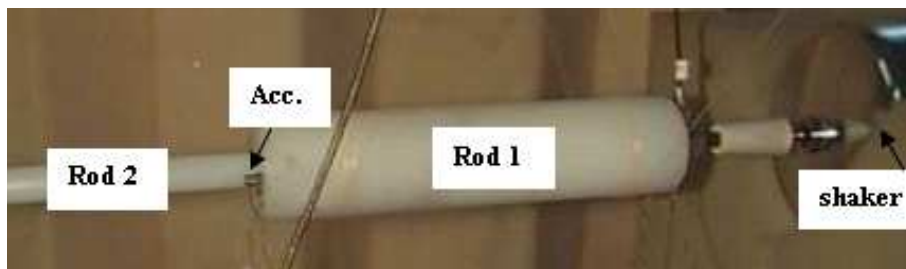


Figure B.7: Accelerometers in details.

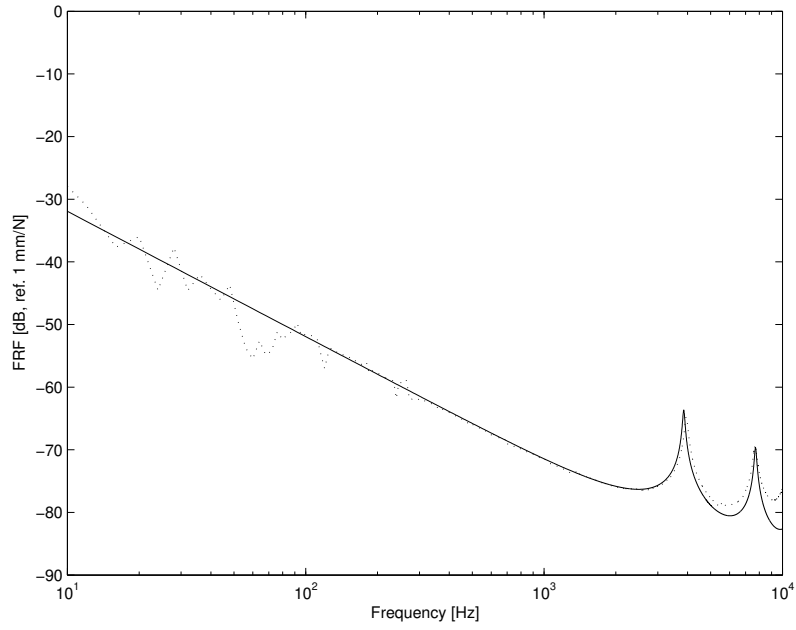


Figure B.8: Numerical (continuous) and experimental (dashed) results for the uncoupled rod case.

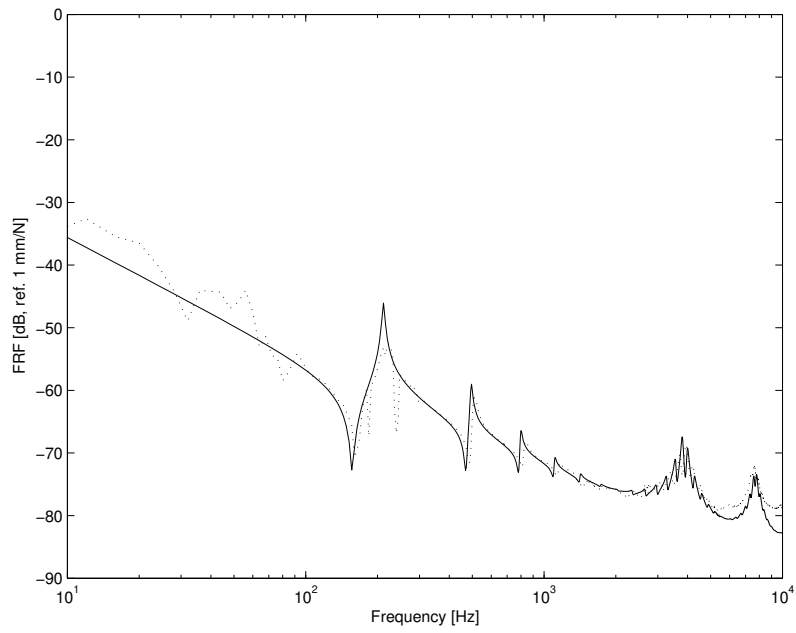


Figure B.9: Numerical (continuous) and experimental (dashed) results for the coupled rods case.

B.0.5 Numerical results: case 2

For the second case, an axial force P is applied at the middle of rod 1. See Figures B.10 and B.11 for the rod scheme and SE model, respectively. For the FE model, the same mesh is adopted. In this numerical example, the SE model consist of three 2-noded spectral elements shown in Figure B.11.

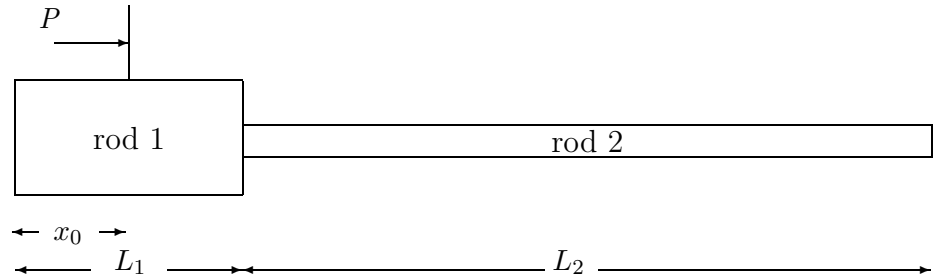


Figure B.10: Coupled rods system with axial force P applied at the middle of rod 1.



Figure B.11: SEM model for the coupled rods applied to case 2.

In Figure B.12, results for the FEM and SEM are compared considering just rod 1 present. In this case, considering the new point force location, we found just one structural mode for the uncoupled case. As a whole, we found equivalent results between FEM and SEM for the uncoupled and coupled rod cases. In addition, Figures B.13 and B.14 present the results considering the FRF coupled rods 1 and 2 and respective comparison between uncoupled and coupled rods using SEM. Again, it is interesting to add that in this setup rod 2 acts as fuzzy attachment to rod 1, which the main idea is to provide additional damping to the modes of rod 1 as well as additional modes at low frequencies (Langley and Bremner, 1999).

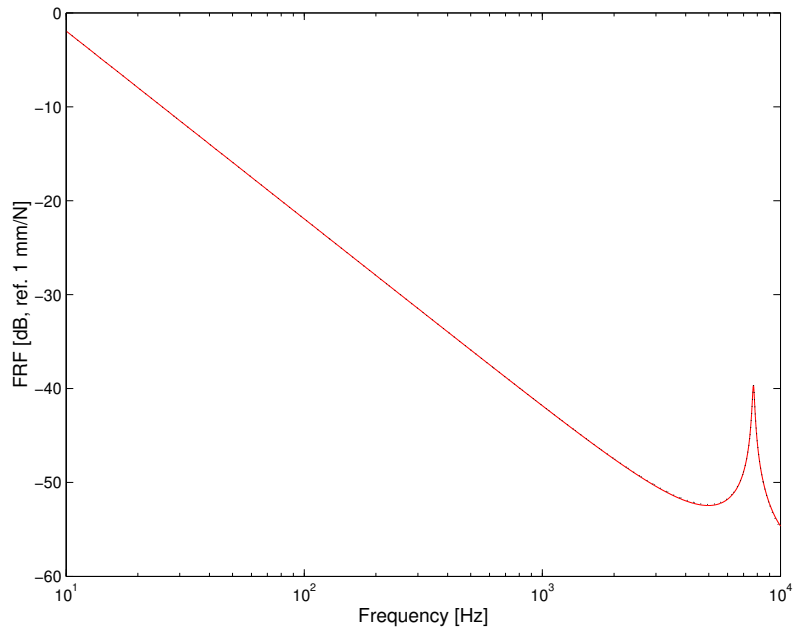


Figure B.12: FRFs for the uncoupled rod 1: comparison of FEM (dashed) and SEM (continuous)

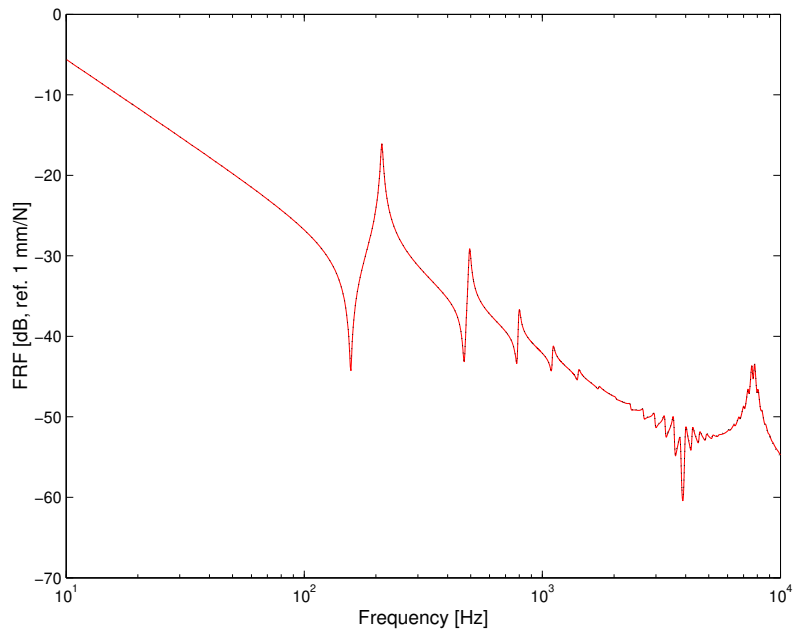


Figure B.13: FRFs for the coupled rods 1 and 2: comparison of FEM (dashed) and SEM (continuous).

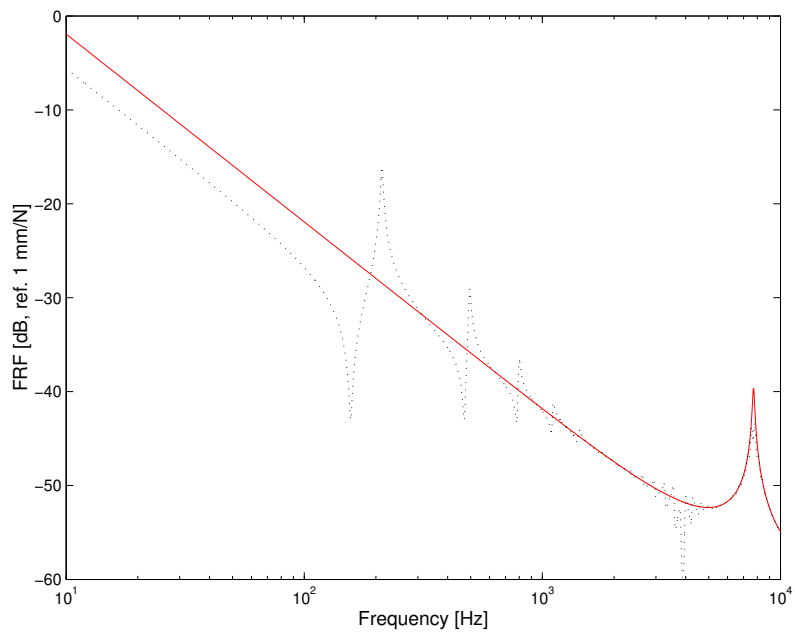


Figure B.14: Comparison for the uncoupled rod 1 (continuous) and coupled rods 1 and 2 (dashed) using the SEM.

Appendix C

The Spectral Element applied to Beams

The SEM applied to beams is developed here based on the elementary Bernoulli-Euler beam theory, which is considered as a simplification of the Timoshenko theory. A more complete description of the SEM applied to beam elements for higher waveguides theory can be found in Doyle (1997).

In this chapter, the Bernoulli-Euler beam theory will be reviewed, which means that the shear stiffness $GA\kappa \implies \infty$ and the rotational inertia $\rho I \implies \infty$ are not considered. Assuming both simplification, the following equation of the movement is derived

$$\frac{\partial^2}{\partial x^2} \left[EA \frac{\partial v^2}{\partial x^2} \right] + \rho A \frac{\partial^2 v}{\partial t^2} = q(x, t) \equiv q_v - \frac{\partial q_\phi}{\partial x} \quad (\text{C.1})$$

where $q(x, t)$ is the extern force which can be separated in the transverse load q_v and the distribute torque q_ϕ .

Assuming that the beam treated here has constant property along its length, the following homogeneous differential equation is defined

$$\frac{d^4 \hat{v}}{dx^4} - \beta^4 \hat{v} = 0 \quad (\text{C.2})$$

Considering Eq. (C.2), particular solutions can be obtained based on solutions of the two equations described by

$$\frac{d^2 \hat{v}}{dx^2} + \beta^2 \hat{v} = 0 \quad \text{and} \quad \frac{d^2 \hat{v}}{dx^2} - \beta^2 \hat{v} = 0 \quad (\text{C.3})$$

with the wavenumbers

$$k_1 = \pm\beta, \quad k_2 = \pm i\beta \quad \text{and} \quad \beta^2 \equiv \sqrt{\frac{\omega^2 \rho A - i\omega \eta A}{EI}} \quad (\text{C.4})$$

Following that, the complete solution can be found using the spectral representation as

$$v(x, t) = \Sigma[\mathbf{A}e^{-i\beta x} + \mathbf{B}e^{-\beta x} + \mathbf{C}e^{i\beta x} + \mathbf{D}e^{\beta x}]e^{i\omega t} \quad (\text{C.5})$$

where \mathbf{A} , \mathbf{B} , \mathbf{C} and \mathbf{D} are coefficients determined from the boundary conditions on the element.

C.0.6 Dynamic Stiffness Matrix - Bernoulli-Euler beam *two nodes element*

In order to develop the dynamic stiffness for a 2 nodes element with length L , displacements \hat{v}_i and node rotation $\hat{\phi}_i$ at the end of the beam, the following expression are defined

$$\hat{v}(0) \equiv \hat{v}_1, \quad \hat{\phi}(0) \equiv \hat{\phi}_1, \quad \hat{v}(L) \equiv \hat{v}_2 \quad \text{and} \quad \hat{\phi}(L) \equiv \hat{\phi}_2 \quad (\text{C.6})$$

Applying Eq.(C.6) into Eq.(C.5), the coefficients \mathbf{A} , \mathbf{B} , \mathbf{C} and \mathbf{D} can be found. Again, if applied Eq.(C.5), the displacement \hat{v}_i and rotation $\hat{\phi}_i$ in any point defined in this beam with length L , the following expression is used to find the response

$$\hat{v}(x) = \hat{g}_1(x)\hat{v}_1 + \hat{g}_2(x)\hat{\phi}_1 + \hat{g}_3(x)\hat{v}_2 + \hat{g}_4(x)\hat{\phi}_2 \quad (\text{C.7})$$

with $\hat{\phi}(x) = \frac{\partial \hat{v}(x)}{\partial x}$. Following that, the functions \hat{g}_i are the frequency dependent beam shape functions defined as

$$\begin{aligned} \hat{g}_1(x) &= (r_1 \hat{h}_1(x) + r_2 \hat{h}_2(x))/\Delta \\ \hat{g}_2(x) &= (r_1 \hat{h}_3(x) + r_2 \hat{h}_4(x))/\Delta \\ \hat{g}_3(x) &= (r_1 \hat{h}_2(x) + r_2 \hat{h}_1(x))/\Delta \\ \hat{g}_4(x) &= (-r_1 \hat{h}_4(x) - r_2 \hat{h}_3(x))/\Delta \end{aligned} \quad (\text{C.8})$$

with the terms in Eq. (C.8) defined as

$$\begin{aligned}
\Delta &= -r_1^2 + r_2^2 \\
r_1 &= i(k_1 - k_2)(1 - e^{-ik_1L}e^{-ik_2L}) \\
r_2 &= i(k_2 + k_2)(e^{-ik_1L} - e^{-ik_2L}) \\
\hat{h}_1(x) &= ik_2(e^{-ik_1x} - e^{-ik_2L}e^{-ik_1(L-x)}) - ik_1(e^{-ik_2x} - e^{-ik_1L}e^{-ik_2(L-x)}) \\
\hat{h}_2(x) &= -ik_2(e^{-ik_2L}e^{-ik_1x} - e^{-ik_1(L-x)}) + ik_1(e^{-ik_1L}e^{-ik_2x} - e^{-ik_2(L-x)}) \\
\hat{h}_3(x) &= (e^{-ik_1x} + e^{-ik_2L}e^{-ik_1(L-x)}) - (e^{-ik_2x} + e^{-ik_1L}e^{-ik_2(L-x)}) \\
\hat{h}_4(x) &= (e^{-ik_2L}e^{-ik_1x} + e^{-ik_1(L-x)}) - (e^{-ik_1L}e^{-ik_2x} + e^{-ik_2(L-x)}) \\
k_1 &= k \\
k_2 &= -ik
\end{aligned}$$

The nodal loads are written then in terms of the displacement degrees of freedom (DOFs) for the structural resultants as

$$\hat{V}(x) = -E I \frac{\partial^2 \hat{\phi}}{\partial x^2}, \quad \hat{M}(x) = E I \frac{\partial \hat{\phi}}{\partial x} \quad (\text{C.9})$$

Applying the boundary conditions to a beam with length L , the matrix equation is found as

$$\begin{Bmatrix} \hat{V}_1 \\ \hat{M}_1 \\ \hat{V}_2 \\ \hat{M}_2 \end{Bmatrix} = \frac{EI}{L^3} [\hat{k}^B] \begin{Bmatrix} \hat{v}_1 \\ \hat{\phi}_1 \\ \hat{v}_2 \\ \hat{\phi}_2 \end{Bmatrix} \quad (\text{C.10})$$

which can be written in the following form

$$\{\hat{F}\} = \frac{EI}{L^3} [\hat{k}^B] \{\hat{u}\} \quad (\text{C.11})$$

where $\frac{EI}{L^3} [\hat{k}^B]$ is defined as the dynamic stiffness matrix of the *two nodes* beam element for the Bernoulli-Euler theory.

The matrix \hat{k}^B is a $[4 \times 4]$ symmetric and in general complex matrix. The individuals terms in this matrix are defined as follows,

$$\begin{aligned}
\hat{k}_{11} &= (z_{11}z_{22} - iz_{12}z_{21})\xi^3/\Delta \\
\hat{k}_{12} &= 0.5(i+1)(z_{12}^2z_{21}^2)\xi^2L/\Delta \\
\hat{k}_{13} &= (iz_{12}z_{22} - z_{11}z_{21})\xi^3/\Delta \\
\hat{k}_{14} &= -(1-i)z_{11}z_{22}\xi^2L/\Delta \\
\hat{k}_{22} &= (iz_{11}z_{22} - z_{12}z_{21})\xi L^2/\Delta \\
\hat{k}_{23} &= -\hat{k}_{14} \\
\hat{k}_{24} &= (z_{12}z_{22} - iz_{11}z_{21})\xi L^2/\Delta \\
\hat{k}_{33} &= \hat{k}_{11} \\
\hat{k}_{34} &= -\hat{k}_{12} \\
\hat{k}_{44} &= \hat{k}_{22}
\end{aligned}$$

with

$$z_{11} = (1 - e^{-i\xi}e^\xi) , \quad z_{12} = (e^{-i\xi} - e^\xi) , \quad z_{21} = (e^{-i\xi} + e^\xi) , \quad z_{22} = (1 + e^{-i\xi}e^\xi) , \\
\Delta = \frac{(z_{11}^2 + z_{12}^2)}{(1+i)} \quad \text{and} \quad \xi = kL.$$

C.0.7 Dynamic Stiffness Matrix - Bernoulli-Euler beam *throw-off* element

For the *throw off* element, the solution for the displacement in any arbitrary point in this element is found with

$$\hat{v}(x) = \hat{g}_1(x)\hat{v}_1 + \hat{g}_2(x)\hat{\phi}_1 \tag{C.12}$$

where the functions \hat{g}_i are beam shape functions defined as

$$\begin{aligned}
\hat{g}_1(x) &= [-k_2e^{-ik_1x} + k_1e^{-ik_2x}]/\Delta \\
\hat{g}_2(x) &= [i(e^{-ik_1x} - e^{-ik_2x})]/\Delta
\end{aligned} \tag{C.13}$$

and $\Delta \equiv (k_1 - k_2)$, $k_1 = k$ and $k_2 = ik$.

Also, making use of Eq. (C.5) and consider $\mathbf{C} = \mathbf{D} = 0$, the following solution can be defined to the *throw off* element

$$v(x, t) = \Sigma[\mathbf{A}e^{-i\beta x} + \mathbf{B}e^{-\beta x}] \tag{C.14}$$

Applying Eq.(C.14) into Eq.(C.9) and performing a solution for the degrees of freedom (DOFs) at the point $x = 0$, the matrix relation can be found as

$$\begin{Bmatrix} -\hat{V}(0) \\ -\hat{M}(0) \end{Bmatrix} \equiv \begin{Bmatrix} \hat{V}_1 \\ \hat{M}_1 \end{Bmatrix} = EI \begin{bmatrix} (i-1)k^3 & ik^2 \\ ik^2 & (1-i)k^3 \end{bmatrix} \begin{Bmatrix} \hat{v}_1 \\ \hat{\phi}_1 \end{Bmatrix} \tag{C.15}$$

which can be rewritten in the following form

$$\{\hat{F}\} = EI[\hat{k}^B]\{\hat{u}\} \quad (\text{C.16})$$

where $EI[\hat{k}^B]$ is defined as the dynamic stiffness matrix to the Bernoulli-Euler beam *throw off* element. This is a symmetric and complex matrix which exhibit a damping behavior in the time domain (Doyle, 1997). One important to add is that such kind of element conduct energy out of the system, which can be interpreted as damping effect.

C.0.8 Numerical Example

In order to show the applicability of the SE method applied to a beam element, a simple example which consist of a Cantilever beam is proposed. The result is compared with a FE model implemented in the MSC.NASTRAN commercial software using BAR elements. A more detailed description regarding BAR elements can be found in NASTRAN (2004b).

In this example, the beam is supposed to be made of aluminum with the properties defined in Table C.1. Also, in this example I_1 and I_2 are assumed to be equal, which means that the cross section is perfectly round.

Table C.1: Physical properties to the Cantilever beam model.

parameter	mean value \bar{m}	dimension
E	7.1×10^9	N/m ²
ρ	2700	kg/m ³
ν	0.33	—
η	1.0×10^{-2}	—
L	1.0	m
A	6.158×10^{-4}	m ²
I	3.0×10^{-8}	m ⁴

In this example a Cantilever beam is defined with a load force $P = 1$ N applied in the middle of the beam. A fixed-free boundary condition is applied at one end of the beam as shown in Figure C.1 with the equivalent SE model in Figure C.2.

In Figure C.3 a point mobility receptance response is checked, while in Figure C.4 the response at the end of the cantilever beam is verified. In general, a good agreement between FE and SE receptance responses is found.

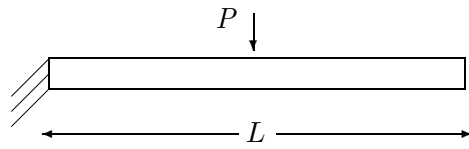


Figure C.1: Cantilever beam model.

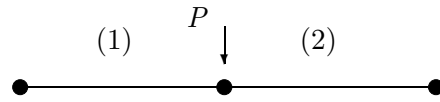


Figure C.2: SEM model applied to a Cantilever beam model.

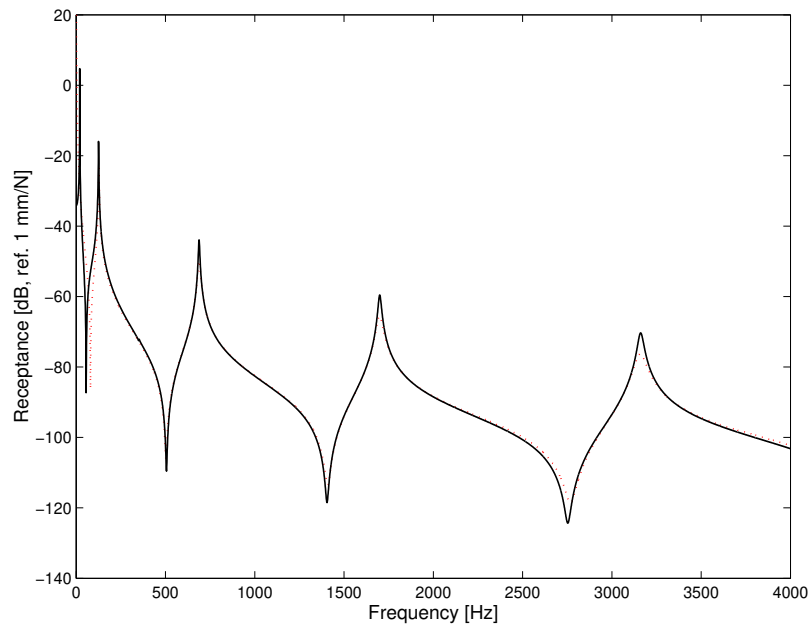


Figure C.3: Comparison of FEM (dashed) and SEM (continuous) results at the point mobility for the Cantilever beam model.

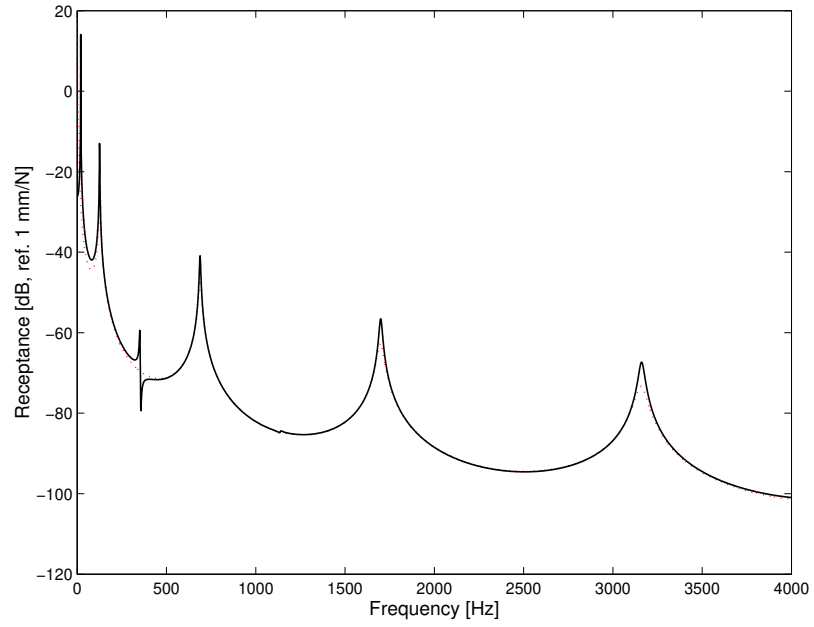


Figure C.4: Comparison of FEM (dashed) and SEM (continuous) results at the end of the Cantilever beam model.

Appendix D

The Spectral Element applied to Plates

The Kirchhoff plate equation described in Ugural (1981) is defined as follows

$$D\nabla^2\nabla^2w(x, y) - \omega^2\rho hw(x, y) = F(x, y) \quad (\text{D.1})$$

where $D = Eh^3/12(1-\nu^2)$, h is the thickness, ν is Poisson's ratio, ρ is the density, and $w(x, y)$ represents the transverse displacement of the plate. Two approaches are now possible. One consists in choosing a boundary condition in one direction, say the y direction, and the other consists in assuming a Fourier series solution in this direction, imposing periodicity, but leaving the boundary condition enforcement for afterwards.

The first approach, used for example in Lee and Lee (1999), is currently, to our knowledge, restricted to the simply supported solution. Assuming a sinusoidal solution for a flat plate that is simply supported along two opposite parallel sides, the transverse displacement can be written as

$$w(x, y) = \sum_{n=1}^{\infty} [\mathbf{A}_n e^{-ik_{1n}x} + \mathbf{B}_n e^{ik_{1n}x} + \mathbf{C}_n e^{-k_{2n}x} + \mathbf{D}_n e^{k_{2n}x}] \sin(k_{yn}y) \quad (\text{D.2})$$

The wave-numbers can be computed by replacing Eq. (D.2) in Eq. (D.1), and using the following properties of the sine function: $d^2 \sin(k_{yn}y)/dy^2 = -k_{yn}^2 \sin(k_{yn}y)$ and $d^4 \sin(k_{yn}y)/dy^4 = k_{yn}^4 \sin(k_{yn}y)$. It is important to mention here that these properties are essential in developing the method and they are the limiting factor for extending the method to other boundary conditions. The wave-numbers are given by

$$k_{1n} = \sqrt{k_p^2 - k_{yn}^2}, \quad k_{2n} = \sqrt{k_p^2 + k_{yn}^2}, \quad k_p = (\omega^2\rho\omega/D)^{1/4}, \quad \text{and} \quad k_{yn} = n\pi/L_y \quad (\text{D.3})$$

The coefficients \mathbf{A}_n , \mathbf{B}_n , \mathbf{C}_n and \mathbf{D}_n are found using the transverse and angular displacements at the two ends as boundary conditions, and using the moment and effective shear force expressions (Ugural, 1981)

$$M_x = D \left[\frac{\partial^2 w}{\partial x^2} + \nu \frac{\partial^2 w}{\partial y^2} \right] \text{ and } V_x = Q_x + \frac{\partial M_{xy}}{\partial y} = -D \left[\frac{\partial^3 w}{\partial x^3} + (2 - \nu) \frac{\partial^3 w}{\partial x \partial y^2} \right] \quad (\text{D.4})$$

One may look at the proposed solution to the wave equation as a wave propagation solution in the x -direction and by a sum of sine functions in the y -direction. These sine terms can be interpreted as propagation modes (Gautier et al., 2003). Each mode n will only propagate for frequencies that are higher than the frequency where the wave-number associated to it, in Eq. (D.3), becomes real, i.e., $k_p \geq k_{yn}$. Given a desired frequency range, it is then straightforward to determine how many propagation modes, N , should be taken into account.

The thin plate spectral element matrix can be obtained by writing the shear force and the moment using the displacements and the slopes at the two extremities along x . Considering an element with length L_x in the x -dimension, the transverse displacement and the slope at positions $x = 0$ and $x = L_x$ is given by

$$\begin{Bmatrix} w_1 \\ \phi_1 \\ w_2 \\ \phi_2 \end{Bmatrix} = \begin{bmatrix} 1 & 1 & 1 & 1 \\ -ik_1 & ik_1 & -k_2 & k_2 \\ e^{-ik_1 L_x} & e^{ik_1 L_x} & e^{-k_2 L_x} & e^{k_2 L_x} \\ -ik_1 e^{-ik_1 L_x} & ik_1 e^{ik_1 L_x} & -k_2 e^{-k_2 L_x} & k_2 e^{k_2 L_x} \end{bmatrix} \begin{Bmatrix} \mathbf{A} \\ \mathbf{B} \\ \mathbf{C} \\ \mathbf{D} \end{Bmatrix} = [\alpha] \begin{Bmatrix} \mathbf{A} \\ \mathbf{B} \\ \mathbf{C} \\ \mathbf{D} \end{Bmatrix} \quad (\text{D.5})$$

and the shear force and the moment are given by

$$\begin{Bmatrix} V_1 \\ M_1 \\ V_2 \\ M_2 \end{Bmatrix} = D \begin{bmatrix} \alpha_1 & -\alpha_1 & \alpha_2 & -\alpha_2 \\ \beta_1 & \beta_1 & \beta_2 & \beta_2 \\ -\alpha_1 e^{-ik_1 L_x} & \alpha_1 e^{ik_1 L_x} & -\alpha_2 e^{-k_2 L_x} & \alpha_2 e^{k_2 L_x} \\ -\beta_1 e^{-ik_1 L_x} & -\beta_1 e^{ik_1 L_x} & -\beta_2 e^{-k_2 L_x} & -\beta_2 e^{k_2 L_x} \end{bmatrix} \begin{Bmatrix} \mathbf{A} \\ \mathbf{B} \\ \mathbf{C} \\ \mathbf{D} \end{Bmatrix} = [\beta] \begin{Bmatrix} \mathbf{A} \\ \mathbf{B} \\ \mathbf{C} \\ \mathbf{D} \end{Bmatrix} \quad (\text{D.6})$$

where

$$\alpha_1 = ik_1^3 + ik_y^2(2 - \nu)k_1; \quad \alpha_2 = -k_2^3 + k_y^2(2 - \nu)k_2; \quad \beta_1 = k_1^2 + \nu k_y^2; \quad \beta_2 = -k_2^2 + \nu k_y^2 \quad (\text{D.7})$$

and the subscript n was dropped for simplicity. Thus, combining the equations above to write the element matrix gives

$$\{V_1 \ M_1 \ V_2 \ M_2\}^T = [\beta][\alpha]^{-1} \{w_1 \ \phi_1 \ w_2 \ \phi_2\}^T \quad (\text{D.8})$$

It is interesting to note that the element matrix is independent of the term $\sin(k_{yn}y)$ and the sum in k_{yn} can be performed for each element independently, or it can be done after the global matrix assembled. In order to complete the process, the force must be projected on the basis of sine function in terms of k_{yn} related to the y -direction. This representation takes into account the position of the concentrated driving force, y_0 , and it is given by

$$F = F_0 \frac{2}{L_y} \sin(k_{yn}y_0) \quad (\text{D.9})$$

The final solution will be given by the sum in the y -direction expressed in Eq. (D.2), which can be interpreted as a propagation mode superposition. The global matrix is assembled with the standard direct stiffness method (Craig, 1981).

The second approach, proposed by Doyle (1997), consists in writing the displacement solution as a Fourier series along direction y :

$$w(x, y) = \sum_{n=1}^N [\mathbf{A}_n e^{-ik_{1n}x} + \mathbf{B}_n e^{ik_{1n}x} + \mathbf{C}_n e^{-k_{2n}x} + \mathbf{D}_n e^{k_{2n}x}] e^{-ik_{yn}y} \quad (\text{D.10})$$

where $k_{yn} = n2\pi/\bar{L}_y$ and \bar{L}_y is the Fourier series period, which, as it will be shown later, is not necessarily equal to the plate length along y . This solution will not impose the simply supported boundary condition, but, instead, will impose a spatial periodicity along direction y . In order to impose a given boundary condition, Doyle (1997) proposes the use of an image method. Pavic (2001) recently formulated image methods, such as the boundary source substitution and the boundary conversion method, that can be used to impose different boundary conditions in a systematic way. The idea of using image sources - fictitious forces used to impose the desired boundary conditions, such as mirror sources used in acoustics to model a rigid surface, but the approach still requires an *ad hoc* solution, which does not always exist.

In order to impose a simply supported line along x at a given y_0 it is necessary to impose a force distribution equal to the force distribution along the beam span, but located symmetrically with respect to the simply supported edge and with a negative sign (a positive sign would produce a simply guided boundary condition). Therefore, to impose two parallel simply supported edges in a plate excited by a point force, three image sources are needed,

as shown schematically in Figure D.1 (the image sources are shown in gray), and the Fourier series period becomes $\bar{L}_y = 4L_y$.

It should be noted that the dynamic stiffness matrix is the same for both approaches. Therefore, Eqs. (D.5)–(D.8) are also used in Doyle’s formulation, but the solution will now be obtained by summing on the Fourier series terms in Eq. (D.10), and the point forces (actual and image) will be expressed as:

$$F_n = \frac{F_0}{L_y} e^{ik_y n y_0} \quad (\text{D.11})$$

In this work, only the simply-supported boundary condition is treated, using both the standard solution proposed by Lee and Lee (1999) and the Fourier series solutions according to Doyle (1997). Nevertheless, using the techniques proposed by Pavic (2001) along with Doyle’s formulation for the spectral element, it should be possible to extend the SE formulation for reinforced plates with other boundary conditions.

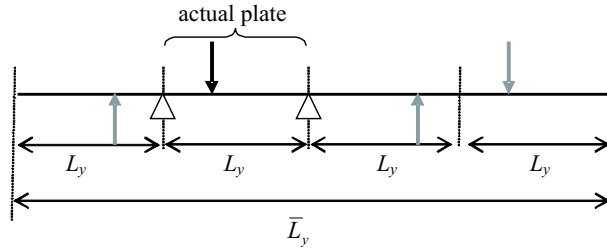


Figure D.1: Scheme of image sources for two simply supported edges.

D.0.9 Introducing the beam reinforcements on the plate element

Stiffener beams can be introduced in the SEM plate element them as ideally attached to the plate, where the effective shear force and the moments at the end of the plate are equal to those in the beam (Ungar, 1961).

Figure D.2 shows the equilibrium for a plate with an edge rigidly connected to a beam.

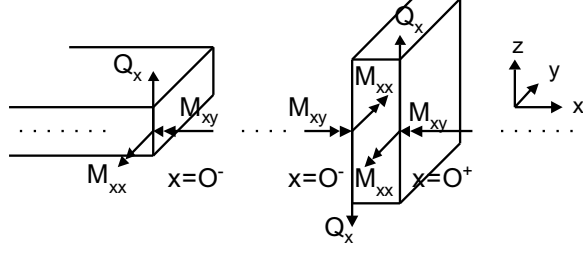


Figure D.2: Equilibrium for a plate with an edge rigidly connected to a beam (Donadon et al., 2004).

When the flexural waves reach the beam, they introduce both flexural and torsional motion in the beam. The equations of movement for Figure D.2 become,

$$EI_b \frac{\partial^4 u(y)}{\partial y^4} - \omega^2 \rho A u(y) = \left(Q_x + \frac{\partial M_{xy}}{\partial y} \right)_{x=0^-} - \left(Q_x + \frac{\partial M_{xy}}{\partial y} \right)_{x=0^+} \quad (\text{D.12})$$

$$GJ_b \frac{\partial^2 \theta(y)}{\partial y^2} + \omega^2 \rho I_p \theta(y) = (M_{xx})_{x=0^-} - (M_{xx})_{x=0^+} \quad (\text{D.13})$$

where $u(y)$ is the transverse displacement of the beam, $\theta(y)$ is the torsion angle of the beam, EI_b and GJ_b are the flexural and torsional stiffness of the beam, respectively, and ρA and ρI_p are the mass and the polar mass moment of inertia per unit length of the beam, respectively. Thus, a modified boundary condition can be established at position $x = 0^+$ to take into account the effective shear force and the moment including the beam effects as

$$V_x = -D \left[\frac{\partial^3 w}{\partial x^3} + (2 - \nu) \frac{\partial^3 w}{\partial x \partial y^2} \right] + EI_b \frac{\partial^4 w}{\partial y^4} - \omega^2 \rho A w \quad (\text{D.14})$$

$$M_x = -D \left[\frac{\partial^2 w}{\partial x^2} + \nu \frac{\partial^2 w}{\partial y^2} \right] - GJ_b \frac{\partial^3 w}{\partial x \partial y^2} - \omega^2 \rho I_p \frac{\partial w}{\partial x} \quad (\text{D.15})$$

The beam effect in the boundary conditions must be applied at the position of the stiffener. Here, the stiffener will be placed at right end of the spectral plate element. Using the same procedure used to derive Eq. (D.5), the modified matrix $[\beta_n]$ can be obtained

$$[\beta_n] = D \begin{bmatrix} \alpha_1 & -\alpha_1 & \alpha_2 & -\alpha_2 \\ \beta_1 & \beta_1 & \beta_2 & \beta_2 \\ (\delta_1 - \alpha_1)e^{-ik_1L_x} & (\delta_1 + \alpha_1)e^{ik_1L_x} & (\delta_1 - \alpha_2)e^{-k_2L_x} & (\delta_1 + \alpha_2)e^{k_2L_x} \\ (\delta_2 - \beta_1 + \kappa_1)e^{-ik_1L_x} & (-\delta_2 - \beta_1 - \kappa_1)e^{ik_1L_x} & (\delta_3 - \beta_2 + \kappa_2)e^{-k_2L_x} & (-\delta_3 - \beta_2 - \kappa_2)e^{k_2L_x} \end{bmatrix} \quad (D.16)$$

where the modifying terms are

$$D\delta_1 = EI_b k_y^4 - \omega^2 \rho A; \quad D\delta_2 = -iGJ_b k_y^2 k_1; \quad D\delta_3 = -GJ_b k_y^2 k_2; \quad D\kappa_1 = i\omega^2 \rho I_p k_1; \quad D\kappa_2 = \omega^2 \rho I_p k_2 \quad (D.17)$$

Replacing this result in Eq. (D.8) gives the dynamic stiffness matrix.

D.0.10 Numerical results for a plate with reinforcements

In order to illustrate the use of the SE method, a plate that is simply supported in the yz -plane and free-free in the xz -plane, shown in Figure D.3, is modelled (Arruda et al., 2004).

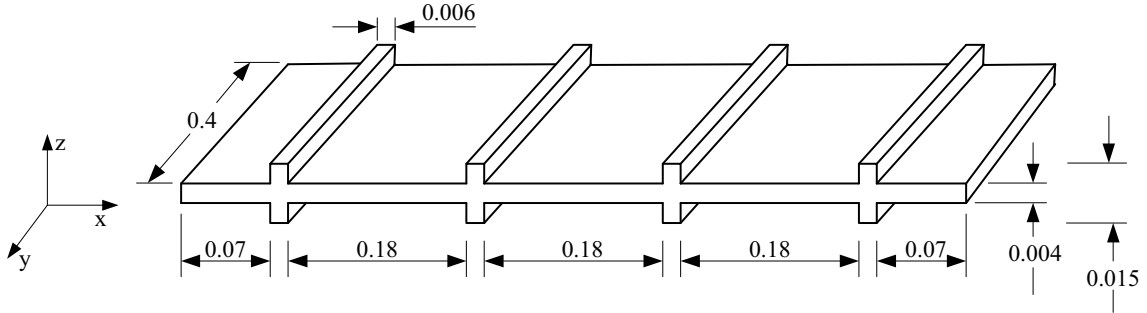


Figure D.3: Schematic diagram of the stiffened plate (units in meters).

In this numerical example, also a comparison with FE method is made to check the SE methodology applied to plates simply supported for two cases of applications, with and without reinforcements. The plate is assumed to have the following properties described in Table D.1. The receptance at the driving point located at position $(x, y) = (333.4, 160.0)$

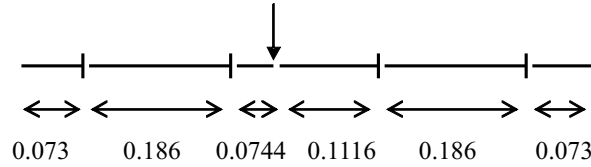


Figure D.4: Scheme of the spectral elements used in the model (Arruda et al., 2004).

mm for the SEM and FEM solutions for both cases, with and without reinforcements are compared.

Table D.1: Physical properties defined to the plate.

parameter	mean value \bar{m}	dimension
E	69×10^9	N/m ²
ρ	2700	kg/m ³
ν	0.3	—
L_x	0.400	m
L_y	0.704	m
h	0.004	m

For the first case, without reinforcements, the SEM model were evaluated using only 2 elements in order to include the driving point. For the second case, 4 reinforced plate and 2 simple plate elements as indicated in the scheme shown in Figure D.4 were used.

In case of the SEM, the responses were obtained with 10 propagation modes for the frequency range DC-2 kHz, while the FEM model was carried out with a commercial code MSC.NASTRAN (2004ab) using SHELL elements, with 4 nodes and 6 DOFs per node, and BAR elements in case with reinforcements shown in Figure D.4.

In the present case, results obtained with the Fourier series approach and image sources were not distinguishable from the sinusoidal solution using 40 Fourier lines.

Figures D.5 and D.6 shown the results obtained by FEM and SEM. The agreement in general is very well. Nevertheless, some improvements can be done in the FE model to achieve better results in the higher frequency range (Craig, 1981). This can be done changing the mode truncation in modal frequency response analysis as shown in Figure D.6, where the mode truncation is changed to a higher value. In general, it is recommended for better accuracy with the FE model, that all modes up to at least two or three times the highest

forcing frequency should be retained.

Finally, Figure D.7 shows the effect of a damping loss factor of $\eta = 0.01$ applied to the case of reinforcement plate. The results for the receptances responses are nearly identical.

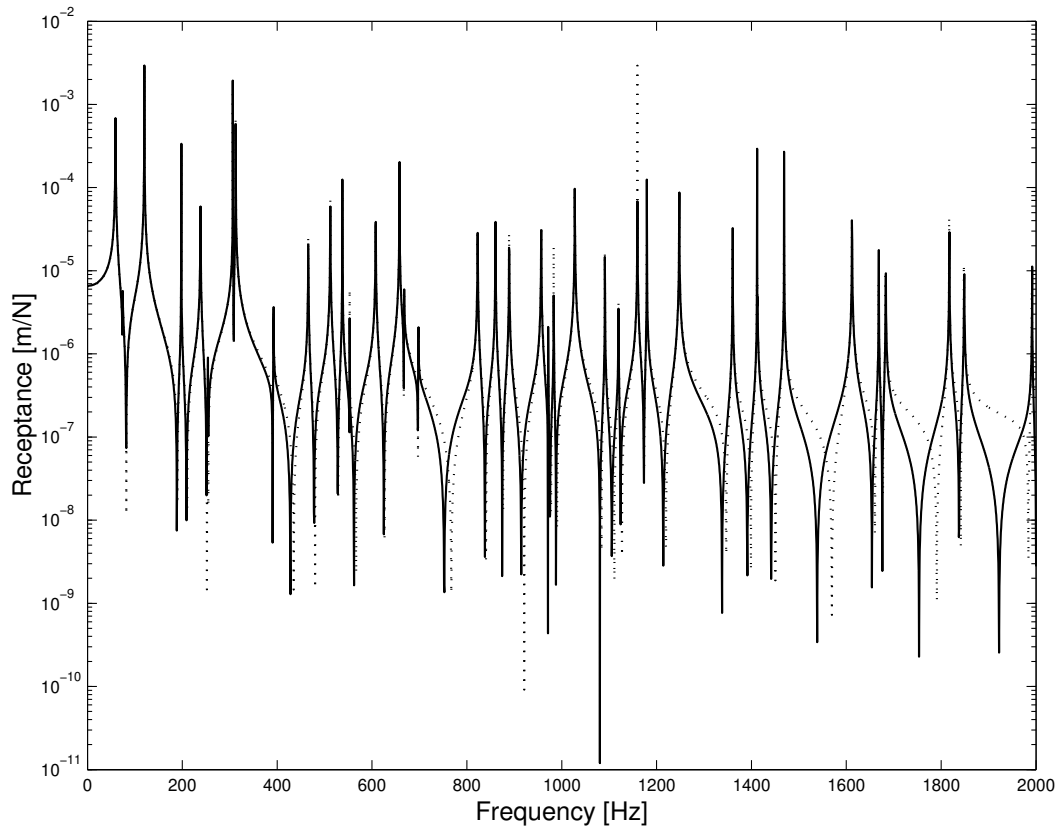


Figure D.5: Comparison of FEM (dashed) and SEM (continuous) results for the plate without reinforcements.

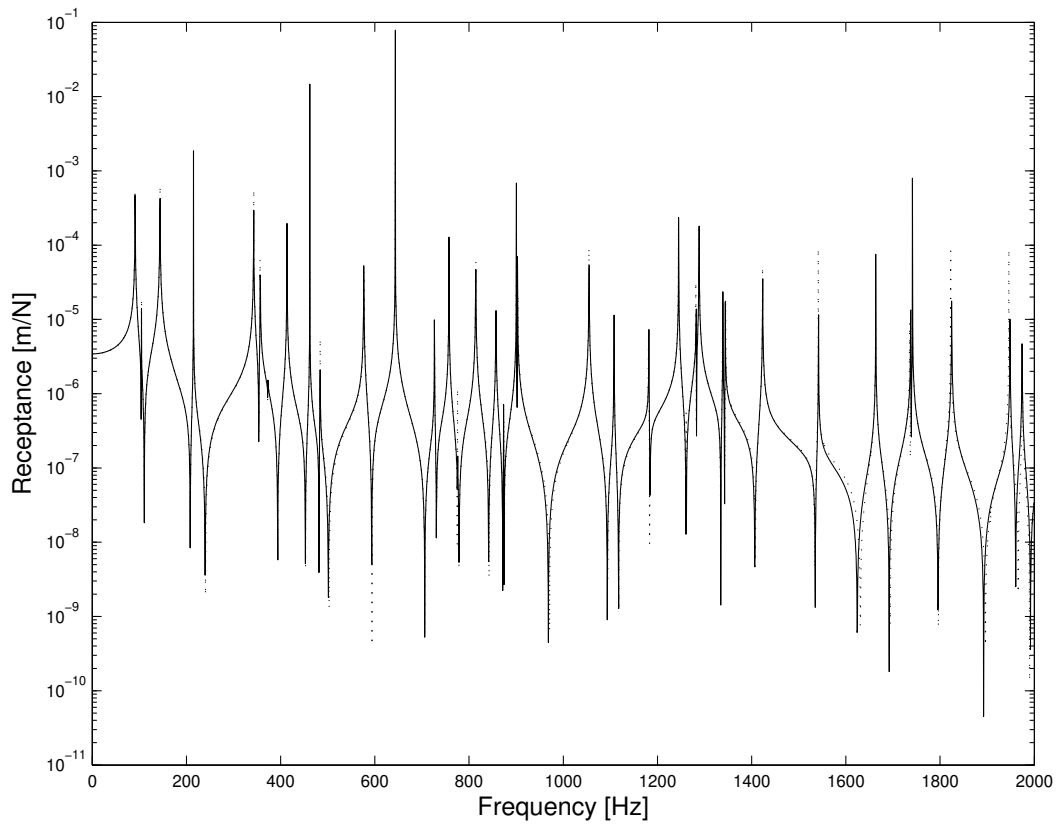


Figure D.6: Comparison of FEM (dashed) and SEM (continuous) results for the plate in Fig.D.3 (Arruda et al., 2004).

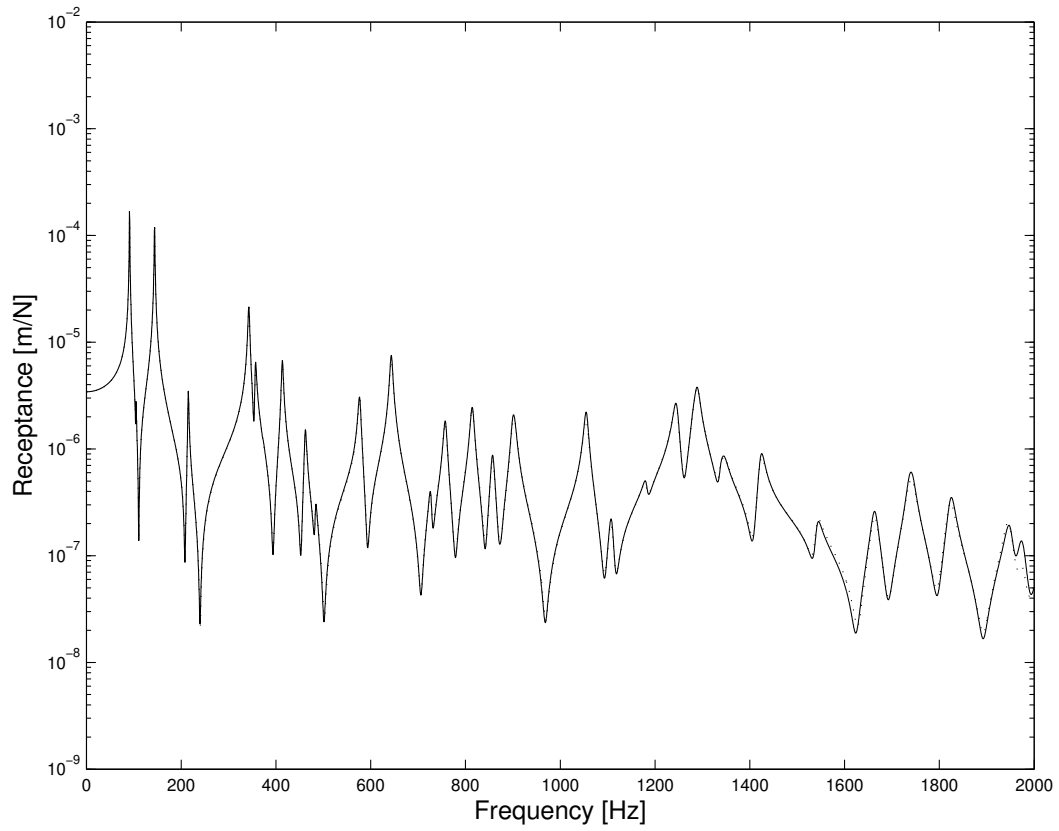


Figure D.7: Comparison of FEM (dashed) and SEM (continuous) results for the plate in Fig.D.3 with $\eta = 0.01$ (Arruda et al., 2004).